RESEARCH REPORT UMP GRANT
Laporan Prestasi Skim Geran UMP

Final	V	Progress		*Progress Period : _November 2019_____*	*√ Please tick*

PROJECT DETAILS *(Keterangan Projek)*

A		
	Grant No	RDU1703194
	Faculty/CoE	FIST
	Project Title	Development of Piezoelectric Thin Film of ZnO for Vibration Sensor Application
	Project Leader	AP Dr Agus Geter Edy Sutjipto
	Project Member	1. Ashry B Jusoh 2. Mazni Mustafa

PROJECT ACHIEVEMENT *(Pencapaian Projek)*

B

ACHIEVEMENT PERCENTAGE				
Project progress according to milestones achieved up to this period	**0 - 25%**	**26 - 50%**	**51 - 75%**	**76 - 100%**
Percentage (please state %)				100

EXPENDITURE *(Perbelanjaan)*

C

Budget Approved *Peruntukan diluluskan*	**Amount Spent** *Jumlah Perbelanjaan*	**Balance** *Baki*	**% of Amount Spent** *Peratusan Belanja*
RM 26,300	**RM 15,168.30**	**RM 11,131.70**	**58%**

RESEARCH OUTPUT *(Output Penyelidikan)*

D

NO OF PUBLICATION

KPI FOR NO OF PUBLICATION

	ISI	Scopus	Index Proceedings	Others
KPI				
Achievement				

The contribution of funder (UMP, MOHE, MOSTI, Industry etc.) as the fund provider must be acknowledged at all times in all forms of publications. Please state the grant number (RDU/UIC) and grant name.

	ISI	**Scopus**
Number of articles/ manuscripts/books *(Please attach the First Page of Publication)*	1. 2.	1. IOP Conference Series: Materials Science and Engineering. DOI: 10.1088/1757-899X/290/1/012043 2. IEEE Xplore. DOI: 10.1109/ICASET.2019.8714394 3. Materials Science Forum, TTP, Accepted 4. Materials Science Forum, TTP, Accepted

Conference Proceeding *(Please attach the First Page of Publication)*	**International**	**National**
	1. 2.	1. NCON-PGR 2018 UMP 2.

HUMAN CAPITAL DEVELOPMENT

KPI FOR HUMAN CAPITAL DEVELOPMENT

	PhD Student	Master Student
KPI		
Achievement		

Human Capital Development	**Number**				**Others** (please specify)
	On-going		**Graduated**		
Citizen	Malaysian	Non Malaysian	Malaysian	Non Malaysian	
PhD Student		1			
Masters Student					
Undergraduate Student					
Total					

Name of Student:	ALI G. M. Shaitir
ID Matric No:	PKC16009
Faculty:	FIST
Thesis title:	Synthesis of ZnO Thin Film using Spin Coating for Vibration Sensor Application
Graduation Year:	Planned in 2021
Name of Student:	
ID Matric No:	
Faculty:	
Thesis title:	
Graduation Year:	
*** enter for more space*	

INTELECTUAL PROPERTIES

KPI FOR INTELECTUAL PROPERTIES

Patent, Copyright, Trademark,Industrial Design: _____

Patent, Copyright, Trademark, Industrial Design ect	None

OTHERS

KPI FOR OTHERS

Prototype, Technology,Collaborations etc: _____

Prototype, Technology, Collaborations etc	**None**

ASSET *(Aset)*

E

Bil	**Peralatan** *(Equipment)*	**Model**	**No Daftar Aset** *(Asset Tagging No)*	**Amount** (RM)	**Lokasi** *(Location)*

PRODUCT DESCRIPTION FOR UMP R&D DIRECTORY (SHORT & BRIEF) *Only for Final Report*

F

ZnO thin film with spin speed of 2000 rpm and annealing temperature of 300 °C which has dimension of 113.25 nm thickness, area 0.78 cm² can produce output of 27.3mV under 40 kHz vibration of Bransonic CPX 5800 H.

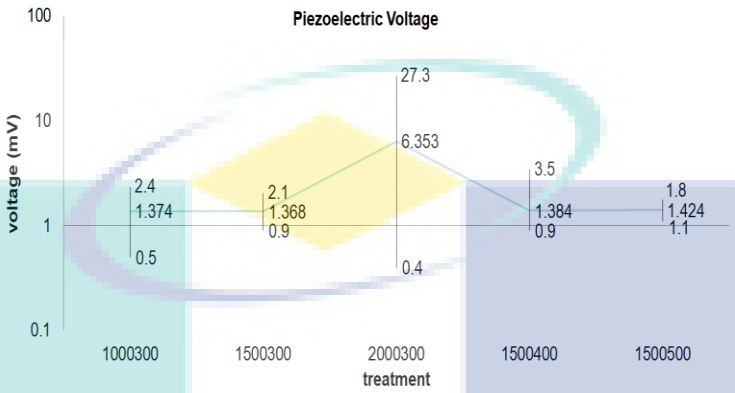

PRODUCT PICTURE FOR UMP R&D DIRECTORY *Only for Final Report*

G

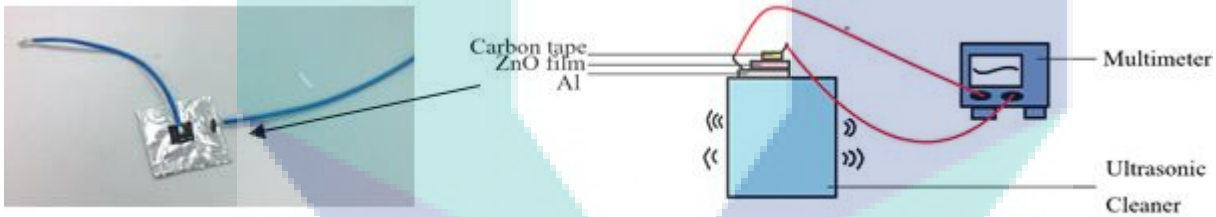

Piezoelectric ZnO Thin Film

SUMMARY OF RESEARCH FINDINGS (*Ringkasan Penemuan Projek Penyelidikan)*

H

ZnO thin film generated high voltage sensitivity of 0.55 V/gr.

ZnO thin film with spin speed of 2000 rpm and annealing temperature of 300 °C which has dimension of 113.25 nm thickness, area 0.78 cm² can produce output of 27.3mV under 40 kHz vibration of Bransonic CPX 5800 H.

PROBLEMS / CONSTRAINTS IF ANY *(Masalah/ Kekangan sekiranya ada)*

I

Could not utilize VOT 11000 since PhD student got scholarship from his sponsorship (government of Lybia).

Date : 30 November 2019 *Tarikh*	**Project Leader's Signature:** *Tandatangan Ketua Projek*

COMMENTS, IF ANY/ ENDORSEMENT BY FACULTY (*Komen, sekiranya ada / Pengesahan oleh Fakulti)*

J

Recommend / Not Recommend / KIV / Need Ammendment

.....

.....

.....

Name:
Nama:

Signature:
Tandatangan:

Date:
Tarikh:

**** Dean/TDR/Director/Deputy Director**

COMMENTS, IF ANY/ ENDORSEMENT BY RMC PNI (*Komen, sekiranya ada / Pengesahan oleh RMC PNI)*

K

Recommend / Not Recommend / KIV / Need Ammendment

.....

.....

.....

Name:
Nama:

Signature:
Tandatangan:

Date:
Tarikh:

DEVELOPMENT OF PIEZOELECTRIC THIN FILM OF ZINC OXIDE ON ALUMINUM SUBSTRATE FOR VIBRATION SENSOR APPLICATION

AGUS GETER EDY SUTJIPTO

RESEARCH VOTE NO:

RDU1703194

Faculty of Industrial Sciences & Technology

University Malaysia Pahang

2019

DEDICATION

Dedicated to my family and my colleagues, my FYI and PhD students, and lab assistances.

ABSTRACT

This thesis deals with ambient energy harvesting by using zinc oxide thin film. The objective of this thesis is to prove the ZnO film as a piezoelectric material can produce electric when vibration is applied and determine its optimal piezoelectric voltage. The thesis describes the sol gel spin coating technique to fabricate zinc oxide thin film. Zinc acetate dehydrate, absolute ethanol and diethanolamine were used in this thesis to act as sol gel precursor. Sol gel was coated on glass slide which wrapped by aluminum foil. The thin film was formed after preheating and annealing. The thin film was characterized by X-ray diffraction (XRD), Field Emission Scanning Electron Microscopy (FESEM), Photoluminescence spectroscopy (PL) and Ultraviolet- visible spectroscopy (UV-Vis) as well as analyzed using vibration technique. From XRD results, the films were preferentially diffracted at 65° which corresponding to (1 1 2) diffraction phase. From FESEM results, it was observed that when the spin speed was increased at same annealing temperature, the grain size was decreased and the thickness was also decreased. When the annealing temperature was increased at same spin speed, the grain size was increased and the thickness was increased. From the PL results, it was observed that there was only film with spin speed of 2000 rpm and annealing with 300 °C had slightly left wavelength which is around 380 nm. Annealing temperature would affect only the intensity of PL wavelength. From the result of UV-Vis, it was observed that when the spin speed was increased at same annealing temperature, the band gap was decreased. When the annealing temperature was increased at same spin speed, the band gap was decreased. Piezoelectric test had proven the ZnO film could produce electricity. The maximum voltage (20.7 mV) was produced by the ZnO film with spin speed of 2000 rpm and annealing with 300 °C.

TRANSLATION OF ABSTRACT

Tesis ini berkaitan dengan penuaian tenaga ambien dengan menggunakan filem zink oksida. Objektif projek ini adalah untuk membuktikan filem ZnO sebagai bahan piezoelektrik boleh menghasilkan elektrik apabila getaran digunakan dan menentukan voltan piezoelektrik optimum. Tesis ini menerangkan teknik lapisan gel putaran sol untuk mereka-reka filem zink oksida. Kering zink oksida, etanol mutlak dan diethanolamine digunakan dalam tesis ini untuk menjadi sebagai sol gel pelopor. Sol gel telah disalut pada slaid kaca yang dibalut dengan kerajang aluminium. Filem akan dibentuk selepas peapemanasan dan penyepuhlindapan. Filim telah dicirikan oleh pembelauan sinar-X, Field Pelepasan Scanning Electron Microscopy (FESEM), Photoluminescence spektroskopi (PL) dan Ultraviolet spektroskopi (UV-Vis) serta dianalisis dengan teknik getaran. Daripada keputusan XRD, filem-filem telah dibelaukan pada 65 ° yang sepadan dengan (1 1 2) fasa. Daripada keputusan FESEM, saiz butiran dan ketebalan telah menurun apabila meningkatkan kelajuan putaran pada suhu penyepuhlindapan yang sama. Saiz butiran dan ketebalan telah meningkat apabila meningkatkan suhu penyepuhlindapan pada kelajuan putaran yang sama. Daripada keputusan PL, hanya filem dengan kelajuan putaran 2000 rpm dan penyepuhlindapan dengan 300 ° C telah meninggalkan panjang gelombang daripada yang lain, iaitu 380 nm. Suhu penyepuhlindapan akan menjejaskan hanya intensiti PL gelombang. Dari hasil UV-Vis, apabila kelajuan putaran telah meningkat pada suhu penyepuhlindapan sama, jurang band ini telah berkurangan. Apabila suhu penyepuhlindapan telah meningkat pada kelajuan putaran sama, jurang band ini telah berkurangan. Ujian piezoelektrik telah membuktikan filem ZnO yang boleh menghasilkan tenaga elektrik. Voltan maksimum (20.7 mV) telah dihasilkan oleh filem ZnO dengan kelajuan putaran 2000 rpm dan penyepuhlindapan dengan 300 ° C.

TABLE OF CONTENTS

LIST OF TABLES

LIST OF FIGURES

LIST OF SYMBOLS

~	-	approximately
%	-	percent
λ	-	wavelength
2θ	-	Bragg angle
^{o}C	-	degree celcius
Å	-	angstrom (10^{-10})
g	-	grams
h	-	hour
t	-	time
s	-	seconds
rpm	-	rotation per minutes

LIST OF ABBREVIATIONS

FESEM	-	Field Emission Scanning Electron Microscopy
PL	-	Photoluminescence
UV-Vis	-	Ultraviolet-Visible Microscopy
XRD	-	X-ray diffraction

CHAPTER 1

INTRODUCTION

1.1 INTRODUCTION

Electricity is generated from non-renewable natural sources such as fossil fuel, coal, natural gas, and petroleum. The electricity is being used in many fields such as automotive, health care and communication devices. For example, for application in medical science, nano-devices and wireless sensors require electricity for their power sources. To use in powering the wireless nano-devices, the regular energy source, battery is facing the limitation due to its big size, heavy weight and short operation lifetime (Prashanthi, et al., September 2013; Kumar & Kim, May 2012). Even though battery has high capacitance, it is not energy efficient. Most of the energy input has been lost as heat, light, sound or vibration. Battery has low power density. In addition, battery is not environmental friendly power resource. Therefore, it has drawn the emergence of research in alternative energy sources to fulfill the needs of wireless sensing problem.

Moreover, these non-renewable natural sources have caused the depletion of ozone layer and global warming. To maintain sustainably development for human civilization, many researches are now focusing on searching renewable alternative way to solve the shortage of natural resources and reduce the pollution (Aricò, Bruce, Scrosati, Tarascon, & Schalkwijk, April 2005).

To break through the insufficiency of traditional power sources and achieve green energy technology, energy harvesting has drawn attention from scientist. Energy harvesting is a device that can convert the unused ambient energy to electricity. The type of energy harvesting depends on the type of energy and applications. Energy harvesting is distinguished as radiant energy harvesting, mechanical energy harvesting, thermal energy harvesting, vibration energy harvesting and others. Energy harvesting is mostly

used for low-powered electronic applications, such as wireless devices. This technologies use material at micro- or nano- scale to charge wireless devices and wireless sensor networks.

There are many benefits of energy harvesting. One of the benefits is to reduce usage of battery power. Device with low-powered can be charged by energy harvester and rely on internal energy storage rather than rely on battery power. Self-powered wireless sensor is easy to install. Therefore, it can reduce installation cost. Energy harvesting also can reduce maintenance cost as there is not necessary to replace battery. Self- powered device can be used in long term as long as the ambient energy is available. Energy harvester also reduces environmental impact (Chen, He, & Sun, 2014; Wong & Dahari, 2015).

Among these few types of energy harvesting, vibration energy harvester has drawn more attention in the world as it is available almost everywhere at all times. It can be used in many fields such as implanted devices, electronic devices, mobile devices and wireless sensor devices (Khaligh, Zeng, & Zheng, March 2010). There are three ways to generate electrical energy from vibration energy which are electromagnetic, piezoelectric and electrostatic. It is hard to fabricate the circuit of electromagnetic as it has low voltage and cannot produce high current. Electrostatic cannot be used in practical as it requires external voltage sources (Shang, Li, Wen, & Zhao, November 2013). Therefore, piezoelectric vibration harvester has been focused more.

The piezoelectric effect converts mechanical energy (vibration, air flow and human physical motion (Kumar & Kim, May 2012)) into electrical energy. In 1880, Curie and his brother discovered the piezoelectric effect. During World War I, the application of piezoelectric effect in solar device had been launched. After that, new applications such as microphones, accelerometers, actuators and ultrasonic motors were developed (Spies, Pollak, & Mateu, June, 2015). Nuffer and Bein proposed that piezoelectric energy harvester acts as a knock sensor to detect irregular combustion in transportation industry (Nuffer & Bein, October 2006). It has become common and easy to find the application of piezoelectric material.

Thin film technology has great potential to produce micro- or nano- scale devices as piezoelectric thin film. Thin film is a 2D nanomaterial which means that two of the dimensions are not confined to the nanoscale. Thin film exists in platelike shape. It offers many benefits in various applications for example, high energy density harvester, high sensitivity but low power sensors and high resolution circuit board. Moreover, compare to bulk piezoelectric materials, piezoelectric thin films are more suitable to be integrated into micromechanical systems (MEMS) or nanoelectromechanical systems (NEMS) (Eom & Trolier-Mckinstry, Nov, 2012).

1.2 PROBLEM STATEMENT

There are many novel ideas of renewable energy harvesting application. However, the major challenges faced by developers are to construct an energy harvester that is cheap, efficient and can work all the time especially when the ambient unused energy is absent. From this case, the combination of semiconductor and piezoelectric plays an important role in energy harvesting.

Piezoelectric semiconducting materials (ZnO, AlN, ZnS, GaN) have been used in many fields to generate power. Among these materials, ZnO has been focused more due to its favorable properties (high electron mobility, high power stability and inherent piezoelectric properties).

There are many studies revealed that the characterization and vibration sensing performance of ZnO nanostructures as piezoelectric energy harvester under different annealing temperature, but the energy harvester based on ZnO thin film was rarely reported.

This paper presents the fabrication process of ZnO thin film by spin coating and the measurement of the energy harvester based on ZnO thin film. The characterizations (crystallographic orientation, composition of ZnO, thickness of thin film and the current output) of ZnO thin film are determined. In this present work, ultrasonic cleaner is used to determine the effect of vibration on the voltage produced from ZnO thin film.

1.3 OBJECTIVES OF RESEARCH

The objectives of this research are stated as below.

1.3.1 To fabricate ZnO based thin film by spin coating

1.3.2 To characterize ZnO thin film using X-ray Diffraction (XRD), Field Emission Scanning Electron Microscopy (FESEM), photoluminescence and UV-Vis spectroscopy

1.3.3 To prove ZnO thin film piezoelectric as vibration energy harvester can produce electric

1.3.4 To determine the optimal piezoelectric voltage by varying the temperature and speed during spin coating

1.4 STATEMENT OF CONTRIBUTION

The scopes of study are

1.4.1 To synthesis ZnO sol gel

Zinc oxide comes from group II-IV semiconductor which has a wide band gap (3.37eV). The properties of ZnO that made it as the candidate of this study are environmental friendly, low cost, chemical stability towards air and biologically safe. It is able to coat for large area. ZnO sol was prepared by adding with precursor sol of zinc acetate dehydrate in 70 ml of absolute ethanol solution and diethanolamine (DEA).

1.4.2 To fabricate ZnO based thin film.

Thin film coating process involves solution preparation, coating and drying. ZnO sol was deposited on an aluminum foil which acts as an electrode by spin coating process. Aluminum foil was being chosen because it is low cost, non-toxic, good electricity, and stable at high temperature. The method of spin coating was used because it is simple and low cost.

1.4.3 To analyze the ZnO thin film by using XRD, FESEM, photoluminescence and UV-Vis spectroscopy to examine the surface morphology and physical properties.

1.4.4 To investigate the effect of vibration on voltage produced from piezoelectric ZnO thin film.

CHAPTER 2

LITERATURE REVIEW

2.1 INTRODUCTION OF PIEZOELECTRIC EFFECT

Piezoelectric is derived from Greek word where “piezo” means pressure and “electric” means electricity. Piezoelectric effects characterize into two types, which are direct and indirect. Direct piezoelectric effect means that an electric charge is being generated across the material when a mechanical strain (stress) is applied to the piezoelectric material. Conversely, indirect piezoelectric effect means that a deformation of material happens when an electric field is applied to the piezoelectric material (Nechibvute, Chawanda, & Luhanga, 2012).

The requirement of piezoelectric material is that the atomic arrangement have no center of symmetry. There is only twenty out of thirty-two crystal classes that have piezoelectric effect. The most important piezoelectric material is quartz (SiO_2).

Figure 2.1 shows piezoelectric phenomenon. Piezoelectric material generates current when a pressure is applied as shown in Figure 2.1a. When a pressure is applied on piezoelectric material, polarization occurs and a charged density is generated in crystals of piezoelectric material. One side of crystal has net positive charge and a net negative charge is at opposite site. The polarization establishes an electric field and causes current flow. Polarization will remain as long as the force is applied. The effect is called as direct polarization effect. Polarization will be disappeared and no current flow when the pressure applied is stopped (Vives, 2008). In contrast, mechanical deformation of piezoelectric material will be occurred when a voltage is applied. The effect is then called as indirect polarization effect.

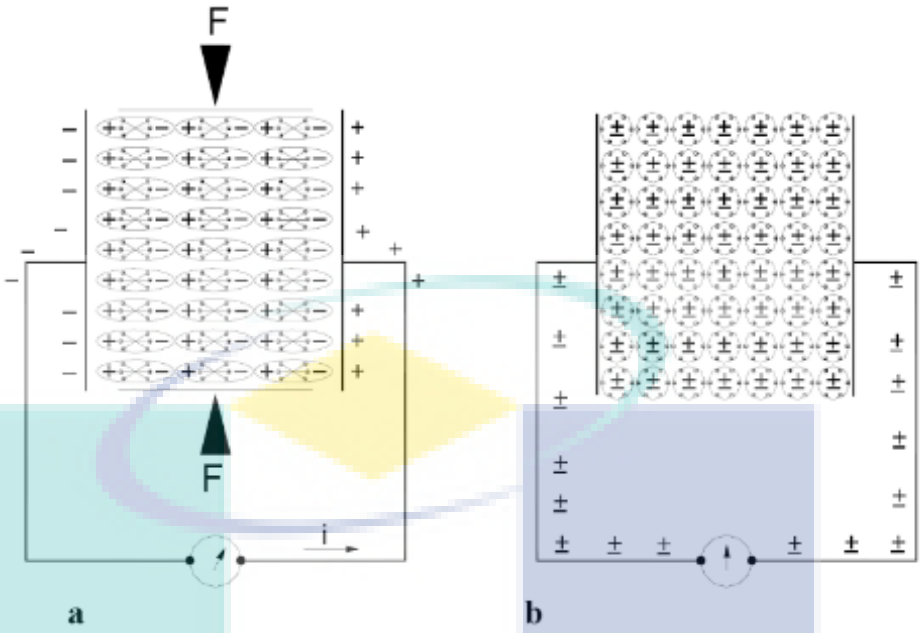

Figure 2. 1. An illustration of piezoelectric phenomenon (a) direct piezoelectric effect, (b) neutral state of piezoelectric material (Vives, 2008).

2.2 PIEZOELECTRIC MATERIAL, ZNO

Zinc oxide (ZnO) comes from group II-IV group semiconductor. It is a transparent conducting oxide. ZnO has a hexagonal wurtzite structure with non centrosymmetric characteristic as shown in Figure 2.2 (a). It possess strong piezoelectric and pyroelectric properties. Besides that, it has a wide band gap which is about 3.37 eV at room temperature. This means that it is suitable to use for short wavelength application such as laser. It also has high exciton binding energy which is about 60 meV so that excitonic emission is efficient at room temperature (Wang, Zhong Lin, 2004).

Zinc oxide, semiconducting material possess piezoelectric characteristic. It generates a small piezoelectric coefficient. It has a preferable highly c-axis oriented with a peak of (002). C-axis preferential thin film is important for piezoelectric devices because along with c-axis, ZnO crystal has the largest coupling constant. This means that, c-axis oriented ZnO film has shorter carrier path in c-axis and hence has lower resistivity. Therefore, it has high mobility of electrons (Yahya, 2011). The lattice parameters of ZnO structure are a = 0.325 nm and c = 0.521 nm. $Zn^{2+}$and O^{2-} ions are tetrahedral bonded and it has overlapping at the centers of charge of positive and negative ions (Alias & Mohamad, 2013). When a stress is applied at the top of tetrahedron, a dipole moment will be induced due to the displacement of the charge. The dipole moment will generate a

piezopotential and the potential drop will maintain as long as the stress is maintained. When an external cable is connected, piezopotential will drive the flow of electron and induce a voltage (Wang & Wu, 2014).

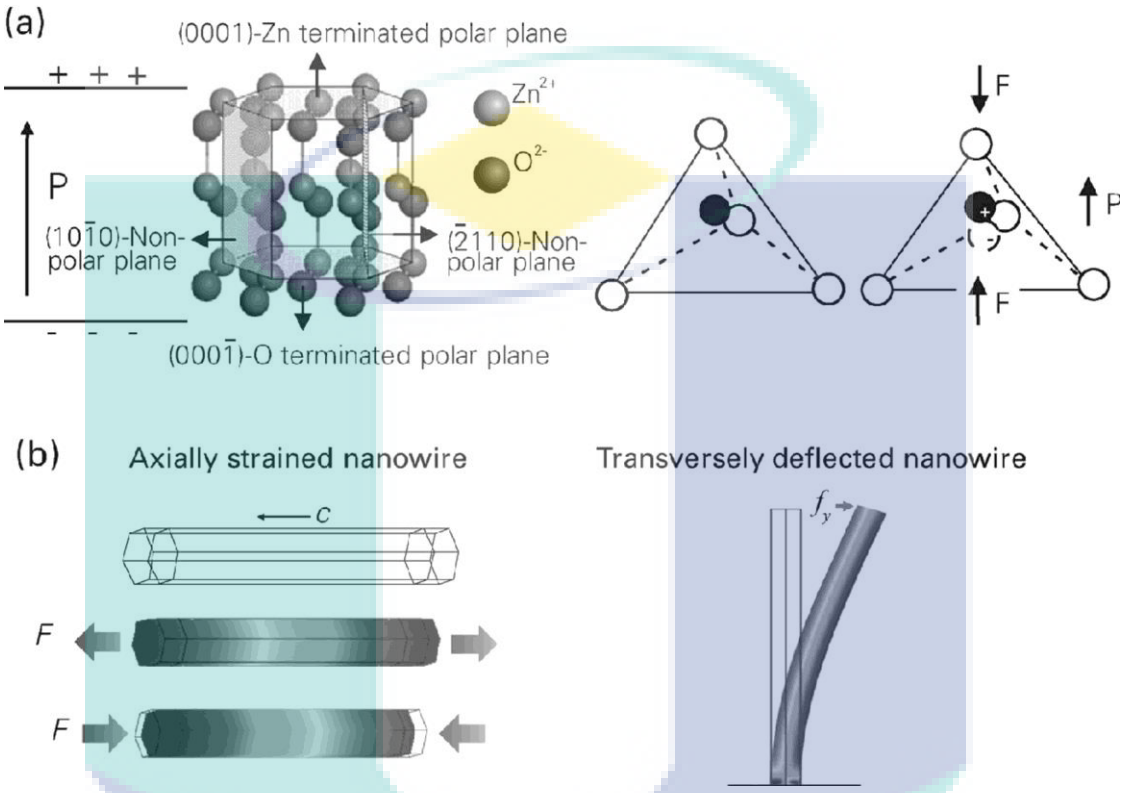

Figure 2.2. Piezopotential in wurtzite crystal (Wang & Wu, 2014).

2.3 SOL GEL DEPOSITION

Sol gel is a process to synthesis nanoscale materials. It is used to fabricate metal oxides nanoparticles. Sol gel process is most common method for synthesize ZnO nanoparticles. ZnO thin film can be made by sol-gel processing.

The advantages of sol gel process are controllability of compositions (Nanda & Gupta, 2010), simple, cost effective, inexpensive, non-vacumm and low temperature treatment. Besides that, homogeneity of solution is easily controlled to form a uniform film. (Kondraties, Kink, & Romanov, 2013).

Sol gel process involves transition phase of a liquid sol to a solid gel by hydrolysis and condensation reaction (Znaidi, L., 2010). Figure 2.3 shows the illustration of sol gel

process. Sol gel process is generally involves 3 principle steps, which are preparation of precursor solution, deposition of sol on suitable substrate by appropriate technique and heat treatment.

It starts with hydrolysis of the molecular precursor. As reported in the literature review, metal salts in alcoholic solution was used to fabricate ZnO film. Therefore, a solution of inorganic metal salts or metal-organic compound (alkoxide) is used and dissolved in appropriate alcoholic solvent (Levy & Zayat, 2015). Polymerization reaction of precursor forms oxo-, hydroxyl or aqua-bridges (Schodek, Ferreira, & Ashby, 2009; Znaidi, L., 2010). The particles can be extracted by using spin-coated or cast onto a substrate. After that, it undergoes gelation and evaporation of solvent to form a dense or nanoporous film. Solid nanoparticles are obtained through nucleation and growth process. Heat treatment is treated to form a dense film (Pierre, A. C., 1998).

Route two in figure 2.3 shows the sol undergoes condensation by dehydration. Drying process is required to remove excess solvent. It will cause shrinkage of a gel due to rising of capillary pressure. A dried gel, which is also called as xerogel is formed (Brinker & Scherer, 2013). A dense film is formed by annealing. Sol gel process is used to fabricate thin films, ultrafine particles, nanothickness films and nanoporous membrane.

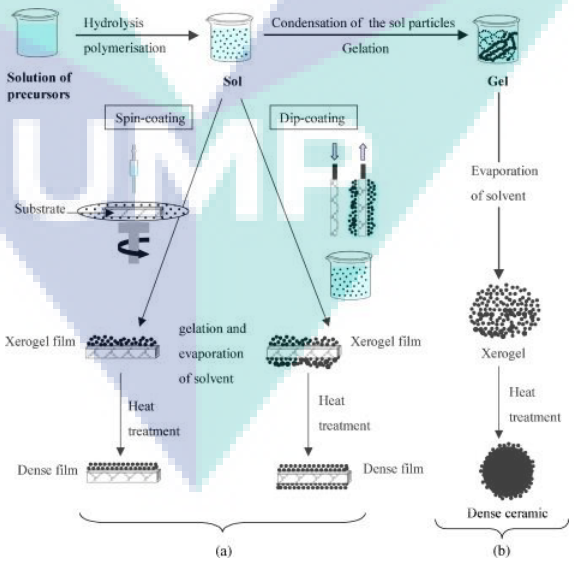

Figure 2. 3. Steps of preparation of (a) thin films and (b) powders by sol gel process (Znaidi, L., 2010)

2.4 PRECURSOR MATERIAL

The common salts that are widely used to synthesis ZnO thin films are zinc nitrate hexahydrate, zinc chloride and zinc acetate. Zinc Chloride is used for electrodeposition. The use of high concentration of zinc acetate dehydrate leads to formation of development of thin film morphology. It also leads to formation of ZnO without impurities. With using zinc acetate dehydrate, extra capping agents can be avoided (Akgun, Kalay, & Unalan, 2012).

According to Heridia E., et al., (2014), the ZnO thin films were prepared by sol gel method using precursor solution of zinc acetate dehydrate dissolved in absolute ethanol, deionized water and acetic acid. They revealed that zinc acetate dehydrate had high solubility in absolute ethanol (E.Heredia, et al., October 2014). According to Habibi & Sardashti, (2008), the sol gel process was to control the nano-scale over the structure of a material. By using zinc acetate and MEA as precursor, a stable, transparent and high quality of sol produced (Habibi & Sardashti, December 2008).

According to Yahya, (2011), sol gel method was used to fabricate ZnO thin film due to ease of production, low in cost and low temperature needed. In the research, materials that used as precursor of ZnO sol were zinc acetate dehydrate which acted as starting material, monoethanolamine (MEA) and 2-methoxyethanol acted as a stabilizer and as solvent respectively. Anhydrous zinc acetate was used to prevent the induction of large amount of water to the sol gel and to control the reaction. The function of aminoethanols such as monoethanolamine and diethanolamine was to act as ligands to Zn^{2+} to stabilize the solution against any precipitation, prevent uncontrollable growth of particle, prevent particle from aggregation, and increase the pH due to presence of amine. The ZnO particles were not in perfect spherical shape due to different surface energy of crystallographic directions (Yahya, 2011).

Table 2.1 summarizes the sol gel undoped ZnO thin film methods.

Table 2. 1: Sol gel undoped ZnO thin film methods

Reference	Precursor (mol L^{-1})	Alcohol	Additive (r)	Aging time	Substrate	Pre-heat treatment	Post-heat treatment
Wang et. al. (Wang, et al., 2006)	ZAD (0.5)	A. EtOH	DEA (1)	-	Quartz	400	400 - 800
Natsume and Sakata (Natsume & Sakata, 2000)	ZAD (0.02)	MeOH	-	-	Pyrex	80	500 - 575
Liu et. al. (Liu, Li, Ya, Xin, & Jin, 2008)	ZAD (0.6)	EtOH, PEG (14 g/L)	DEA (1)	-	Glass	100	500
Kumar et. al. (Kumar, Kaur, & Mehra, 2007)	ZAD (0.2)	EtOH	DEA (1)	48 h	p-Si (1 0 0)	250	350 - 450
Bae and Choi (Bae & Choi, 1999)	ZAD (0.25)	2-PrOH	DEA (1.5)	-	Alumina	300	400 - 900
Zhu et. al. (Zhu, et al., 2008)	ZAD (0.75)	2- ME	MEA (1)	-	Glass	60	400-550
Abdel Aal et. al. (Abdel Aal, Mahmoud, & Aboul-Gheit, 2009)	ZAD	2-PrOH	NaOH	-	Glass	-	550
Heridia E. et. al. (E.Heredia, et al., October 2014)	ZAD	A. EtOH	MEA	-	a- SiO_2	200	450

2.5 SOLVENT, ABSOLUTE ETHANOL

Absolute ethanol is been chosen as it gives rise to form spherical shape of particle. This is because absolute ethanol has hydroxyl group to interact with nanoparticle in nucleation, growth and termination process (P.B., Moloto, & Sikhwivhilu, 2012). Hydroxyl group in absolute ethanol also reduces the formation of porosity and irregular grains. Dissolution of ZnAc in absolute ethanol also can lead to self-hyrolysis of zinc salt to form ZnO. Besides that, absolute ethanol forms smaller size of ZnO particles when compared nanoparticles formed when using acetone. The use of alkali is avoided to have better control of purity of final product (Gattorno & Oskam, 2006).

2.6 THIN FILM PREPARATION METHOD

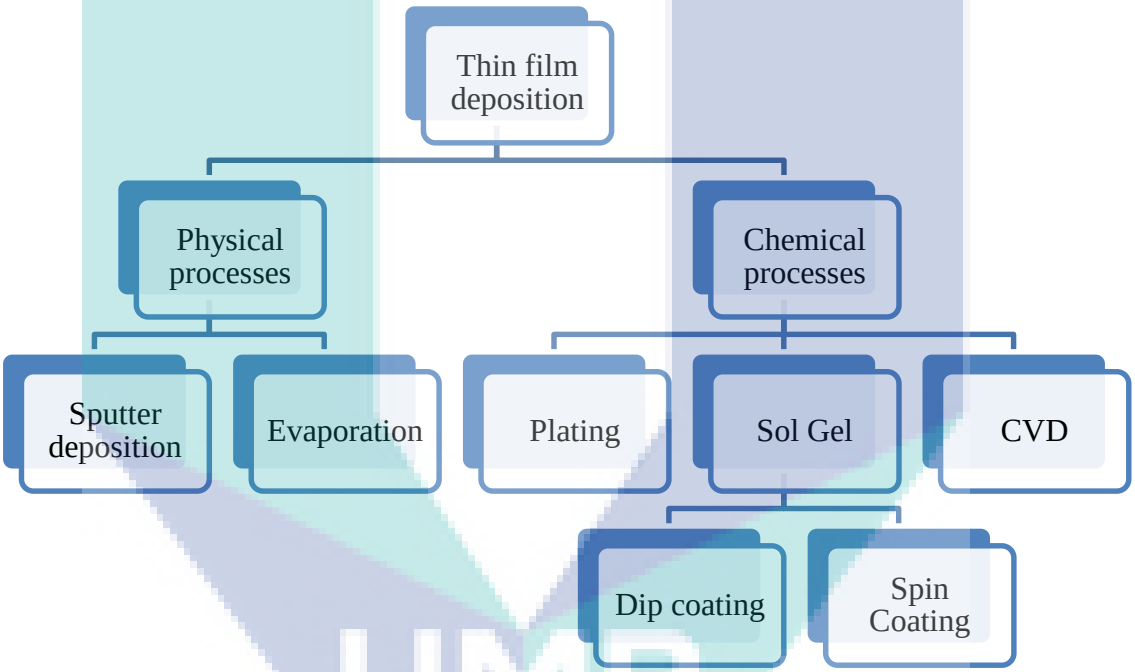

Figure 2. 4. Thin film preparation techniques.

There are many methods in fabricating thin film as showed in figure 2.4. It divides into chemical deposition (plating, chemical solution deposition, spin coating, chemical vapor deposition, plasma enhanced CVD) and physical deposition (thermal evaporator, sputtering, cathodic arc deposition). In this study, spin coating is used to deposit ZnO thin film on aluminum foil. Spin coating is a simple and fast process for depositing thin coating on a flat substrate. A typical spin coater has a high rotation speeds around 1000-10 000 rpm. The steps of spin coating start with depositing fluid into substrate. Then, accelerating the substrate to final radial velocity. The action of spinning causes the liquid precursor or

sol-gel precursor to spread out uniformly on the surface of substrate. The thickness of coating is dependent on the rate of evaporation and the spin speed. Lastly, solvent is evaporated from the film and resulting further thining film is formed. The typical coating thickness values are below 1 μm (Schweizer & Kistler, 2012).

The advantage of spin coating is that the thickness of film can be easily controlled by changing spin speed or using different viscosity photoresist. Uniform thin film can be formed during coating process. Besides that, spin coating is easy, low cast and fast operating system (Sahu, Parija, & Panigrahi, 2009). It can be used commercially available equipment. It can also be used at all stages of processing on all types of substrate layers. It consumes short time and forms high resist film thickness homogeneity. However, it is highly depending on the position of cavity. Size and shapes of cavities have influence on the resist uniformity. The reproducibility of spin coating is very less.

2.7 ANNEALING EFFECT

The process of annealing metal oxide thin film is to control the surface roughness, improve structure and modify surface morphology. The number and size distribution of crystallites depends on annealing temperature and time. Phase transition from amorphous to polycrystallines occurs in annealing process (Monk, Mortimer, & Rosseinsky, 2007).

Shivaraj, et al., (2015) had reported the effect of annealing temperature on the grain size, surface roughness, surface morphology and photoluminescence properties of ZnO thin films prepared by dip coating and spin coating. They were able to observe that when increasing in annealing temperature, the grain size also increased under XRD as showed in figure 2.5. SEM images showed the surface morphology could be clear distinguished for spin coated film. The study revealed that annealing temperature increased, the wavelength intensity increased under photoluminescence test (Shivaraj, Murthy, Krishna, & Satyanarayana, 2015).

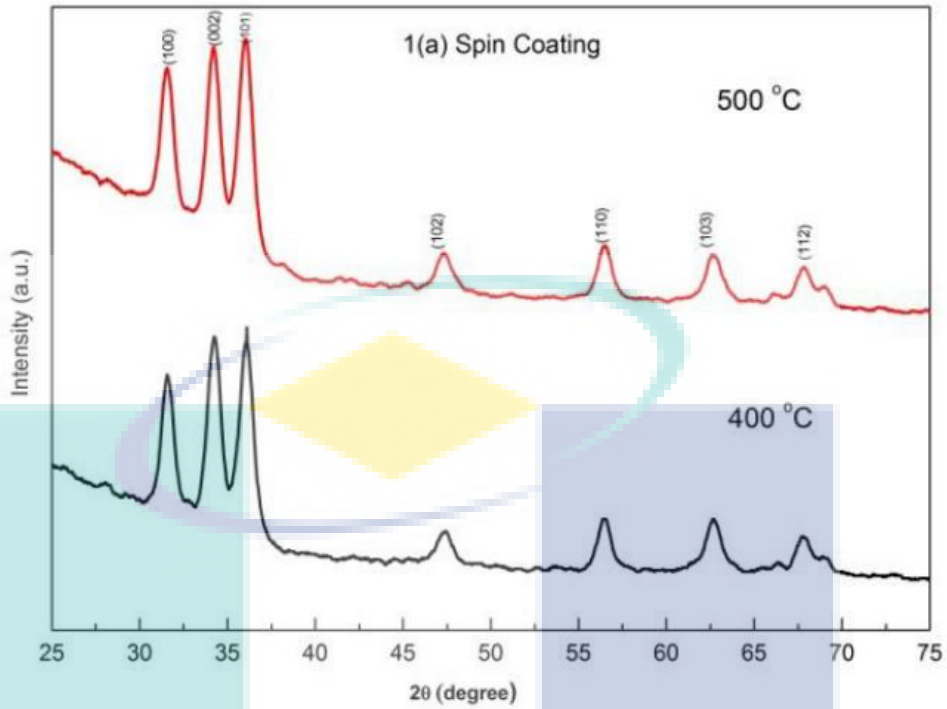

Figure 2. 5. XRD pattern ZnO thin film by spin coating at different annealing temperature (Shivaraj, Murthy, Krishna, & Satyanarayana, 2015).

2.8 ENERGY HARVESTING TEST

Joshi, et al., (2014) revealed that a range of annealing temperature from 100 °C to 500 °C, the optimum annealing temperature for ZnO thin film was 300 °C. ZnO thin film showed highly c-axis oriented, surface morphology with uniformity in grain for this optimum temperature. It presented a better performance with higher peak output volage of 147 mV when testing with vibration sensing performance (Joshi, Nayak, & Rajanna, March 2014).

2.9 APPLICATION OF PIEZOELECTRIC

Piezoelectric transducers generate electricity when a force is applied. They do not need bias voltage. Therefore, piezoelectric materials provide advantages for power harvesting. Piezoelectric transducer connects with two rectifying diode to generate dc output voltage. The ongoing development of piezoelectric materials has led to huge market. The application of piezoelectric material can be seen from things for daily use to specialized devices, such as air bag sensor, knock sensor, inkjet printers, telephones, ultrasonic imaging and depth sounders.

In 2010, Dr. Ville Kaajakari had developed a microstructured piezoelectric shoe power generator which can be embedded in the sole of a shoe. The design of shoe power generator is shown in figure 2.6. The transducer could replace the regula heel absorber and generate voltage. The voltage generated could be converted into usable power output to charge battery or powering electronic. He also mentioned that the shoe power generator can be used for powering sensors and locator devices such as Global Positioning System (GPS) which require a milliwatt power source (Ville, K., 2010).

Figure 2. 6. Shoe Power Generator (Ville, K., 2010)

Piezoelectric materials are also used in transportation industry. Piezoelectric has been applied in passenger cars, such as knock sensors, distance sensors and fuel injection systems. Distance sensors are used in vehicles as ultrasonic transducer. It is used when parking. When backing, transducer will emit ultrasonic waves. The waves will be reflected back when there is obstacle. The transducer will then received the reflected wave and convert it into electrical system. The distance is calculated from the travelling time of ultrasonic waves (Nuffer & Bein, October 2006).

Another application of piezoelectric is self-powered sensors for monitoring of highway bridges. Health monitoring of highway bridges is very important to avoid the loss of human life. Wireless sensor powered by batteries has used to develop health monitoring system for bridges. However, millions of batteries need to be replaced from time to time and high maintenance fees have caused the limitation of wireless sensor. Therefore, energy harvesting is the solution to solve this problem. In 2009, Edward and his team had proposed the testing of wireless sensor system which is powered by energy harvesting on State Route 11 bridge in Potsdam, NY, USA. The test showed the feasibility of energy harvesting for the application of Strucural Health Monitoring (SHM) (Sazonov, Li, Curry, & Pillay, 2009) . Energy harvesting also can be used in health monitoring of wear detection of train wheels (Wu & Thompson, 2010).

CHAPTER 3

MATERIALS AND METHODS

3.1 INTRODUCTION

In this chapter, the research methodology is explained. This research involves four stages which are the procedure of synthesis of ZnO sol gel, fabrication of ZnO thin film on Al foil as substrate using spin coating technique and heat treatment, characterization of ZnO thin film and energy harvesting test. Spin coating technique was used to fabricate ZnO thin film on Al substrate. ZnO thin film was characterized by using X-ray diffraction (XRD), Field Emission Scanning Electron Microscope (FESEM), Photoluminescence spectroscopy (PL), and Ultraviolet-Visible Spectroscopy (UV-Vis). The energy harvesting test was analysed using vibration as mechnanical force.

3.2 MATERIAL SYNTHESIS METHODS

Figure 3.1 shows the flow chart of research methodology.

3.2.1 Material and Apparatus

The material used in this research were zinc acetate dehydrate (ZnAc), absolute ethanol, ethanol, diethanolamine (DEA).

The apparatus used in this research were microscope glass slide, aluminum foil, diamond cutter, magnetic stirrer, hot plate, ultrasonic cleaner, spin coater, carbon tape, and schott bottle.

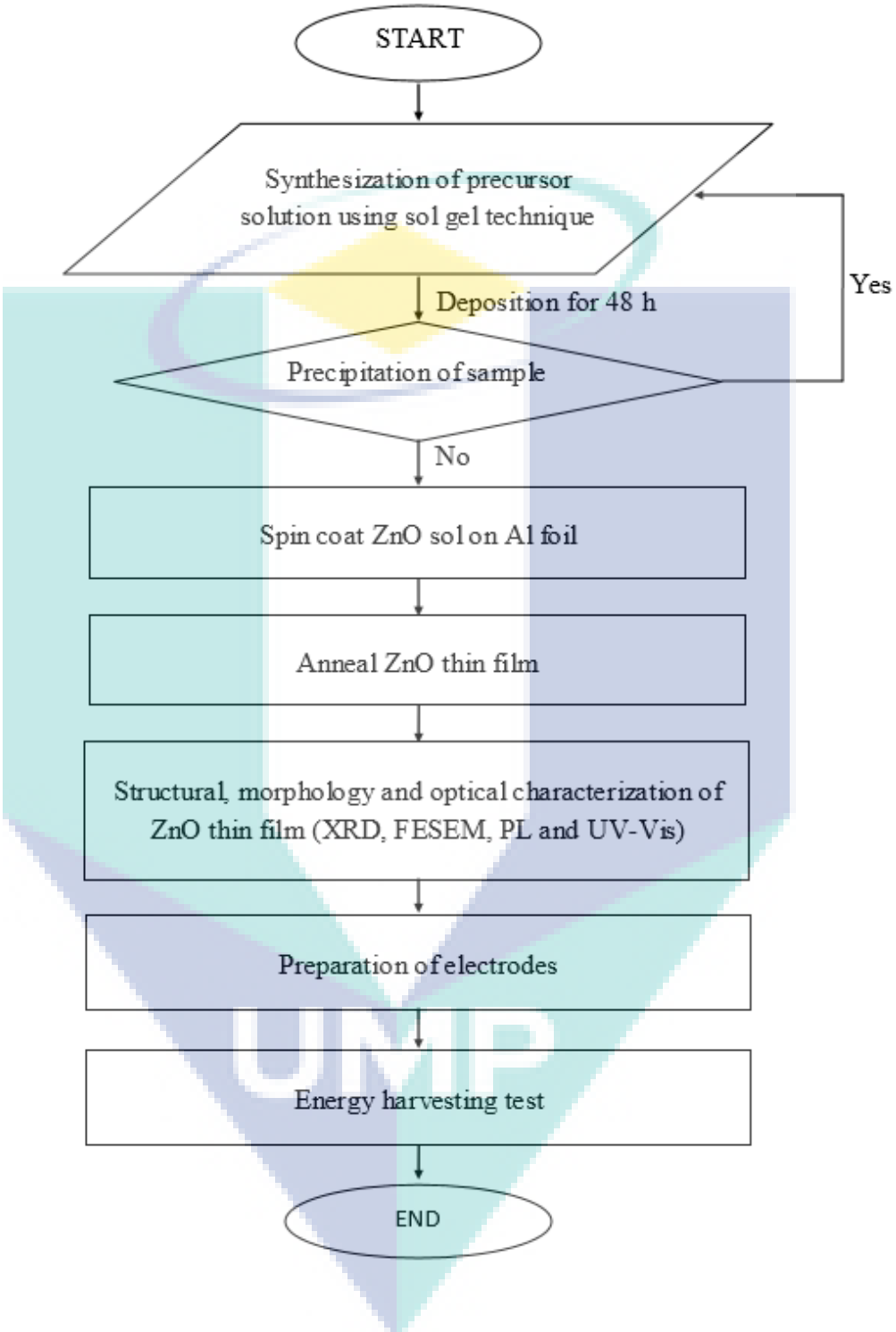

Figure 3. 1. Flow chart of methodology research

3.2.2 Preparation of Precursor Solution

Figure 3.3 presents the flow chart of preparation of sol gel by using zinc acetate dehydrate (ZnAc), absolute ethanol and diethanolamine (DEA).

ZnO sol gel was prepared by dissolving 0.2 mol of zinc acetate dehydrate ($Zn(CH_2CO_2)_2 \cdot 2H_2O$) (purity 99.95 %) in 70 ml of absolute ethanol. The mixture was stirred using magnetic stirrer for 45 min at 60 °C. The mixture was become milky as shown in figure 3.2. Then, diethanolamine (DEA) which acts as stabilizer was added drop by drop to the ZnO sol with interval of 1 min until the solution became clear. The molar ratio of DEA/zinc acetate as 1:1. The addition of DEA was used to affect the change of pH value from neutral to alkali. The alkaline nature of sol can help the growth of ZnO films. By adding the stabilizer, the sol was become transparent. After another 45 min of stirring, a homogeneous sol was obtained and transferred to a sealed bottle for deposition for 48 h.

At the mean time, microscope glass slides were cut with the dimension of 2.5 cm x 2.5 cm. Slides were then washed by ultrasonic cleaner and rinsed with ethanol. Aluminum foil is folded to cover the glass slide. Aluminum foil was also rinsed with ethanol.

Figure 3. 2. ZnAc dissolved in absolute ethanol

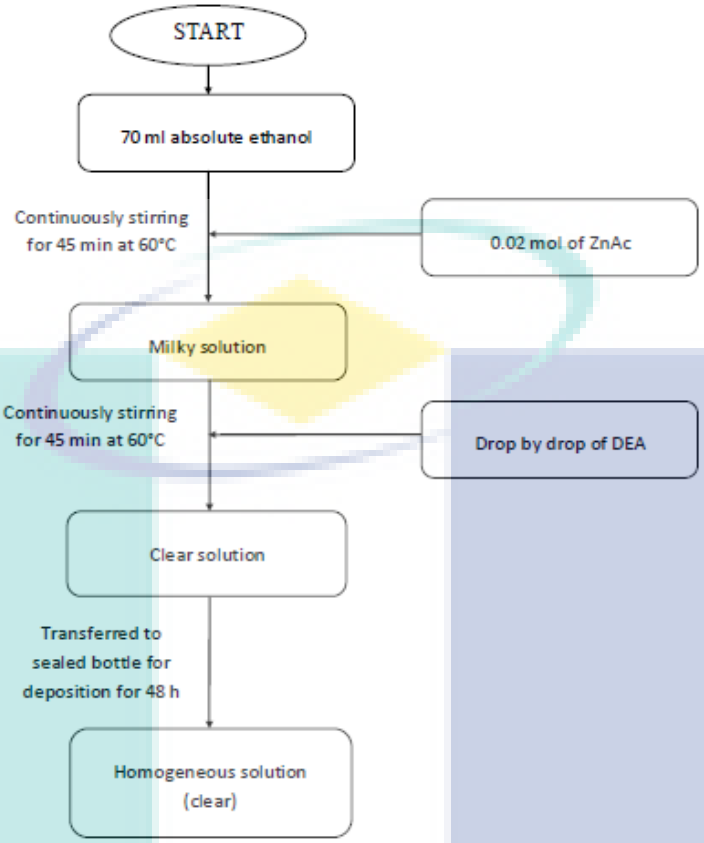

Figure 3. 3. Flow chart of preparation of precursor solution

3.3 FABRICATION OF ZNO THIN FILM

3.3.1 Spin speed

Laurell WS-650MZ-23 spin coater was used in this research. Figure 3.4 shows spin coating instrument. The ZnO thin film was fabricated on aluminum foil using spin coating technique. In this research, spin speed acted as one of the manipulated variables.

A spin coater with 1000-2000 rpm with spinning duration up to 30 s was used. The ZnO sol was spin-coated on the aluminum foil with different speeds (1000 rpm, 1500 rpm and 2000 rpm) for 30 s to fabricate different thickness of ZnO thin film. After deposition, the films were preheated at 60 °C for 30 s using a hot plate. The spinning process and preheating process were repeated for 5 times to get 5 layers. Finally, the samples were transferred to high temperature furnace

and annealed at 300 °C for 1 h to ensure the complete oxidation, eliminate the organic residue and promote the complete crystallization of ZnO thin films. Figure 3.5 showed the ZnO film formed with spin speed of 2000 rpm and annealing temperature of 300 °C.

Figure 3. 4. Spin coating instrument

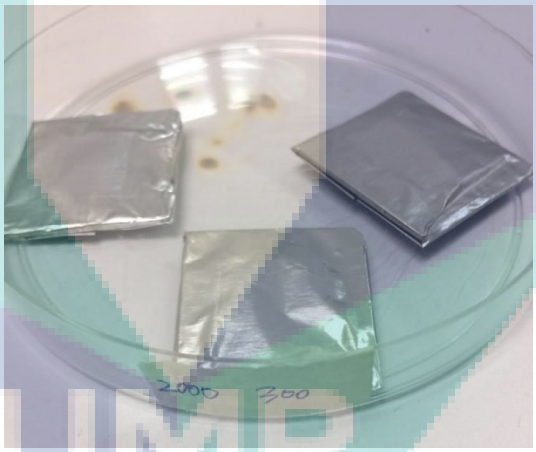

Figure 3. 5. ZnO film formed with spin speed of 2000 rpm and annealing temperature of 300 °C

3.3.2 Heat Treatment

ZnO sol was spin-coated on the aluminum foil at a speed of about 1500 rpm for 30 s. After deposition, the films were preheated at 60 °C for 30 s using a hot plate. The spinning process and preheating process were repeated for 5 times to get 5 layers. After that, the samples were annealed at different temperatures (300 °C, 400 °C and 500 °C) for 1 h using a high temperature vacuum furnace.

3.4 CHARACTERIZATION OF ZNO THIN FILM

The ZnO films were characterized by X-ray diffraction (XRD), Field Emission Scanning Electroscopy Microscope (FESEM), Photoluminescene spectroscopy (PL) and Ultraviolet- visible spectroscopy (UV-Vis) as showed in figure 3.5. The composition of ZnO thin films were observed under XRD technique. The morphology of films were investigated using FESEM with an acceleration of 15 kV and beam current of 20 mA. The optical properties of films were analysed using PL and UV-VIS spectroscopy.

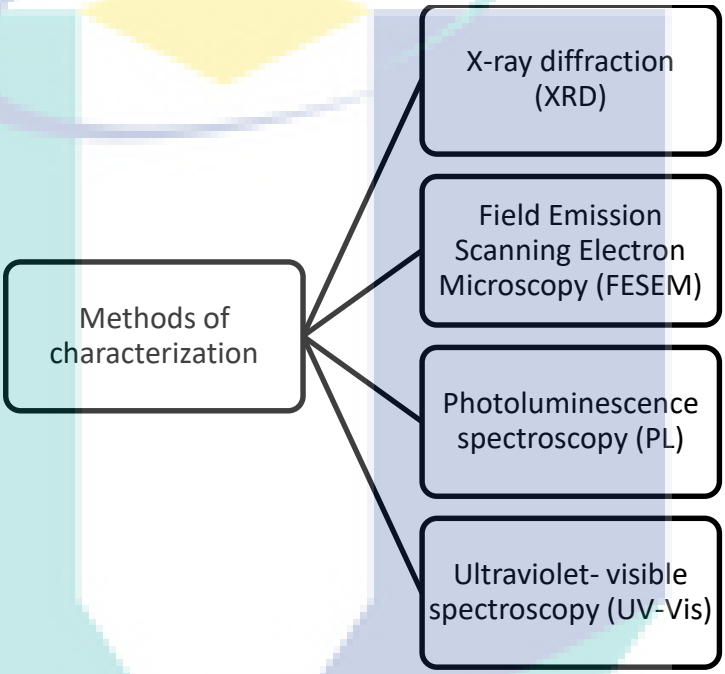

Figure 3. 6. List of methods used to characterize the ZnO films

3.4.1 X-ray Diffraction (XRD)

X ray diffraction is a non-destructive technique. The ZnO films were analyzed using X-ray diffraction (XRD) to examine the composition, crystalline size and phase exists. The instrument used was Miniflex II, Rigaku, Japan. The ZnO films were scanned in 2θ = 10-80 ^{o} at the rate of 0.1 ^{o}/min with Cu Kα (λ = 1.5406 Å) radiation. The films with 5 layers were too thin and could not be detected. Therefore, 35 layers of ZnO film was formed for XRD detection.

3.4.2 Field Emission Scanning Electron Microscopy (FESEM)

Zeiss EVO 50 Scanning Electron Microscope and Baltec-SCD 005 Sputter Coater were used to characterize surface morphology and thickness of ZnO films as shown in figure 3.7.

(a) (b)

Figure 3. 7. FESEM instrument (a) Zeiss EVO 50 SEM and (b) Baltec-SCD 005 Sputter Coater

The areas of ZnO films were cut using scissor. The ZnO films with aluminum foil were mounted on aluminum stub and attached using sticky carbon tape. A layer of platinum was coated on the top of sample holder using sputtering. The purpose of coating platinum as conductive layer was to avoid electron charging and image degradation. The surface morphology and grain size of ZnO films were analysed using FESEM. For each sample, few areas were detected randomly with different magnification.

For measuring the thickness of the film, ZnO sol was coated on glass which act as substrate. The ZnO films with glass substrates were cut with diamond cutter. Then, the glass substrates with films were mounted on aluminum stub with vertical position and attached using sticky carbon tape. A layer of platinum was coated on the top of sample holder using sputerring. The thickness of ZnO flms were analysed. For each sample, few areas were detected randomly with different magnification.

3.4.3 UV-VIS Spectroscopy

Shimadzu UV-1800 spectrophotometer and UVProbe 2.43 software were used to analyse the optical properties of ZnO film.

Two microscope glass slides were rinsed with ethanol. Then, they were placed in S compactment and R compartment respectively to set the baseline. The wavelength was set from 200 nm to 1400 nm. A chime sound was played and the glass slides in S compartment was taken out and replaced with glass slide that coated with ZnO film. The first peak was observed at long wavelength region. It was marked and the value of peak position was observed and used in calculation.

3.4.4 Photoluminescence Spectroscopy

FLS 920 Fluorescence Spectrometer and F900 software were used to analyse the photoluminescence property of ZnO film.

Glass slide coated with ZnO thin film was placed in sample compartment. A glass slide with 330 nm was placed in the spectrometer to act as filter. The value of estimated excitation wavelength was filled and the EML wavelength was filled as 400 nm. The range of emission scan was filled from 320 nm to 640nm. A bell-shaped graph was observed and the peak of the photoluminescence was marked. The energy loss was calculated.

3.5 PIEZOELECTRIC TEST

Piezoelectric test was carried out to measure the voltage that can be produced by the piezoelectric material, ZnO. Bransonic CPX 5800 H Ultrasonic bath and multimeter were used to measure the voltage.

Carbon tape which acted as a conductive electrode was connected with ZnO film. Copper wire was connected with two different electrodes, which are aluminum foil and carbon tape and multimeter to complete the circuit. Figure 3.8 showed the connection of copper wire with two electrodes. The sample was placed on the surface of the water. The schematic diagram for piezoelectric testing was showed in figure 3.9. Ultrasonic cleaner was then switched on. 40 kHz of

frequency was applied to the water within three minutes. The readings for maximum voltage and minimum voltage are video recorded.

Figure 3. 8. Connection of copper wire with two electrodes

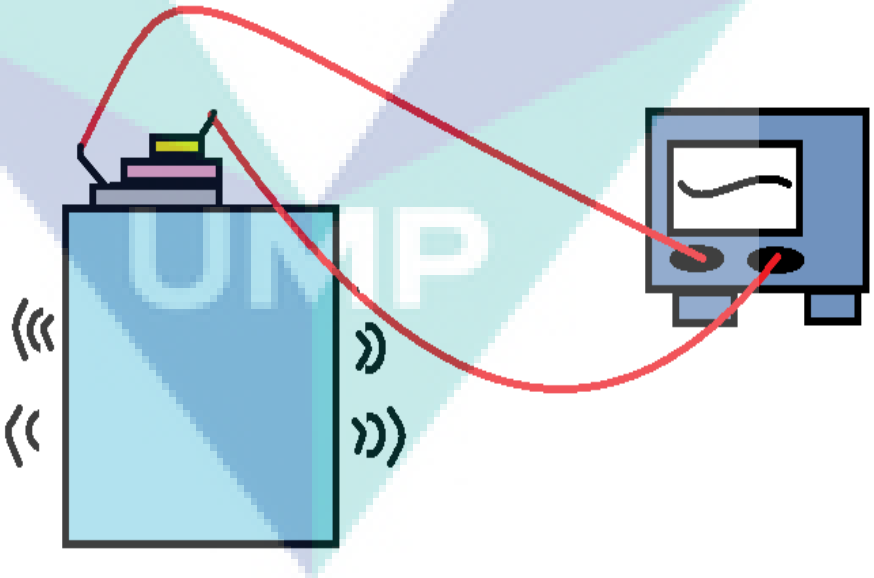

Figure 3. 9. Schematic diagram of piezoelectric testing

CHAPTER 4

RESULTS AND DISCUSSION

4.1 INTRODUCTION

This chapter consists of the results of the characterization of sample and piezoelectric test. A brief summary of the results was discussed in the next paragraph.

The XRD results showed the diffraction phase of each film. All the films showed preferentially oriented at ~65° which corresponding to (1 1 2) diffraction phase. From FESEM results, surface morphology of ZnO films showed all the films were successfully formed as nano size grains. However, there were some agglomeration and cracks could be found on the surface. ZnO films were not homogeneous completely. From the result of UV-Vis, ZnO films were excited at 340-363 nm. They were excited at ultraviolet region. The band gap of all the films were around 3.4-3.6 eV which are higher than theoretical band gap value (3.37 eV). The annealing temperature was increased, the energy band gap was decreased. From results of photoluminescence, ZnO thin film were emitted electron at 385 nm. Ultrasonic vibration test was used to determine the voltage that can be produced by ZnO films. The sample that could produce the highest voltage was ZnO film with spin speed of 2000 rpm and annealing temperature of 300 °C with maximum voltage of 27.3 mV and minimum voltage of 0.4 mV. The sample that could produce the least voltage was ZnO film with spin speed of 1500 rpm and annealing temperature of 400 °C with average voltage of 1.368 mV.

4.2 SYNTHESIS AND CHARACTERIZATION OF ZNO THIN FILM

4.1.1 X-Ray Diffraction Analysis

The crystalline size, phase orientation and lattice parameter of ZnO film were calculated from XRD result. From XRD result, the crystalline size of a crystal is calculated using Scherrer's formula which is shown in equation 4.1.

$$T = \frac{0.9\,\lambda}{\beta \cos\theta} \qquad 4.1$$

where d is the crystallite size in nano meter , λ is wavelength of x-ray (1.5406 Å), β is full width at half maximum of the peak (FWHM) in radian and θ is the Bragg's angle.

The Bragg's law was used in this research to calculate the crystal structure, therefore d-spacing of the crystal can be found.

$$n\lambda = 2d\,sin\,\theta \qquad 4.2$$

where λ is the wavelength, n is number of order, d is lattice spacing, and θ is the diffraction angle.

The lattice parameter of hexagonal crystal structure can be calculated from the equation 4.3.

$$\frac{1}{d^2} = \left(\frac{4}{3}\right)\frac{h^2+kh+k^2}{a^2} + \frac{l^2}{c^2} \qquad 4.3$$

where value of d is the lattice spacing which obtained from equation 4.2, h, k and l are the Miller indices of each peak, a and c are the lattice parameters.

The films were grown by sol-gel technique on Al foil as substrate with different rotation speed and annealing temperature. All films that formed were polycrystalline. In figure 4.1, the films grown with rotation speed of 1000 rpm and annealed at 300 °C presented two peaks at 43.99° and 64.447° which

corresponding to the (1 0 1) and (1 1 2) diffraction planes of hexagonal ZnO. The d-spacing of the crystal was 1.44570 Å whereas the lattice parameter calculated was a= 0.3474 nm and c= 0.5214 nm.

In figure 4.2, the films grown with rotation speed of 1500 rpm and annealed at 300 °C presented two peaks at 65.1421° and 74.04°. These peaks correspond to the (1 1 2) and (0 0 4) diffraction phases of ZnO wurtzite structure. The d spacing of the crystal was 1.4308 Å and the lattice parameter was calculated as a= 0.345 nm and c= 0.5116 nm.

In the pattern of film with rotation speed of 2000 rpm and annealed at 300 °C as shown in figure 4.3, three peaks could be clearly seen at 34.37°, 65.083° and 78.394°, these peaks were corresponding to (0 0 2), (1 1 2) and (1 0 4) diffraction planes of ZnO wurtzite structure respectively. The d-spacing used was 1.43199 Å and the lattice parameter for ZnO film was calculated as a=0.3427 nm and c= 0.5214 with plane (1 1 2).

The diffraction phase of (0 0 2) could be also found at the film with rotation speed of 1500 rpm and annealed at 400°C and 500°C at 34.47° and 33.61° respectively. The (0 0 4) of diffraction phase also could be found at the peak of 74.1° of film with annealed at 400 °C as shown in figure 4.4. The d-spacing used for film with annealed at 400 °C was 1.43303 Å and lattice parameter was a= 0.3435 nm and c= 0.52 nm.

Figure 4.5 showed film with annealed at 500 °C could also find diffraction phase of (1 1 2) and (2 0 2) at the peaks of 64.882° and 75.5°. The d-spacing of this film was 1.43594 Å and lattice parameter was a= 0.341 nm and c= 0.5328 nm.

From figure 4.1 to 4.5, the highest peak was around 45°. The peak was corresponding to aluminum plane as shown in appendice 1. For the plane of ZnO, it could be found that all the films were preferentially oriented in the (1 1 2) direction at ~ 65°. The typical phase (0 0 2) was only found at some films. The presence of (0 0 2) diffraction phase was due to the precursor solution used was ZnAc which promotes the growth of crystal in (0 0 2) direction (Sagar, Kumar,

Mehra, Okada, Wakahara, & Yoshida, 2007). Figure 4.6 showed the combination of XRD spectrum of ZnO films. When the annealing temperature was increased, the intensity peak was decreased. This was due to the large thermal expansion coefficient between ZnO film and substrate.

Figure 4.7 showed the ZnO film with rotation speed of 1500 rpm and annealing temperature of 180 °C. The ZnO film formed by dissolving 0.5 mol of ZnAc into 20ml of absolute ethanol. The mixture was stirred until the solvent evaporated and white powder formed. Then, DEA was added in and a clear gel was formed. The peaks of XRD spectrum were at 33.06 ° and 64.669 ° which corresponding to (1 1 1) and (1 1 2) diffraction plane.

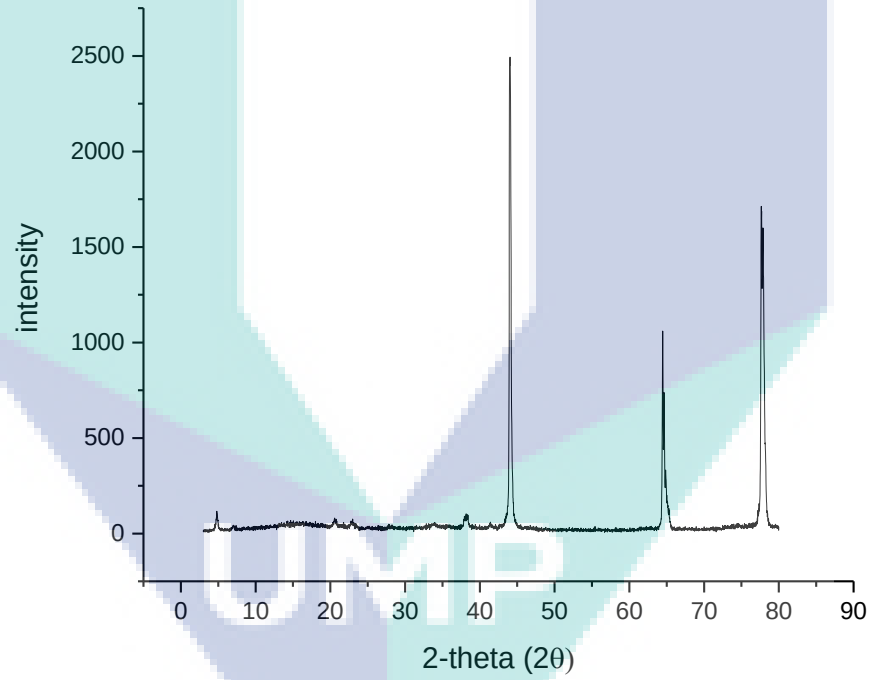

Figure 4. 1. XRD pattern of ZnO thin film with spin speed of 1000 rpm and annealing temperature 300 °C

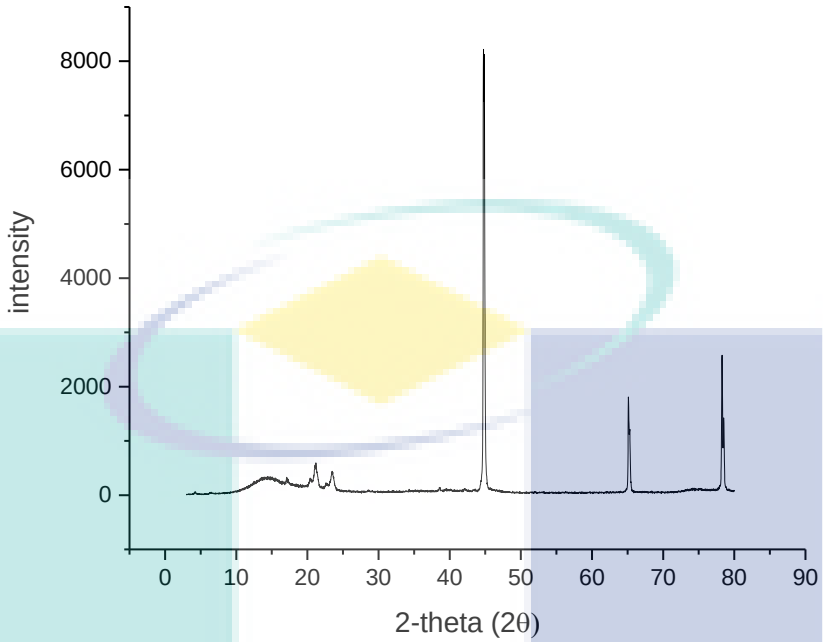

Figure 4. 2. XRD pattern of ZnO thin film with spin speed of 1500 rpm and annealing temperature 300 °C

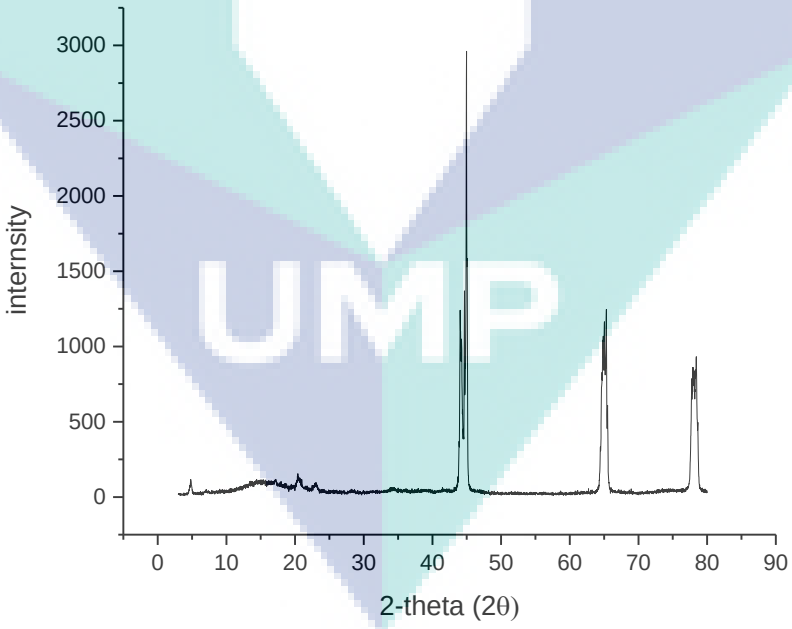

Figure 4. 3. XRD pattern of ZnO thin film with spin speed of 2000 rpm and annealing temperature 300 °C

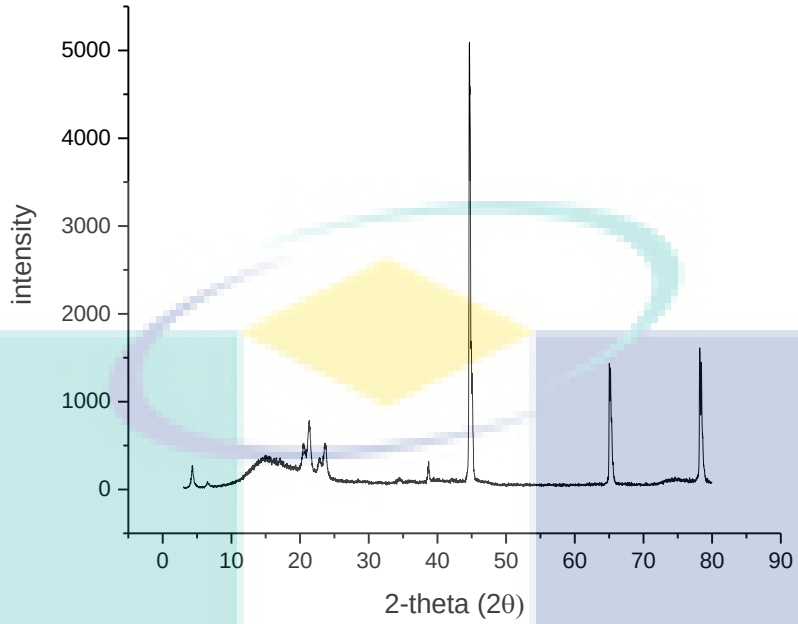

Figure 4. 4. XRD pattern of ZnO thin film with spin speed of 1500 rpm and annealing temperature 400 °C

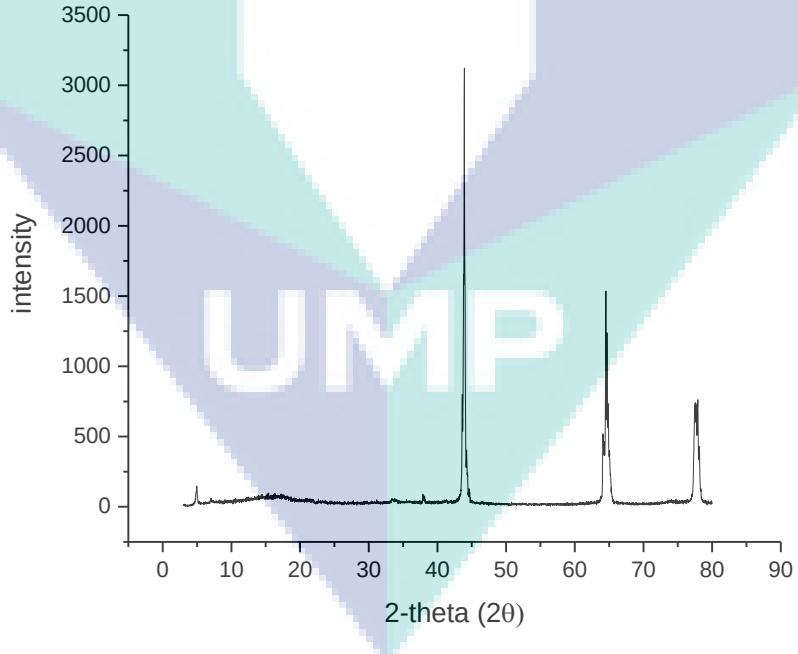

Figure 4. 5. XRD pattern of ZnO thin film with spin speed of 1500 rpm and annealing temperature 500 °C

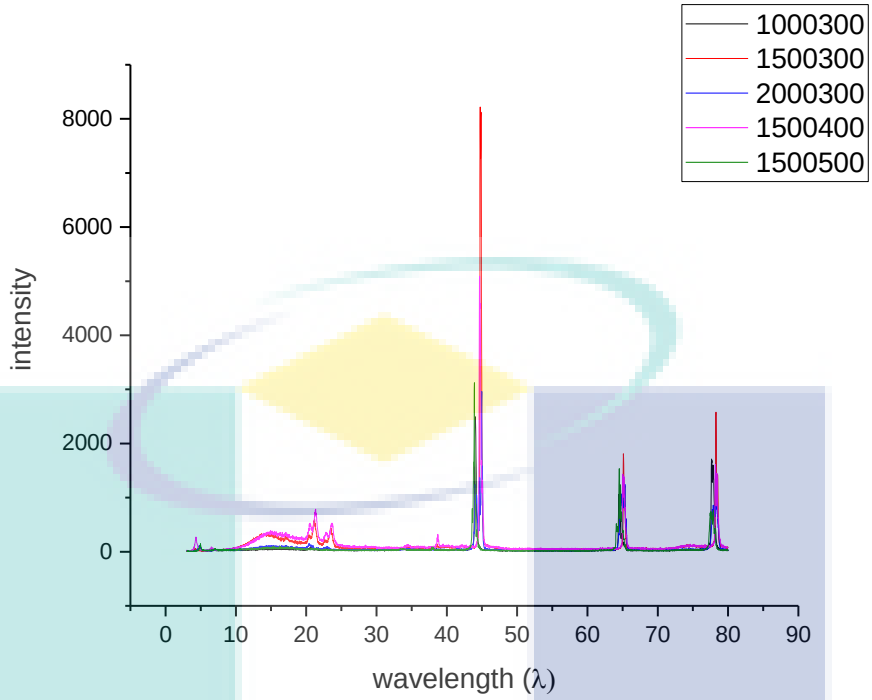

Figure 4. 6. XRD spectrum of each film

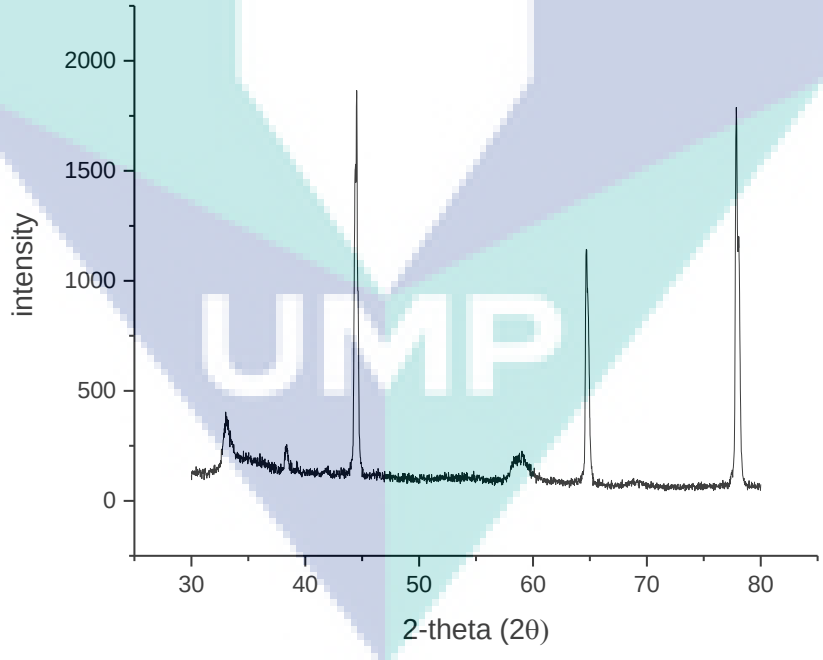

Figure 4. 7. XRD spectrum of ZnO film with rotation speed of 1500 rpm and annealing temperature of 180 °C

Table 4. 1. (h k l) plane, d-spacing ad crystalline size for the ZnO thin films with different spin speed and annealing temperature

Sample	Spin Speed (rpm)	Anneal Temperature (°C)	2θ	(h k l)	d-spacing	FWHM	Average Crystalline Size, nm
A	1000	300	43.9918	(1 0 1)	2.0566	0.181	0.7350
			64.4470	(1 1 2)	1.44570	0.174	
B	1500	300	65.1421	(1 1 2)	1.43083	0.151	1.0324
			74.0400	(0 0 4)	1.27900	2.260	
C	2000	300	34.3700	(0 0 2)	2.60700	1.100	0.5945
			65.0830	(1 1 2)	1.43199	0.260	
			78.3940	(1 0 4)	1.21882	0.256	
D	1500	400	34.4700	(0 0 2)	2.60000	0.560	0.6215
			65.0300	(1 1 2)	1.43303	0.142	
			74.1000	(0 0 4)	1.27800	2.500	
E	1500	500	33.6100	(0 0 2)	2.66400	0.900	0.6786
			64.8820	(1 1 2)	1.43594	0.143	
			75.5000	(2 0 2)	1.25900	4.000	

4.1.2 Morphology Analysis

The morphology of ZnO films were characterized under FESEM. The morphology of ZnO films could not be studied under SEM due to limitation of magnification of SEM spectroscopy. Figure 4. 8. **Surface morphology of ZnO thin with rotation speed of 1000 rpm and annealed at 300 °C with different magnification (a) 5 kx, (b) 50 kx, (c) 150 kx (d) 150 kx with measuring**Figure 4.8 to figure 4.12 showed the surface morphology of films with different magnification. Table 4. 2 showed the nanoparticle size with different condition and annealing temperature. The grain size was increased when the annealing temperature was increased. This is because the fusion of grains was happened due to increment of energy (Quinones-Galvan, et al., 2013).

By using FESEM, cross section of ZnO film was also been analysed. ZnO film was coated on glass substrate to examine the thickness. ZnO film that was coated on Al substrate could not be examined as when cutting, ZnO film was bent and overlap with Al foil. Therefore, by using Al foil as substrate, ZnO layer and Al layer could not be differentiated. Figure 4.13 showed the failure of examining cross section of ZnO film on Al substrate. The method used in figure 4.13 was backscattered mode. Figure 4.14 to figure 4.18 showed the cross section of ZnO film on glass substrate with different magnification at several parts of sample.

It was observed that the thickness was decreased due to increasing of rotation speed. Comparing between figure 4.9, figure 4.11 and figure 4.12, the thickness was increased when annealing temperature was increased. It was due to the grain size was increased when annealing temperature was increased. Therefore, the thickness was increased. Table 4.3 showed the average thickness of ZnO film with different spin speed and annealing temperature.

Figure 4.19 showed the surface morphology of ZnO film with rotation speed of 1500 rpm and annealing temperature of 180 °C. It could clearly observed that the nanoparticle did not form in this film. This was because the film did not have enough energy to form nanoparticle.

Table 4. 2. Nanoparticle size of ZnO films with different rotation speed and annealing temperature

Sample	Rotation speed (rpm)	Annealing temperature (°C)	Grain size (nm)
A	1000	300	19.00
B	1500	300	17.98
C	2000	300	20.38
D	1500	400	20.63
E	1500	500	25.15

Figure 4.8 showed the surface morphology of ZnO film with rotation speed of 1000 rpm and annealed at 300 °C with different magnification at several regions of the sample. The surface of ZnO film did not form uniformly. Some parts of sample had agglomerated. Figure 4.8 (b), (c) and (d) were taken at the part of uniform surface. It could be seen that the grains formed were as small as nano size. The grain size was around 15 – 20.6 nm.

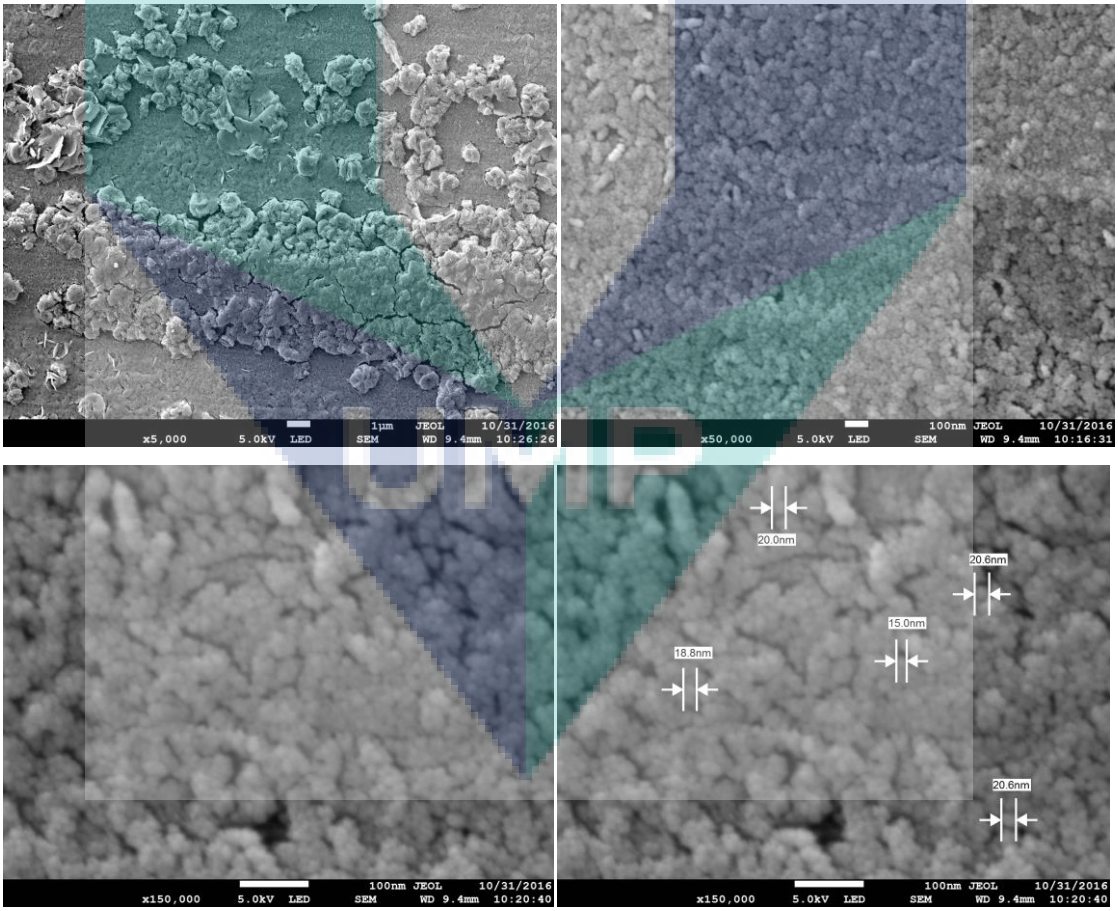

Figure 4. 8. Surface morphology of ZnO thin with rotation speed of 1000 rpm and annealed at 300 °C with different magnification (a) 5 kx, (b) 50 kx, (c) 150 kx (d) 150 kx with measuring

Figure 4.9 showed the surface morphology of ZnO thin with rotation speed of 1500 rpm and annealed at 300 °C with different magnification at several regions of the sample. It could be seen that the film was uniformly formed but with cracking. Figure 4.9 (b), (c) and (d) were taken at the part of uniform surface without cracking. The grain size of ZnO was around 16.9 – 20 nm.

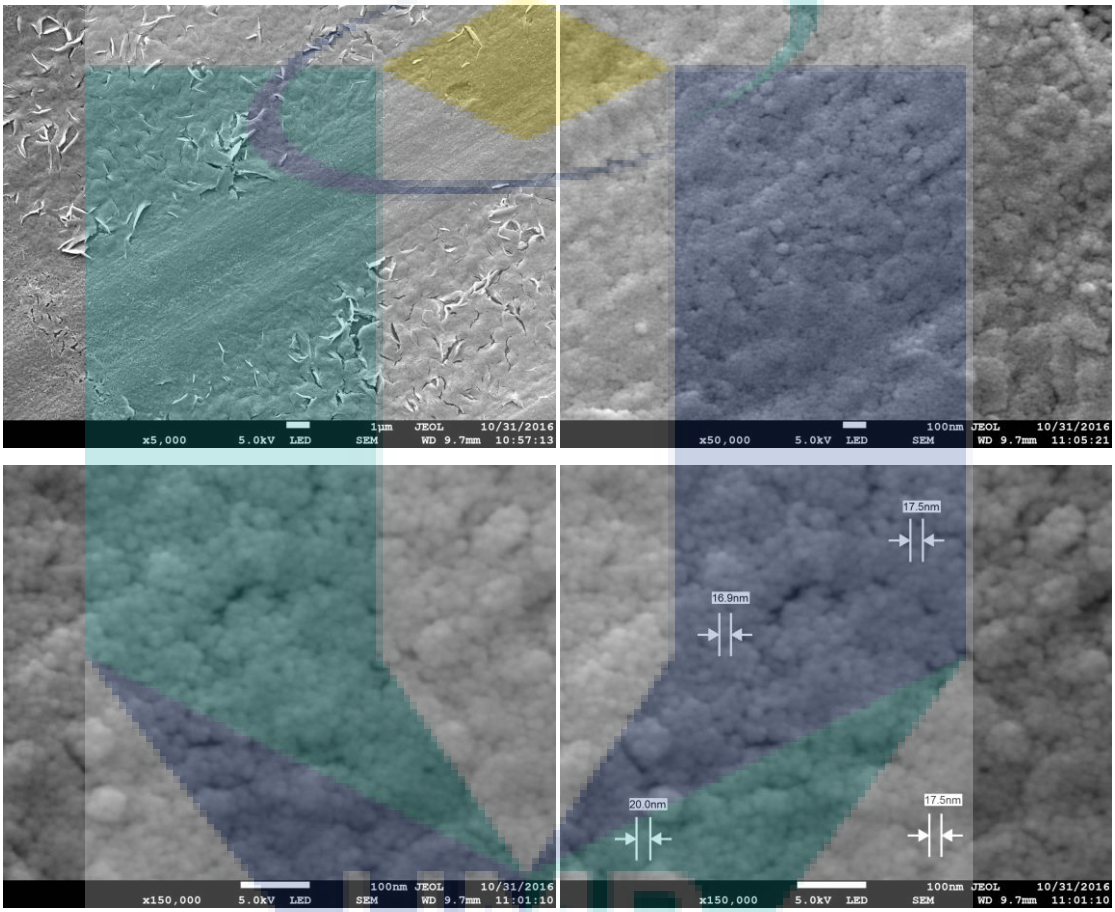

Figure 4. 9. Surface morphology of ZnO thin with rotation speed of 1500 rpm and annealed at 300 °C with different magnification (a) 5 kx, (b) 50 kx, (c) 150 kx (d) 150 kx with measuring

Figure 4.10 showed the the surface morphology of ZnO thin with rotation speed of 2000 rpm and annealed at 300 °C with different magnification at several regions of the sample. It could be seen that the film was uniformly formed but with porosity. Figure 4.10 (b), (c) and (d) were taken at the part of uniform surface without porosity. The grain size of ZnO was around 18.8 – 21.9 nm.

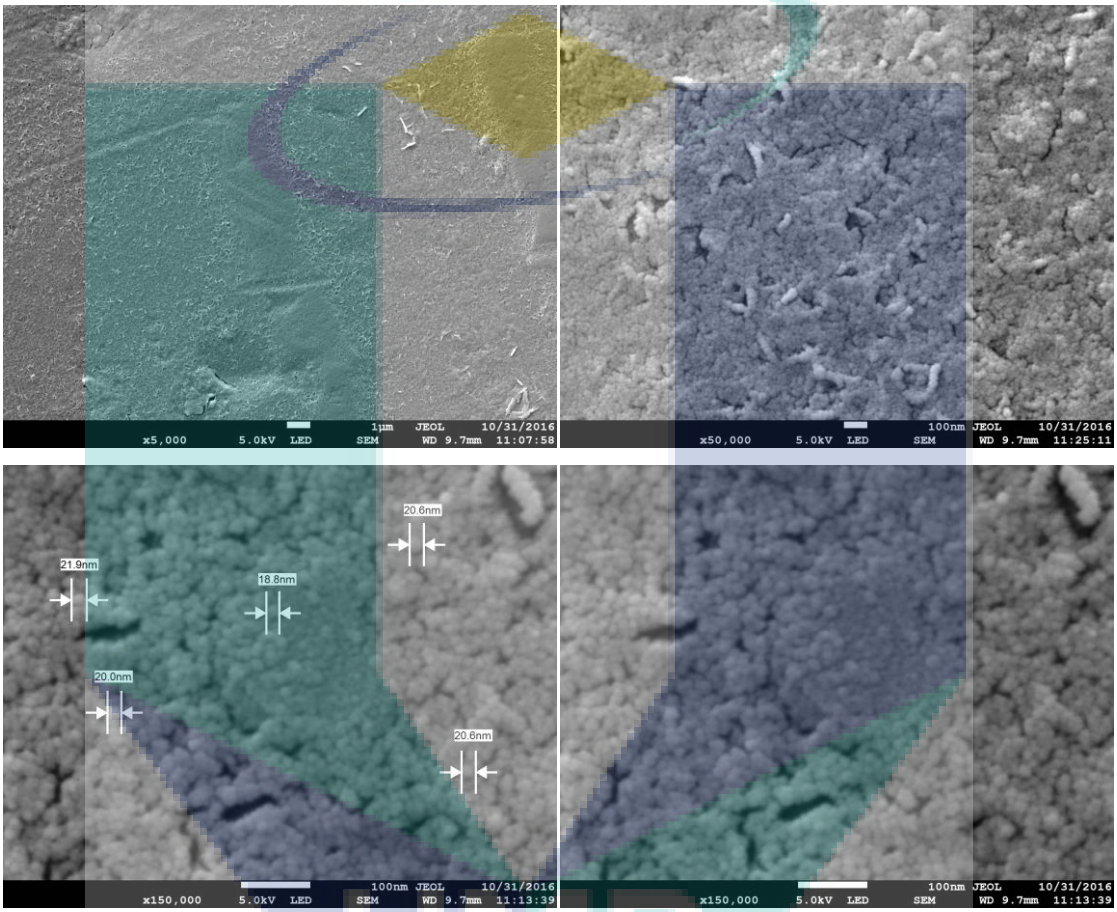

Figure 4. 10. Surface morphology of ZnO thin with rotation speed of 2000 rpm and annealed at 300 °C with different magnification (a) 5 kx, (b) 50 kx, (c) 150 kx (d) 150 kx with measuring

Figure 4.11 showed the surface morphology of ZnO thin with rotation speed of 1500 rpm and annealed at 400 °C with different magnification at several regions of the sample. It could be seen that the film was uniformly formed but with cracking. Figure 4.11 (b), (c) and (d) were taken at the part of uniform surface without any defect. The grain size of ZnO was around 20 – 21.9 nm. When comparing with figure 4.9, the grain size of ZnO was increased due to annealing temperature was increased.

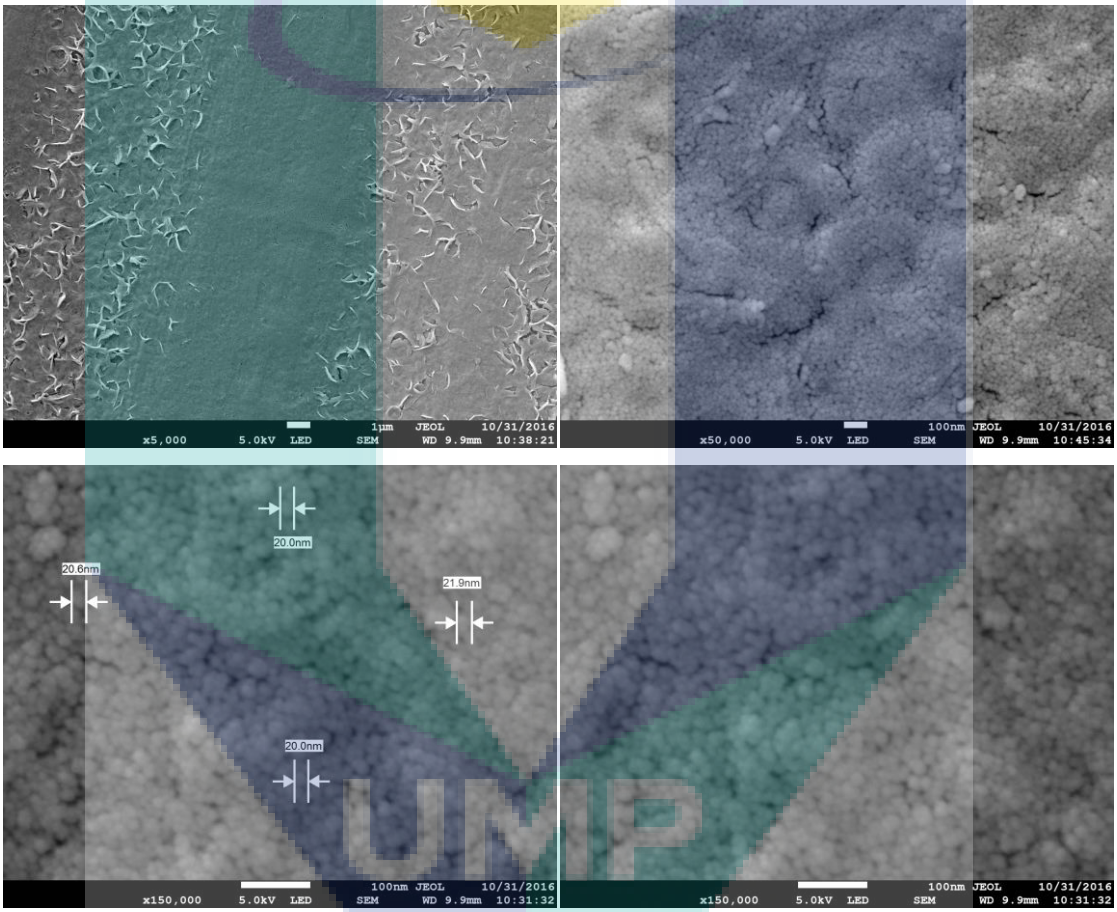

Figure 4. 11. Surface morphology of ZnO thin with rotation speed of 1500 rpm and annealed at 400 °C with different magnification (a) 5 kx, (b) 50 kx, (c) 150 kx (d) 150 kx with measuring

Figure 4.12 showed the surface morphology of ZnO thin with rotation speed of 1500 rpm and annealed at 500 °C with different magnification at several regions of the sample. It could be seen that the film was uniformly formed but with cracking and porosity. Figure 4.12 (b), (c) and (d) were taken at the part of uniform surface without any defect. The grain size of ZnO was around 23.7-26.9 nm. When comparing with figure 4.9 and figure 4.11, the grain size of ZnO was increased due to annealing temperature was increased.

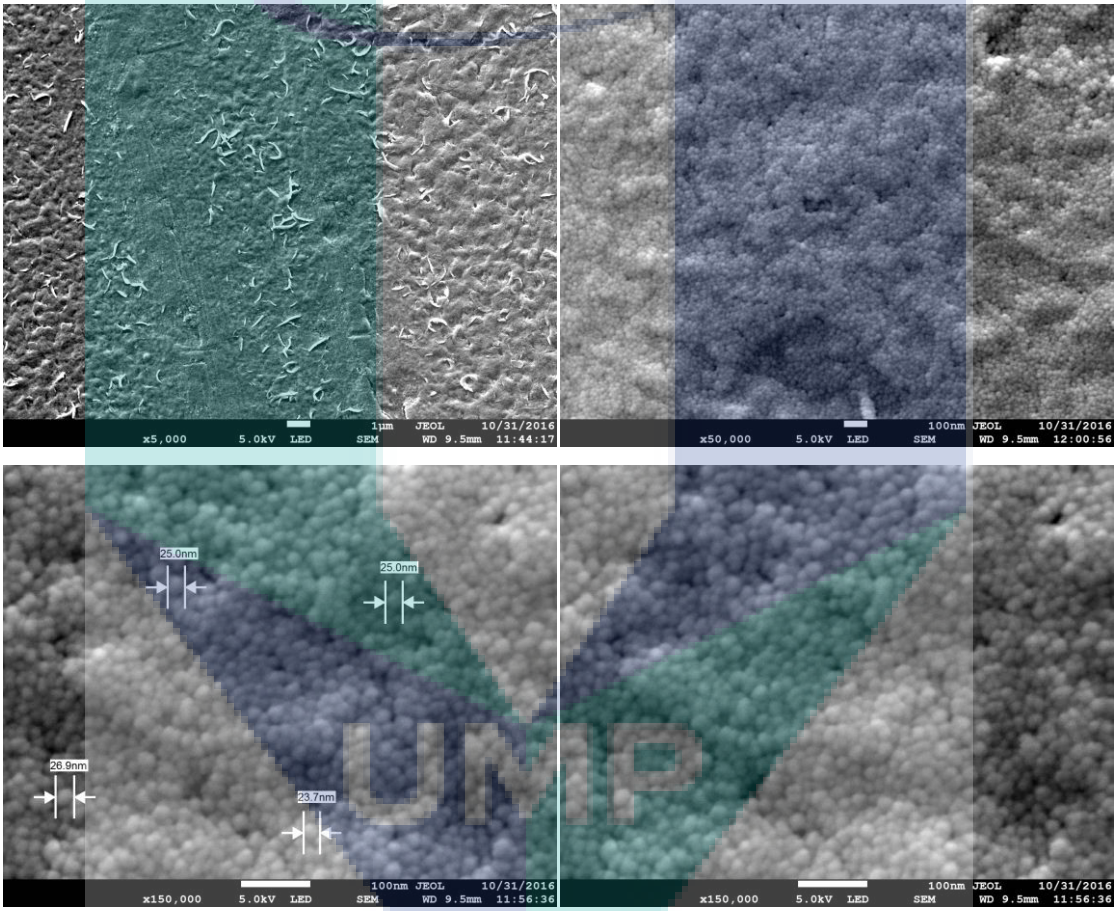

Figure 4. 12. Surface morphology of ZnO thin with rotation speed of 1500 rpm and annealed at 500 °C with different magnification (a) 5 kx, (b) 50 kx, (c) 150 kx (d) 150 kx with measuring

Figure 4.13 showed the cross section of ZnO film on Al substrate with rotation speed of 1000 rpm and annealed at 300 °C. Figure 4.13 (a) was used the backscattered mode. The purpose was to detect the changes in chemical contrast. Therefore, ZnO film and Al substrate can be differentiated. In theoretically, ZnO would have denser color than Al foil as the molecular weight and atomic number was higher than Al. However, from figure 4.12 (a), there was no difference in color. Therefore, the cross section of ZnO film on Al substrate could not be determined. The method had changed to ZnO coated on glass substrate. This was due to glass substrate is brittle. ZnO film would not bend or overlap onto glass substrate. Diamond cutter was used to cut glass substrate in order to get thickness.

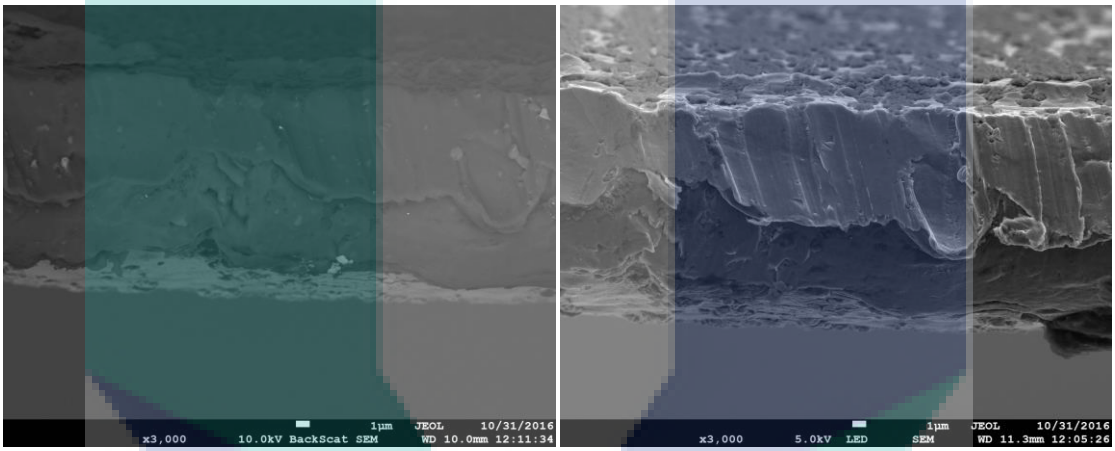

Figure 4. 13. Cross section of ZnO film on Al substrate with rotation speed of 1000 rpm and annealed at 300 °C

Figure 4.14 showed the cross section of ZnO film with rotation speed of 1000 rpm and annealed at 300 °C with different magnification at several parts of sample. From the cross section, it could be found that some parts of ZnO film was not uniformly formed. From figure 4.14 (d), it could be seen that there were some ZnO particle overlapped with glass substrate. This might due to the inproper cutting process. The thickness of ZnO film was 373 nm.

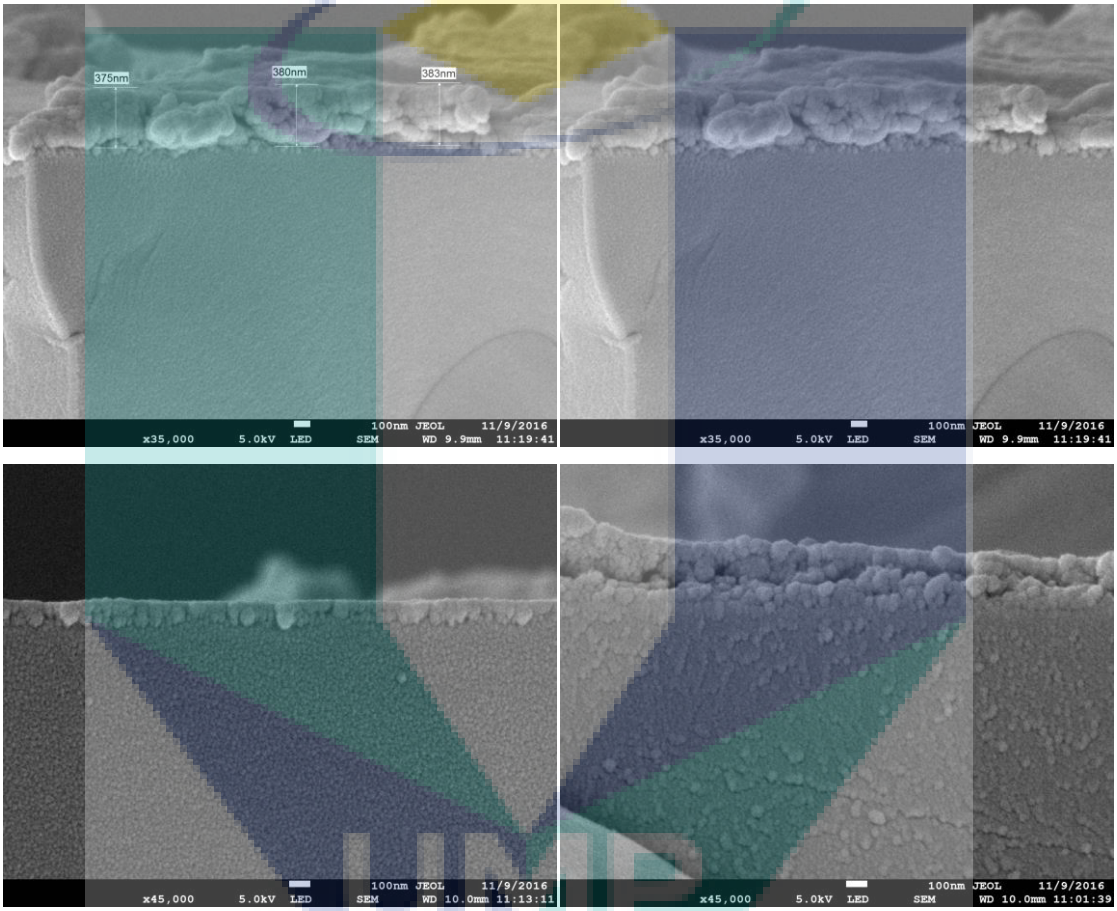

Figure 4. 14. Cross section of ZnO film with rotation speed of 1000 rpm and annealed at 300 °C with different magnification at several parts of sample

Figure 4.15 showed cross section of ZnO film with rotation speed of 1500 rpm and annealed at 300 °C with different magnification at several parts of sample. From the cross section, it could be found that ZnO film was uniformly formed. The thickness of ZnO film was 166.25 nm.

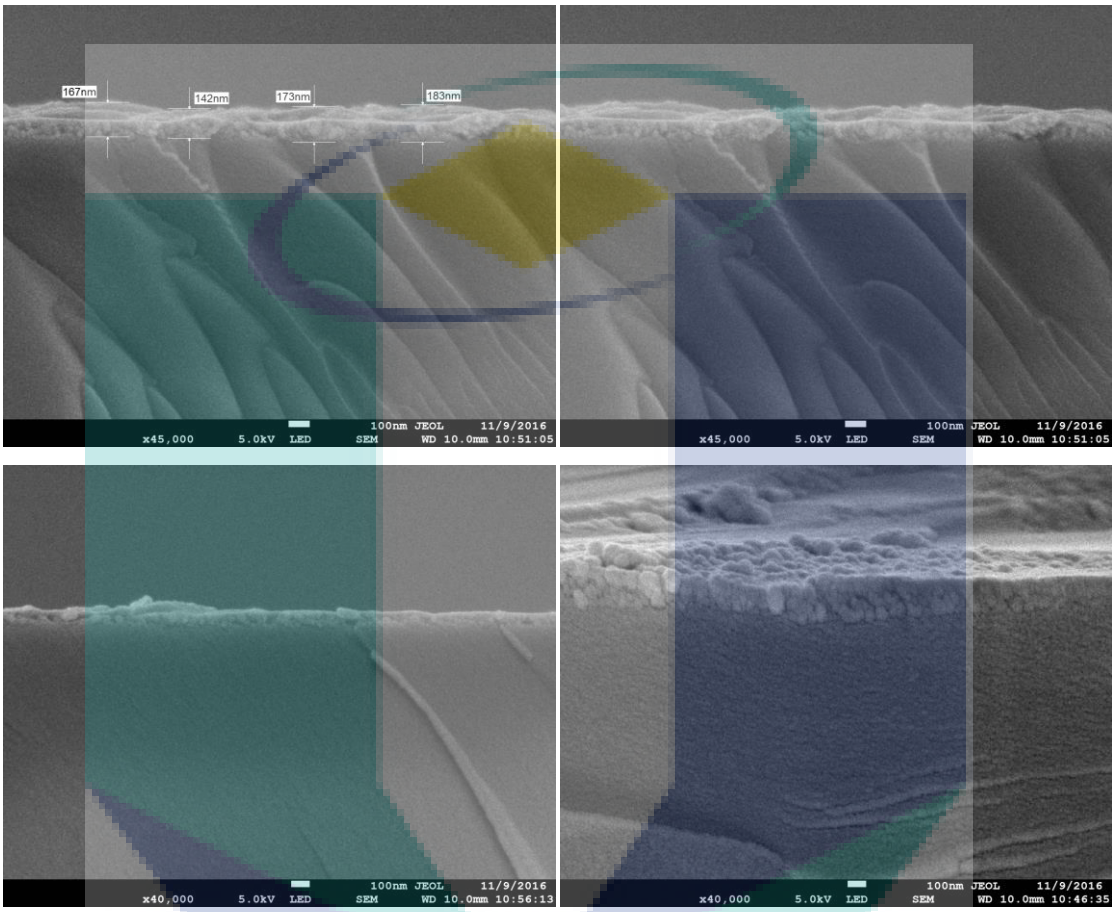

Figure 4. 15. Cross section of ZnO film with rotation speed of 1500 rpm and annealed at 300 °C with different magnification at several parts of sample

Figure 4.16 showed the cross section of ZnO film with rotation speed of 2000 rpm and annealed at 300 °C with different magnification at several parts of sample. From the cross section, it could be found that ZnO film was uniformly formed. The thickness of ZnO film was 113.25 nm.

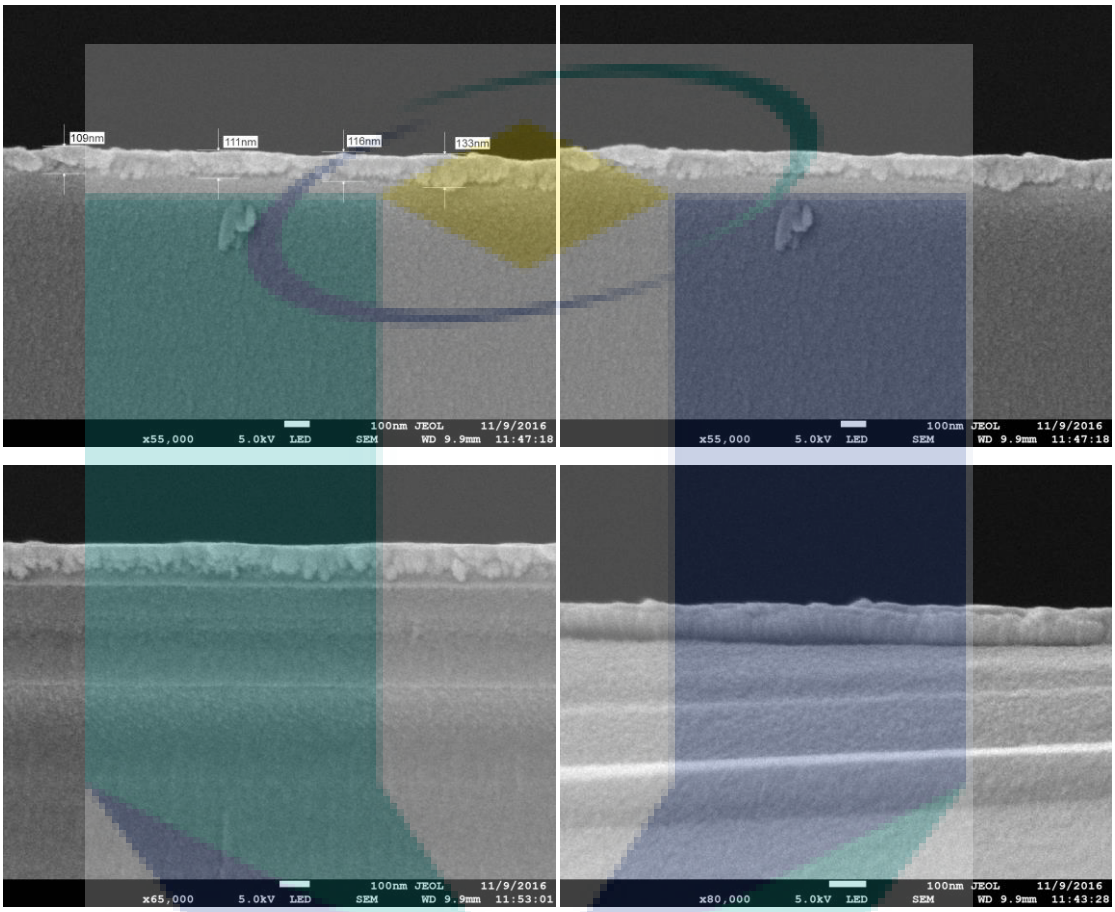

Figure 4. 16. Cross section of ZnO film with rotation speed of 2000 rpm and annealed at 300 °C with different magnification at several parts of sample

Figure 4.17 showed the cross section of ZnO film with rotation speed of 1500 rpm and annealed at 400 °C with different magnification at several parts of sample. From the cross section, it could be found that some parts of ZnO film was not uniformly formed. The thickness of ZnO film was 187.5 nm.

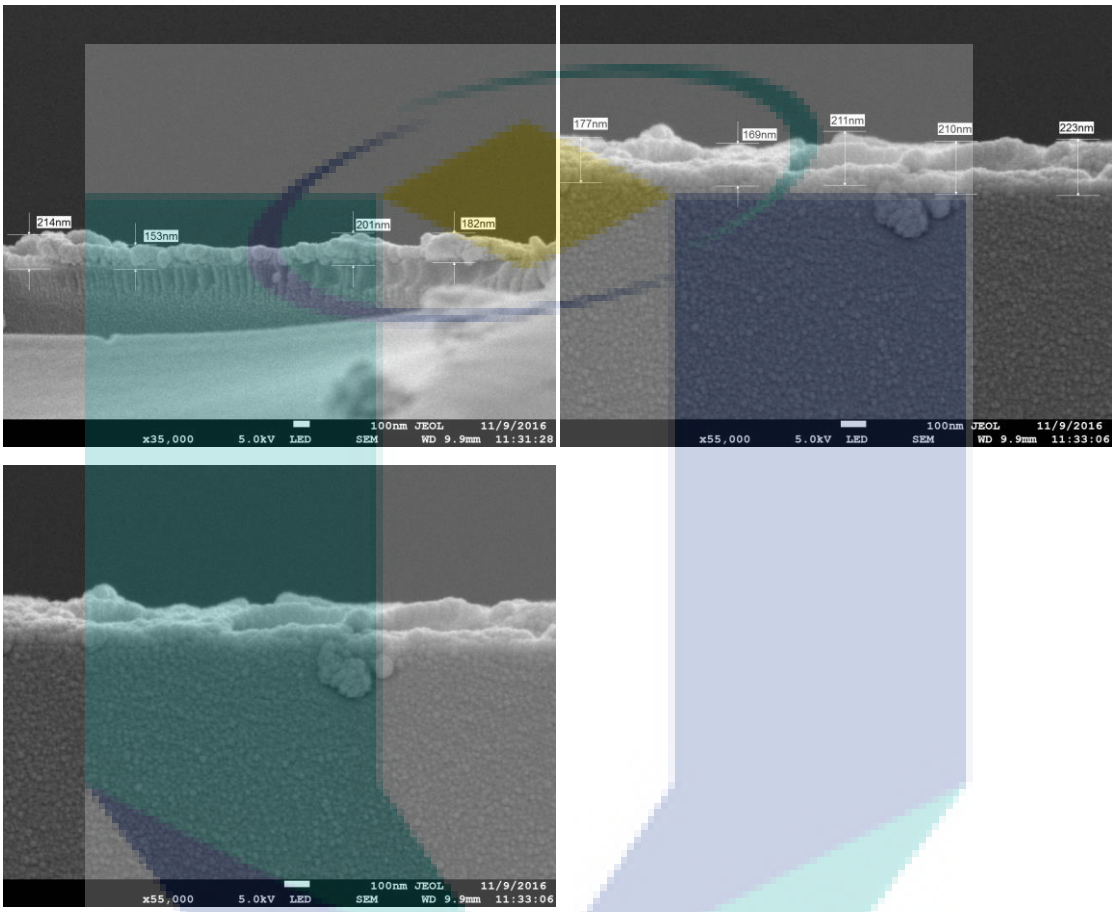

Figure 4. 17. Cross section of ZnO film with rotation speed of 1500 rpm and annealed at 400 °C with different magnification at several parts of sample

Figure 4.18 showed the cross section of ZnO film with rotation speed of 1500 rpm and annealed at 500 °C with different magnification at several parts of sample. From the cross section, it could be found that some parts of ZnO film was uniformly formed. The thickness of ZnO film was 205.25 nm.

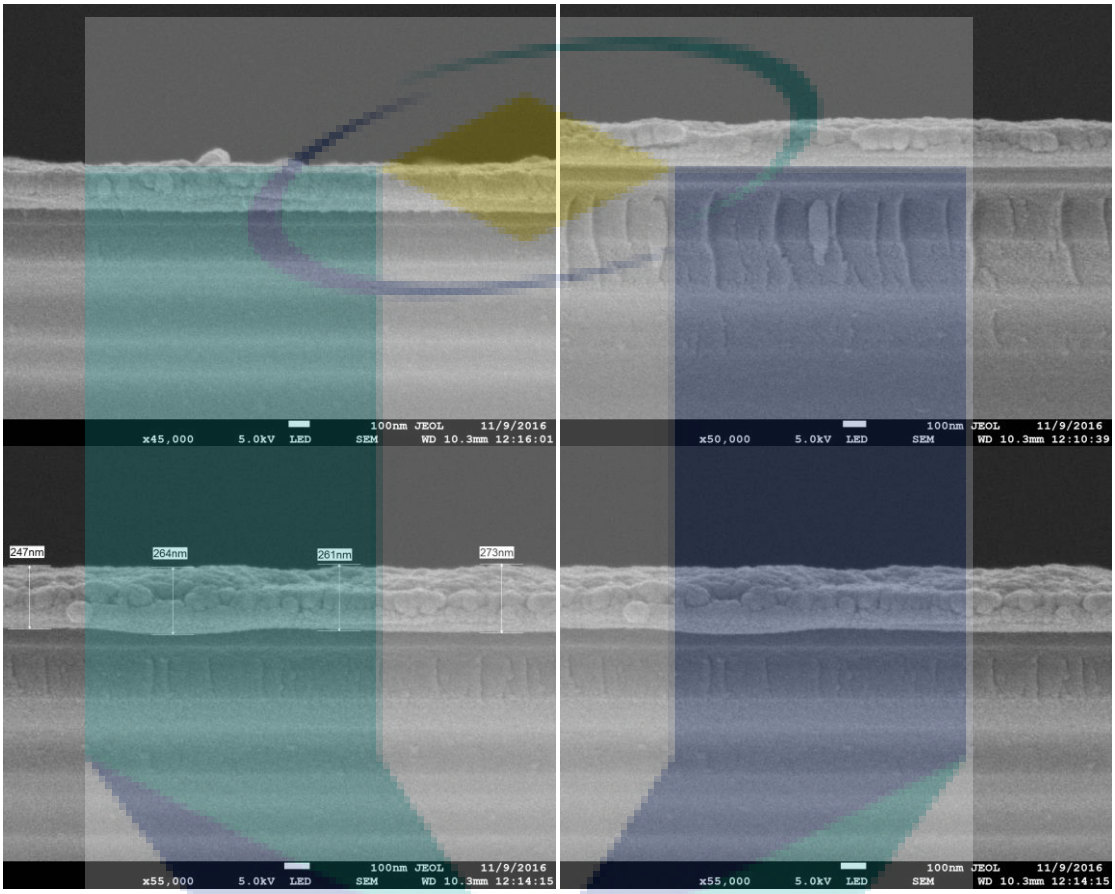

Figure 4. 18. Cross section of ZnO film with rotation speed of 1500 rpm and annealed at 500 °C with different magnification at several parts of sample

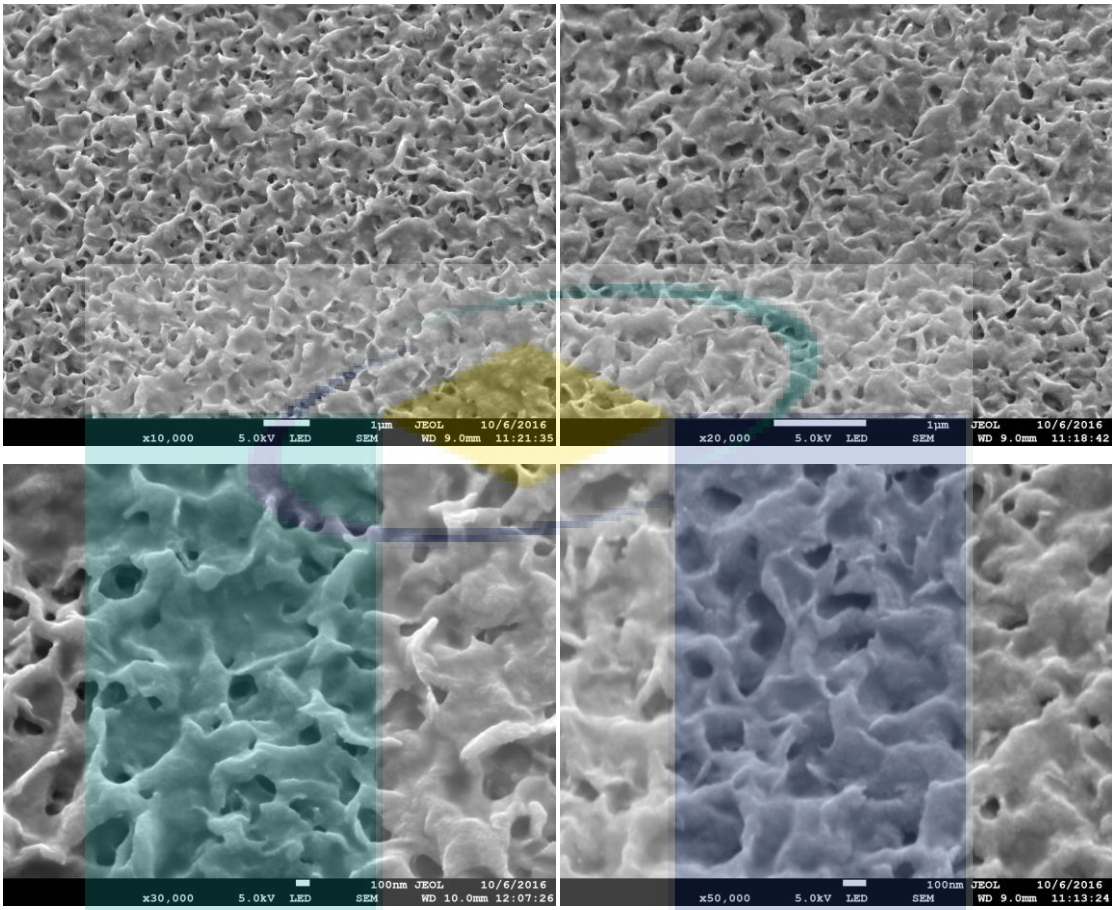

Figure 4. 19. Surface morphology of ZnO film with spin speed of 1500 rpm and annealing temperature of 180 °C

Table 4. 3. Thickness of ZnO thin film with different spin speed and annealing temperature

Sample	Spin Speed (rpm)	Annealing Temperature (°C)	Average Thickness (nm)
A	1000	300	373.00
B	1500	300	166.25
C	2000	300	113.25
D	1500	400	187.50
E	1500	500	205.25

4.1.3 Photoluminescence

PL spectra of ZnO films were shown in figure 4.18. The emission spectrum of ZnO thin film showed the peak was at narrow band ~380 nm. It was corresponding to band edge emission. It was due to free exciton emission. It has ultraviolet region. The PL spectrum also showed a wide broad peak of green emission at ~500 nm. The green emission was due to the existence of intrinsic defects, which are zinc vacancies and oxygen interstitial (Xu, Zheng, Lai, & Pei, 2014) . It could be observed that when the annealing temperature was increased, the wavelength intensity was increased. This was because of the oxygen and zinc atoms in interstitial site moved to lattice sites. It was also due to surface grain area increases (Li, Xu, Li, Shen, & Wang, 2010). From figure 4.18, it can be seen that there was insignificant change in wavelength, this is because the wavelength shift only caused by composition of precursor but not annealing temperature and spin speed. Annealing temperature had only changed the intensity of wavelength (Sagar, Shishodia, Mehra, Okada, Wakahara, & Yoshida, 2007).

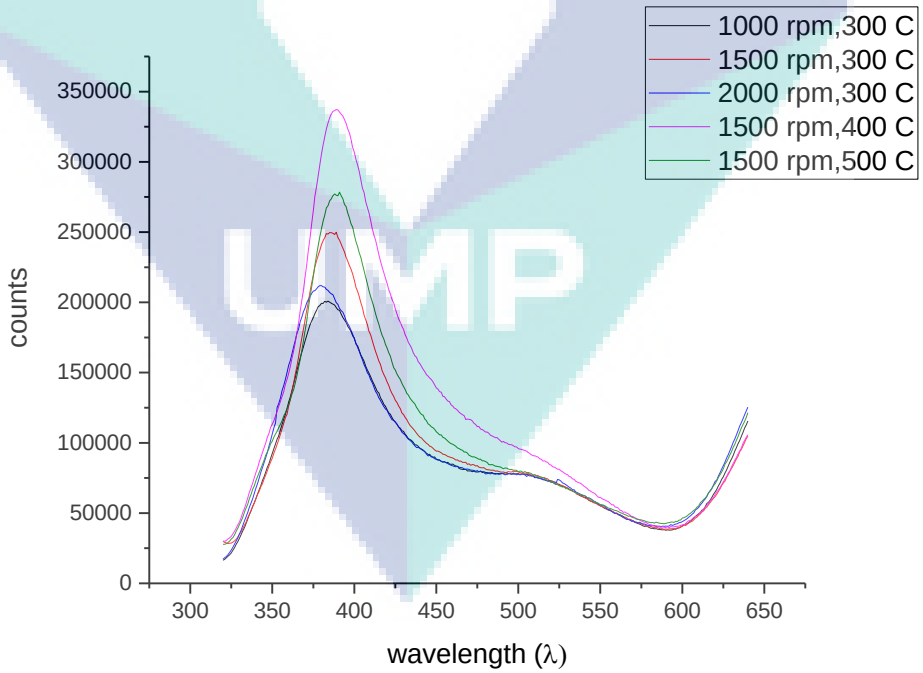

Figure 4. 20. PL spectrum of ZnO thin film with different spin speed and annealing temperature

4.1.4 UV-Vis Analysis

UV-Vis was carried out to calculate the band gap of ZnO nanoparticles. The first excitonic peak was determined by Origin Pro software. The band gap of ZnO film could be calculated using equation 4.4.

$$E_g = \frac{hv}{\lambda} \quad 4.4$$

where E_g is energy band gap of ZnO, h is Plank's constant in eV (4.135 x 10^{-15}), v is the velocity of light (3 x 10^8) and λ is the wavelength of first excitonic peak.

Figure 4.20 to figure 4.24 showed the UV emission spectrum of ZnO with different spin speed and annealing temperature. Table 4.4 showed the energy band gap of each ZnO film with different spin speed and annealing temperature. It could be found that when increasing the annealing temperature, the energy band gap was decreased. The highest band gap (3.6109 eV) was belong to ZnO film with spin speed of 1000 rpm and annealing temperature of 300 °C.

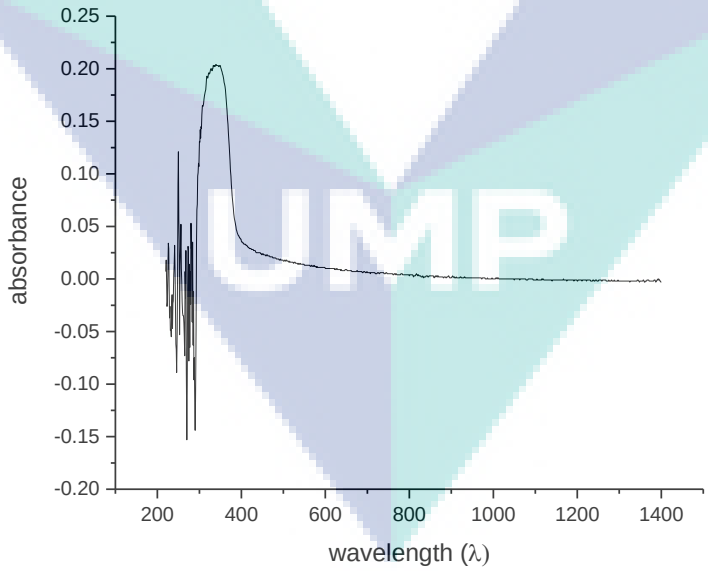

Figure 4. 21. UV spectrum of ZnO film with spin speed of 1000 rpm and annealing temperature of 300 °C

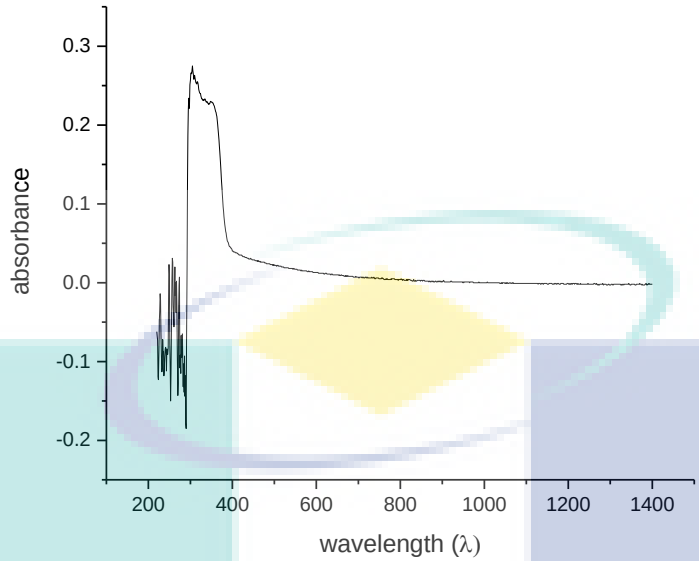

Figure 4. 22. UV spectrum of ZnO film with spin speed of 1500 rpm and annealing temperature of 300 °C

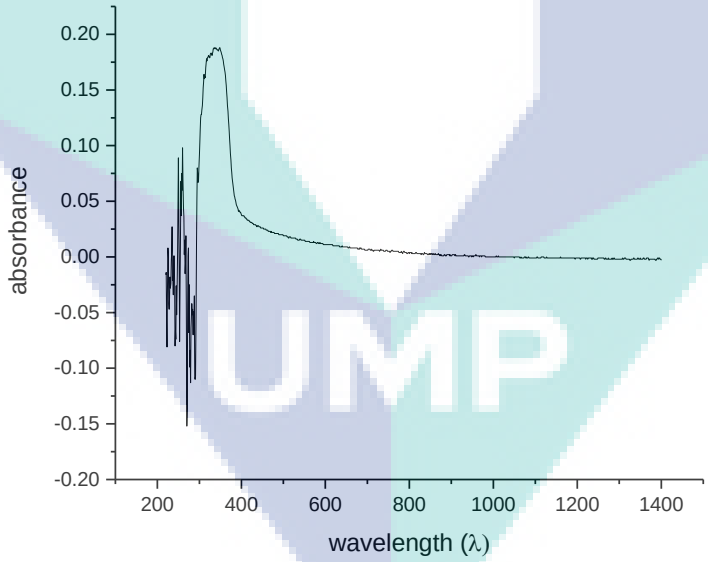

Figure 4. 23. UV spectrum of ZnO film with spin speed of 2000 rpm and annealing temperature of 300 °C

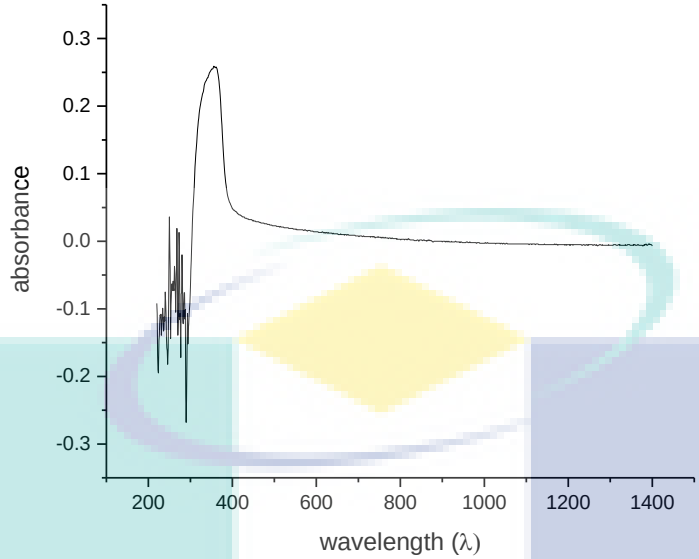

Figure 4. 24. UV spectrum of ZnO film with spin speed of 1500 rpm and annealing temperature of 400 °C

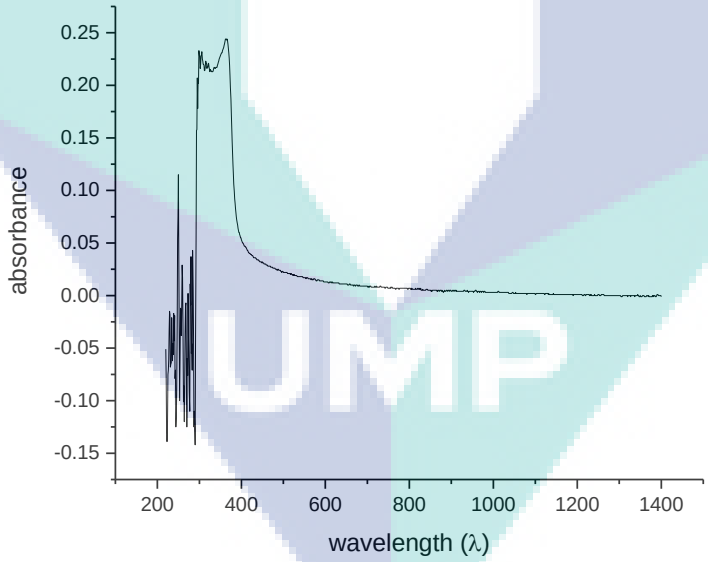

Figure 4. 25. UV spectrum of ZnO film with spin speed of 1500 rpm and annealing temperature of 500 °C

Table 4. 4. Energy band gap of UV emission peak at different spin speed and annealing temperature of ZnO thin film

Sample	Spin Speed (rpm)	Annealing Temperature (°C)	First Excitonic Peak (nm)	Energy band gap (eV)
A	1000	300	343.5477	3.6109
B	1500	300	348.9740	3.5547
C	2000	300	351.8468	3.5257
D	1500	400	359.8267	3.4475
E	1500	500	362.6995	3.4202

4.3 PIEZOELECTRIC TEST

The voltage that produced by ZnO thin film was measured for three minutes with fixed frequency of 40 kHz. During piezoelectric test, the voltage produced was inconsistent. Table 4.10 showed the maximum and minimum voltage that each film could produce.

From the results, it showed when increasing annealing temperature, the voltage produced was increased. When increasing the rotation speed, the voltage produced was increased. The highest voltage was produced by ZnO film with rotation speed of 2000 rpm and annealing temperature of 300 °C. The maximum voltage produced from this film was 27.3 mV, lowest voltage was 0.9 mV and average voltage was 6.353 mV. ZnO film with rotation speed of 1000 rpm and annealing temperature of 300 °C produced the least voltage which was 1.374 mV.

The maximum and minimum voltage that produced by ZnO film with spin speed of 1500 rpm and annealing temperature of 180 °C was 202 mV and 0.142 mV. The average voltage produced was 174 mV. However, the film that produced was not uniform film. The ZnO was accumulated. Therefore, it was believed that the voltage produced could be very high because of the film was thick enough. Figure 4.26 showed the ZnO film with spin speed of 1500 rpm and annealing temperature of 180 °C.

Figure 4. 26. ZnO film with spin speed of 1500 rpm and annealing temperature of 180 °C

Table 4. 5. Voltage that could be produced by each films

Sample	Spin Speed (rpm)	Annealing Temperature (°C)	Average Voltage (mV)	Minimum Voltage (mV)	Maximum Voltage (mV)
A	1000	300	1.374	0.5	2.4
B	1500	300	1.368	0.9	2.1
C	2000	300	6.353	0.4	27.3
D	1500	400	1.384	0.9	3.5
E	1500	500	1.424	1.1	1.8

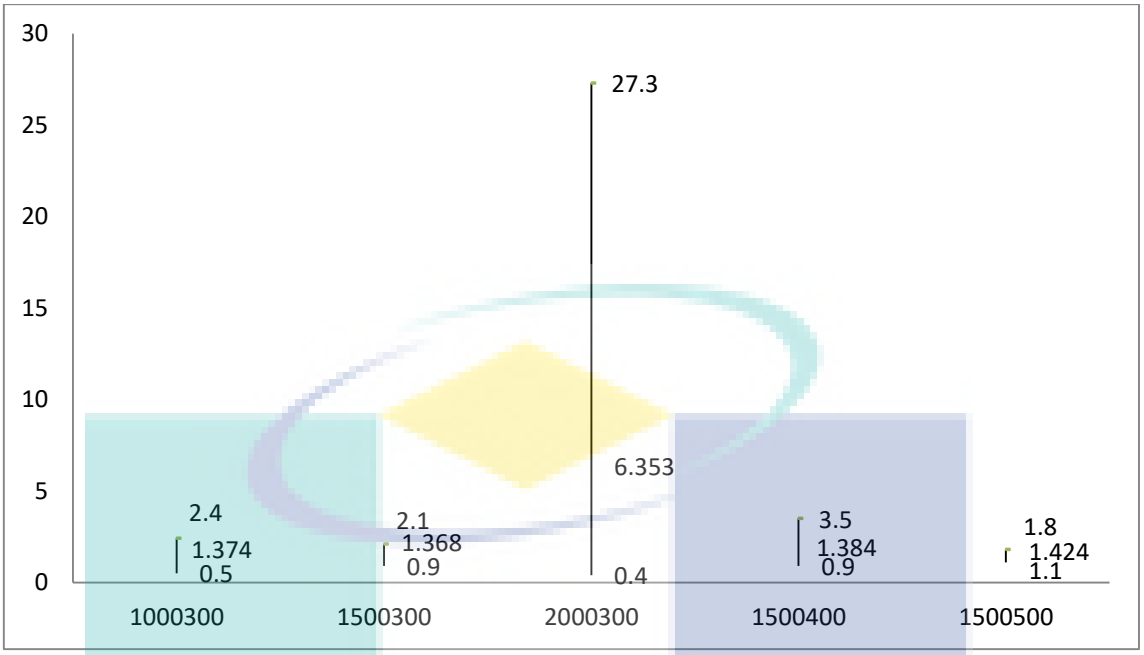

Figure 4. 27. Voltage produced by each film

CHAPTER 5

CONCLUSION AND RECOMMENDATION

5.1 CONCLUSIONS

The objective of this research was to determine the piezoelectric voltage that could be produced by ZnO film. From XRD results, the films were preferentially diffracted at 65° which corresponding to (1 1 2) diffraction phase. From the PL results, it was observed that there was only film with spin speed of 2000 rpm and annealing with 300 °C had slightly left wavelength which is around 380 nm. Piezoelectric test had proven the ZnO film could produce electricity. The maximum voltage (20.7 mV) was produced by the ZnO film with spin speed of 2000 rpm and annealing with 300 °C. The voltage output is sufficient to become source of energy for some millivolt sensor devices.

5.2 RECOMMENDATIONS

There were some limitation in this research, some recommendations was raised in this section to improve the experiment. The film with spin speed of 1500 rpm and annealing temperature of 180 °C was accumulated and could not get uniform film. Dip coating might be used to improve the uniformity of film. One of the limitation in this research was the XRD detection. The films were too thin to be detected by XRD. Therefore, more layers should be coated to be able to detect. The sample preparation is crucial step. A little bit of contaminant will affect the result. Personal Protective Equipment must be worn throughout the entire process. Cleanliness of surrounding must be taken care. Rather than aluminum was used as substrate, ITO glass could be used as substrate. Besides that, the reading of multimeter in piezoelectric test is inconsistent. Keithley instrument should be used so that the reading could be recorded. The other limitation was the sample could not contact directly with the vibrator, therefore, the vibration produced was too weak to be detected by samples. Other vibrators such as ChromTech Ultrasonic Cleaner could be used to improve the vibration strength.

REFERENCES

Abdel Aal, A., Mahmoud, S., & Aboul-Gheit, A. (2009). Sol-Gel and Thermally Evaporated Nanostructured Thin ZnO films for Photocatalytic Degradation of Trichlorophenol. *Nanoscale Research Letters* , 627-634.

Akgun, M. C., Kalay, Y. E., & Unalan, H. E. (2012). Hydrothermal zinc oxide nanowire growth using zinc acetate dihydrate salt. *Material Research* , 1445-1451.

Alias, S. S., & Mohamad, A. A. (2013). *Synthesis of Zinc Oxide by Sol GEl Method for Photoelectrochemical Cells.* Springer Science & Business Media.

Aricò, A. S., Bruce, P., Scrosati, B., Tarascon, J.-M., & Schalkwijk, W. v. (April 2005). Nanostructured materials for advanced energy conversion and storage devices. *Nature Materials* , *4*, 366 - 377.

Bae, H., & Choi, G. (1999). Electrical and reducing gas sensing properties of ZnO and ZnO-CuO thin films fabricated by spin coating method. *Sensors and Actuators B: Chemical* , 47-54.

Brinker, C., & Scherer, G. (2013). *Sol Gel Science.* San Diego: Academic Press.

Brus, L.E. (1984). Electron-electron and electron-hole interaction in small semiconductor crystallites: The size dependence of the lowest excited electronic state. *The Journal of Chemical Physics* , 4403-4409.

Chen, J., He, S., & Sun, Y. (2014). *Rechargeable Sensor Networks: Technology, Theory, and Application: Introducing Energy Harvesting to Sensor Networks.* Singapore: World Scientific.

Concept of energy harvesting. (n.d.). Retrieved November 23, 2016, from Ambiosystems LLC.: http://www.ambiosystems.com/index.php/2-uncategorised/13-concept-of-energy-harvesting

E.Heredia, Bojorge, C., CAsanova, J., Canapa, H., Craievich, A., & Kellermann, G. (October 2014). Nanostrucute ZnO thin films prepared by sol-gel spin-coating. *Applied Surface Science , 317*, 19-25.

Eom, C.-B., & Trolier-Mckinstry, S. (Nov, 2012). Thin-Film piezoelectric MEMS. *MRS Bulletin* , 1007-1017.

Gattorno, G., & Oskam, G. (2006). Forced hydrolysis vc self-hydrolysis of zinc acetate in ethanol and iso-butanol. *The Electrochemical Society* (pp. 23-28). ECS.

Habibi, M. H., & Sardashti, M. K. (December 2008). Structure and morphology of nanostructured zinc oxide thin films prepared by dip- vs. spin-coating methods. *Iranian Chemical Society , 5* (4), 603-609.

Joshi, S., Nayak, M., & Rajanna, K. (March 2014). Effect of post-deposition annealing on transverse piezoelectric coefficient and vibration sensing performance of ZnO thin films. *Applied Surface Science , 296*, 169-176.

Khaligh, A., Zeng, P., & Zheng, C. (March 2010). Kinectic energy harvisting using piezoelectric and electromagnetic technologies-state of the art. *IEEE Transactions on Industrial Electronic , 57* (3), 850-860.

Kondraties, V., Kink, I., & Romanov, A. (2013). Low temperature sol gel technique for processing Al-doped zinc oxide films. *Material Physics and Mechanics 17* , 38-46.

Kumar, B., & Kim, S.-W. (May 2012). Energy harvestingbased on semiconducting piezoelectric ZnO nanostructures. *Nano energy , 1* (3), 342-355.

Kumar, N., Kaur, R., & Mehra, R. (2007). Photoluminescence studies in sol-gel derived ZnO film. *Journal of Luminescence* , 784-788.

Levy, D., & Zayat, M. (2015). *The Sol-Gel Handbook.* John Wiley & Sons.

Li, Y., Xu, L., Li, X., Shen, X., & Wang, A. (2010). Effect of aging time of ZnO sol on the structural and optical properties of ZnO thin films prepared by sol0gel method. *Applied Surface Science* , 4543-4547.

Liu, Z., Li, J., Ya, J., Xin, Y., & Jin, Z. (2008). Mechanism and characteristics of porous ZnO films by sol-gel method with PEG template. *Materials Letters* , 1190-1193.

Monk, P., Mortimer, R., & Rosseinsky, D. (2007). *Electrochromism and Electrochromic Devices.* Cambridge University Press.

Nanda, S., & Gupta, P. (2010). Structural and Optical Properties of Sol-gel Prepared ZnO Thin Film. *Applied Physics Research* , 19-28.

Natsume, Y., & Sakata, H. (2000). Zinc oxide films prepared by sol-gel spin-coating. *Thin Solid Films* , 30-36.

Nechibvute, A., Chawanda, A., & Luhanga, P. (2012). Piezoelectric energy harvesting devices: an alternative energy source for wireless sensors. *Smart Materials Research , 2012*.

Nuffer, J., & Bein, T. (October 2006). Application of piezoelectric materials in transportation industry.

P.B., K., Moloto, M., & Sikhwivhilu, L. (2012). The effect of solvents, acetone, water and ethanol, on the morphological and optical properties of ZnO nanoparticle prepared by microwave. *Journal of Nanotechnology* , 1-6.

Pierre, A. C. (1998). *Introduction to Sol-Gel Processing.* Boston/Dordrecht/London: Kluwer Academic Publishers.

Prashanthi, K., Miriyala, N., Gaikwad, R., Moussa, W., V.Ra, g. R., & Thundat, T. (September 2013). Vibrational energy harvesting using photo-patternable piezoelectric nanocomposite cantilevers. *Nano Energy , 2* (5), 923-932.

Quinones-Galvan, J., Sandoval-Jimenez, I., Tototzintle- Huitle, H., Hernandez-Hernandez, L., de Moure-Flores, F., Compos-Gonzallez, E., et al. (2013). Effect of precursor solution and annealing temperature on the physical properties of sol-gel deposited ZnO thin films. *Results in Physics* , 248-253.

Sagar, P., Kumar, M., Mehra, R., Okada, H., Wakahara, A., & Yoshida, A. (2007). Epitaxial growth of zinc oxide thin films on epi-GaN/sapphire (0001) by sol-gel technique. *Thin Solid Films* , 3330-3334.

Sagar, P., Shishodia, P., Mehra, R., Okada, H., Wakahara, A., & Yoshida, A. (2007). Photoluminescence and absorption in sol-gel-deroved ZnO films. *Journal of Luminescence* , 800-806.

Sahu, N., Parija, B., & Panigrahi, S. (2009). Fundamental understanding and modeling of spin coating process: A review. *Indian Journal of Physics* , 493-502.

Sazonov, E., Li, H., Curry, D., & Pillay, P. (2009). Self-powered sensors for monitoring of highway bridges. *Sensors Journal* , 1422-1429.

Schodek, D. L., Ferreira, P., & Ashby, M. F. (2009). *Nanomaterial, Nanotechnologies and Design.* Butterworth-Heinemann.

Schweizer, P. M., & Kistler, S. F. (2012). *Liquid film coating: scientific principles and their technological implications.* Springer Science & Business Media.

Shang, Z., Li, D., Wen, Z., & Zhao, X. (November 2013). The fabrication of vibration energy harvester arrays based on AlN piezoelectric film. *Journal of Semiconductor , 34* (11), 114013.

Shivaraj, B. W., Murthy, H. N., Krishna, M., & Satyanarayana, B. S. (2015). Effect of annealing temperature on structural and optical properties of dip and spin coated ZnO thin films. *Procedia Materials Science , 10*, 292-300.

Spies, P., Pollak, M., & Mateu, L. (June, 2015). *Handbook of energy harvesting power supplies and application.* CRC Press.

Ville, K. (2010). Microstructured piezoelectric shoe power generator outperforms batteries. *MEMS Investor Journal* .

Vives, A. A. (2008). *Piezoelectric Transducers and Application.* Springer Science & Business Media.

Wang, M., Kim, E., Chun, J., Shin, E., Hahn, S., Lee, K., et al. (2006). Influence of annealing temperature on the structure and optical properties of sol-gel prepared ZnO thin film. *Physica Status Solidi (a)* , 2418-2425.

Wang, Z. L., & Wu, W. Z. (2014). Piezotronics and piezo-phototronics: fundamentals and applications. *National Science Review , 1* (1), 62-90.

Wang, Zhong Lin. (2004). Zinc oxide nanostructures: growth, properties and application. *Journal of Physics: Condensed Matter* , R829-R858.

Wong, H., & Dahari, Z. (2015). Human body parts heat energy harvesting using thermoelectric module. *Energy Conversion (CENCON)* (pp. 211-214). IEEE.

Wu, T., & Thompson, D. (2010). The vibration behavior of railway track at high frequencies under multiple preloads and wheel interactions. *Journal Acoust Soc. A.* , 1046-1053.

Xu, L., Zheng, G., Lai, M., & Pei, S. (2014). Annealing impact on the structural and photoluminescence properties of ZnO thin films on Ag substrate. *Journal of Alloys and Compunds* , 560-565.

Yahya, N. (2011). *Carbon and oxide nanostructures: synthesis, characterisation and application.* Springer Science & Business Media.

Yu, W. W., Qu, L., Guo, W., & Peng, X. (2003). Experimental determination of the extinction coefficient of CdTe, CdSe and CdS nanocrystals. *Chemistry of Materials* , 2854-2860.

Zhu, M., Xia, J., Hong, R., Abu-Samra, H., Huang, H., Staedler, T., et al. (2008). Heat-activated structural evolution of sol-gel-derived ZnO thin films. *Journal of Crystal Growth* , 816-823.

Znaidi, L. (2010). Sol-gel-deposited ZnO thin films: A review. *Material Science and Engineering: B* , 18-30.

PUBLICATIONS UNDER RESEARCH GRANT RDU1703194

JOURNAL

A. G. E. Sutjipto, Yit Pei Shian, Ali Shaitir, Ari Legowo: Ambient Energy Harvesting of Piezoelectric ZnO Thin Film Dependence of Spin Speed and Annealing Temperature. Accepted for publication in Materials Science Forum 2019.

Agus Geter Edy Sutjipto, Low Kai Ti Yuli Panca Asmara, and Ari Legowo: Sample Preparation of TiO2 added ZnO using Powder Metallurgy Route and its Characteristics. Accepted for publication in Materials Science Forum 2019.

T. X. Fen, A. G. Satier, A. Legowo, A.G.E. Sutjipto: Study on the Effect of Mg Dopant on the Properties of ZnO Thin Film Prepared by Sol Gel. Published in IEEE Xplore DOI: 10.1109/ICASET.2019.8714394.

A.G.E. Sutjipto, M.H. Mazwir, H.L. Lee, S. Miskom, A.G. Shaitir, M.A. Jusoh, R. Othman: Effect of Compaction Pressure of Green Body and Heating Current on Photoluminescence Property of ZnO Crystal Grown by Electric Current Heating Method. IOP Conf. Series: Materials Science and Engineering 290, 012043, 2018.

CONFERENCE

A Shaitir, A.G.E. Sutjipto, and Y., Shian: Synthesis and characterizations of ZnO thin films deposited on aluminum metal substrate by sol-gel spin coating technique. In: National Conference for Postgraduate Research (NCON-PGR 2018), 28-29 August 2018, Universiti Malaysia Pahang, Gambang, Pahang. pp. 133-138. ISBN 9789672226055

IEEE.org | IEEE *Xplore* Digital Library | IEEE-SA | IEEE Spectrum | More Sites

Cart (0) | Create Account | Personal Sign In

Institutional Sign In

Browse My Settings Get Help Subscribe

Advertisement

< Previous | Back to Results | Next >

Conferences > 2019 Advances in Science and ...

Study on the Effect of Mg Dopant on the Properties of ZnO Thin Film Prepared by Sol Gel

Publisher: IEEE

<< Results | < Previous | Next >

4 Author(s) Tang Xiao Fen ; Ari Legowo ; Ali Shaitir ; Agus Geter Edy Sutjipto View All Authors

63
Full
Text Views

Export to
Collabratec

Alerts

Manage
Content Alerts

Add to Citation
Alerts

More Like This

Performance of Metal-Semiconductor-Metal Ultraviolet Photodetectors Based on Sol-Gel Derived MgxZn1-xO Semiconductor Thin Films
2018 25th International Workshop on Active-Matrix Flatpanel Displays and Devices (AM-FPD)
Published: 2018

Influence of annealing temperature on structural and optical properties of CdS thin films prepared by sol-gel spin coating method
International Conference on Advanced Nanomaterials & Emerging Engineering Technologies
Published: 2013

View More

Top Organizations with Patents on Technologies Mentioned in This Article

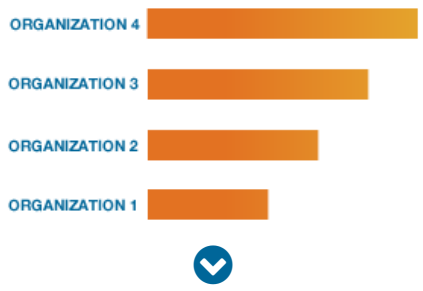

Abstract

Downl

Document Sections

Authors
Figures
References
Keywords
Metrics
More Like This

PDF

Abstract: Thin film technology is the field of thin film deposition process and it is linked to nanotechnology. Thin film technology has been applied in many fields. Mostly thin fi...
View more

Metadata

Abstract:
Thin film technology is the field of thin film deposition process and it is linked to nanotechnology. Thin film technology has been applied in many fields. Mostly thin film is used in electronic components and electronic displays such as LED displays and lighting, thin film solar cell. Semiconducting material, insulating materials or metal silicide conductors are typically made up of these thin films. Doping is one of the methods to change the properties of thin film. There various types of materials could be used as doping element. Different types of element has different properties which will cause properties of ZnO thin film to be changed. Thin film of ZnO could change from semiconductor to insulator or conductor depends on types doping element. However, doping using Mg mostly will changed the band gap of thin film. , ZnO is chosen as semiconducting material since it is transparent conducting oxide. At room temperature, it has wide direct band gap with value of 3.37eV that in group II-IV semiconductor. Due to luminescence in visible and near UV range of spectrum, it is widely used in sensors, light emitting diodes or solar cells. The doping element being chosen is Mg because the similarity in ionic radius between Mg and Zn. After thin film of ZnO is doped with Mg, several properties of ZnO thin film is changed. The research shows that the surface of undoped ZnO thin film will contain much void and uniform grain size. However, the surface thin film that doped with Mg is dense and uniform while the void will decreases with concentration of Mg. This shows that there is improved in surface morphology. Sol gel techniques had many advantages compared to other method. Sol gel method requires low sintering temperature (200 C to 600 C). It is an economical method as it is low cost and it can be carried out using simple and inexpensive equipment. Sol gel method has the ability to change microstructure of film by changing the pH, temperature and viscosity of sol. This thesi...

(View more)

Advertisement

Published in: 2019 Advances in Science and Engineering Technology International Conferences (ASET)

Date of Conference: 26 March-10 April 2019

Date Added to IEEE *Xplore*: 16 May 2019

ISBN Information:

INSPEC Accession Number: 18674061

DOI: 10.1109/ICASET.2019.8714394

Publisher: IEEE

Conference Location: Dubai, United Arab Emirates, United Arab Emirates

Advertisement

Contents

Sign in to Continue Reading

CHANGE USERNAME/PASSWORD
PAYMENT OPTIONS
VIEW PURCHASED DOCUMENTS
COMMUNICATIONS PREFERENCES
PROFESSION AND EDUCATION
TECHNICAL INTERESTS
US & CANADA: +1 800 678 4333
WORLDWIDE: +1 732 981 0060
CONTACT & SUPPORT

About IEEE *Xplore* | Contact Us | Help | Accessibility | Terms of Use | Nondiscrimination Policy | Sitemap | Privacy & Opting Out of Cookies
A not-for-profit organization, IEEE is the world's largest technical professional organization dedicated to advancing technology for the benefit of humanity.

© Copyright 2019 IEEE - All rights reserved. Use of this web site signifies your agreement to the terms and conditions.

IEEE Account
- » Change Username/Password
- » Update Address

Purchase Details
- » Payment Options
- » Order History
- » View Purchased Documents

Profile Information
- » Communications Preferences
- » Profession and Education
- » Technical Interests

Need Help?
- » **US & Canada:** +1 800 678 4333
- » **Worldwide:** +1 732 981 0060
- » Contact & Support

About IEEE *Xplore* | Contact Us | Help | Accessibility | Terms of Use | Nondiscrimination Policy | Sitemap | Privacy & Opting Out of Cookies

A not-for-profit organization, IEEE is the world's largest technical professional organization dedicated to advancing technology for the benefit of humanity.
© Copyright 2019 IEEE - All rights reserved. Use of this web site signifies your agreement to the terms and conditions.

Study on the Effect of Mg Dopant on the Properties of ZnO Thin Film Prepared by Sol Gel

Tang Xiao Fen
Faculty of Industrial Sciences & Technology
Universiti Malaysia Pahang
fen2883@gmail.com

Ari Legowo
Aviation Engineering Technology and Science
Higher Colleges of Technology
Abu Dhabi Men's College, UAE
alegowo@hct.ac.ae

Ali Shaitir
Faculty of Industrial Sciences & Technology
Universiti Malaysia Pahang
alishaiter@yahoo.com

Agus Geter Edy Sutjipto
Faculty of Industrial Sciences & Technology
Universiti Malaysia Pahang
agusgeter@ump.edu.my

Abstract*— Thin film technology is the field of thin film deposition process and it is linked to nanotechnology. Thin film technology has been applied in many fields. Mostly thin film is used in electronic components and electronic displays such as LED displays and lighting, thin film solar cell. Semiconducting material, insulating materials or metal silicide conductors are typically made up of these thin films. Doping is one of the methods to change the properties of thin film. There various types of materials could be used as doping element. Different types of element has different properties which will cause properties of ZnO thin film to be changed. Thin film of ZnO could change from semiconductor to insulator or conductor depends on types doping element. However, doping using Mg mostly will changed the band gap of thin film. , ZnO is chosen as semiconducting material since it is transparent conducting oxide. At room temperature, it has wide direct band gap with value of 3.37eV that in group II-IV semiconductor. Due to luminescence in visible and near UV range of spectrum, it is widely used in sensors, light emitting diodes or solar cells. The doping element being chosen is Mg because the similarity in ionic radius between Mg and Zn. After thin film of ZnO is doped with Mg, several properties of ZnO thin film is changed. The research shows that the surface of undoped ZnO thin film will contain much void and uniform grain size. However, the surface thin film that doped with Mg is dense and uniform while the void will decreases with concentration of Mg. This shows that there is improved in surface morphology. Sol gel techniques had many advantages compared to other method. Sol gel method requires low sintering temperature (200˚C to 600˚C). It is an economical method as it is low cost and it can be carried out using simple and inexpensive equipment. Sol gel method has the ability to change microstructure of film by changing the pH, temperature and viscosity of sol. This thesis discuss about the sol gel spin coating techniques to produce Mg doped ZnO thin films. Zinc acetate dehydrate, absolute ethanol and diethanolamine used as sol gel precursor while magnesium chloride as source of doping element. Sol gel was coated onto glass slides that wrapped with aluminium foil using spin coated instruments. After that, the thin film was annealing at 400˚C for one hour. The thin films with varying concentration of Mg and spin speed is characterized using XRD, FESEM, PL, UV-Vis and four point probes. Thin films that fabricated with 5 wt% Mg and spin speed of 2000 rpm has better result in term of characterization of XRD and FESEM among all Mg doped ZnO thin films since it has more crystal growth of MgO and it has the best surface morphology with uniform nanoparticles structure eventhough it has moderate transparency and energy band gap. Furthermore, the resistivity of this samples is also higher compared to sample with 5 wt% and 3000 rpm but lower than sample with 10 wt% and 2000 rpm. Sample with 10 wt% and 2000 rpm has the best results among all sample in application pf photonic since the intensity peaks of PL is the highest.

Keywords—thin film, nanotechnology, ZnO, Mg doping, Sol gel

I. INTRODUCTION

Many of thin film synthesis and properties have been reported [1-5] as well as changes of materials properties based on materials addition or dopant and treatment [6-13]

Thin films are materials that consists of a layer of thickness that ranges from fraction nanometers to micrometers [14]. Thin film plays very important role in our daily life especially in the field of nanotechnology. Nanotechnology merging into the films shows many advantages including enhance efficiency and lower total cost [15]. Thin film nanotechnology can be applied in many types of application includes integrated circuit chips, microelectronic optical system, light emitting diodes (LED), thin film batteries or photovoltaic solar cell [16].

ZnO is chosen to synthesis thin film this is because ZnO has low acoustic absorption, high mechanical stability and low loss [17]. ZnO is a semiconductor with n-type. It has wide and direct band gap around 3.3eV. It also has high excitonic binding energy around 60 mega eV that make it suitable for excitonic devices. This property enables it to be applied in many applications like photo catalysis, gas sensors and optoelectronic [18-19]. Mg is chosen to be used as dopants. Mg is the lightest metal which expected to reduce weight of devices and increases flexibility in spinning process. The ionic radius of Mg^{2+} ion which is 0.0527 nm is similar to Zn^{2+} ion

which is 0.060 nm [20]. This cause no significant changes in lattice size when Mg^{2+}ion is incorporated into ZnO [18].

There are many techniques to synthesis thin film. Among this few techniques, sol gel spin coating has several advantages compared to other includes low cost, easy doping, simple method and high accuracy control of materials composition [21]. Moreover, this method has ability to obtain atomic scale mixing of individual components [22].

In this modern era, ZnO thin film had been widely used due to its advanced properties that contributed to many types of applications especially nanotechnology applications. Changes made on different parameter such as thickness, annealing temperature and doping will affects the synthesis thin film. For example, N.Nithya and co-workers observed that the properties of ZnO thin film in term of optical and structural will change according to thickness of the [23]. For instances, F.A.Garces and his friends found that through doping of impurity such as aluminium (Al) or magnesium (Mg) will affected the lattice parameter and crystalline texture of the films and give better structural properties compared to undoped ZnO thin film [24].

The objectives of this research are to synthesis ZnO thin film that doped with using sol gel method and spin coating method and to characterize Mg doped ZnO thin film using XRD, FESEM, PL, UV-Vis and four point probe by varying spin speed and concentration of Mg dopants.

II. METHODOLOGY

A. Synthesis of ZnO sol gel that Doped with Mg

The materials used in this research includes magnesium chloride powder, zinc acetate dihydrate (Zn(CH2CO2)2•2H2O) (purity 99.95%), diethanolamine (DEA) and absolute ethanol. Zinc acetate dihydrates acts as precursors while absolute ethanol and diethanolamine used as solvent and stabilizing agents. Moreover, magnesium chloride acts as the source of magnesium doping. The substrate used for Mg doped ZnO thin film to be coated is glass slide that wrapped with aluminium foil.

Mg doped sol-gel was produced by using magnesium chloride, zinc acetate dihydrate, absolute ethanol and diethanolamine. Three different concentration of Mg doped sol-gel were prepared which are 0 wt%, 5 wt% and 10 wt%. For 0 wt% Mg, magnesium chloride was not being used. Firstly, ZnO sol-gel which refer to 0 wt% was formed by dissolved 0.2 mol zinc acetate dehydrate in absolute ethanol in beaker. After that, using magnetic stirrer, the mixture was stirred at 60˚C for duration of one hour. During stirring, the mixture was turn milky. After one hour, DEA acts as stabilizing agents was dropped into the mixture in interval of one minute until the milky solution turns clear. The molar ratio of DEA to zinc acetate dehydrate is 1:1. After the solution continue stirs for one hour, a homogeneous sol was produced and sealed by using Para film in order for deposition of 48 hours. For 5 wt% and 10 wt% Mg doped ZnO sol-gel, magnesium chloride powder was added into solution after mixture of zinc acetate dehydrate and absolute ethanol.

B. Fabrication of Mg Doped ZnO Thin Film

Laurell WS-650MZ-23 spin coater was used to fabricated Mg doped ZnO thin film onto glass slides that wrapped with aluminium foil. Spin speed was one of the manipulated variables in this research. Different spin speed was used to produce different thickness of thin films. The time for spinning process was 60s. After one layer of coating, the sample was preheated at 80˚C using a hot plate. This process was repeated for 40 times in order to get 40 layers. ZnO thin film that doped by Mg with 0 wt%, 5 wt% and 10 wt% was fabricated by using spin coating techniques with 2000 rpm. After characterization of the samples, the 5 wt% Mg has the better result. Thus, the 5 wt% Mg thin films were manipulated with 2000rpm, 2500 rpm and 3000 rpm. Thus, five samples with different concentration of Mg and spin speed has been produced which are 0 wt% with 2000 rpm, 5 wt% with 2000 rpm, 5 wt% with 2500 rpm, 5 wt% with 3000 rpm and 10 wt% with 2000 rpm.

Lastly, all samples that fabricated through spin coating techniques were annealed at temperature of 400˚C for duration of one hour using Thermo Scientific Lindberg Blue M box furnace. The thin films of ZnO with different concentration of Mg and spin coated using different spin speed were characterized by using XRD, FESEM, UV-VIS, PL and four point probe in order to determine the optical, structural, morphological and electrical properties of thin films.

III. RESULTS AND DISCUSSION

A. XRD Analysis

XRD analysis were used to determine and analyze the phase exists, composition and crystallite size of ZnO thin films that doped by different concentration of Mg and fabricated through different spin speed. These films are produced by spin coating sol-gel method and fabricated on glass slides that wrapped with aluminium foil. From Figure 1, XRD results shows that all samples of thin films were polycrystalline and oriented in distinct order. The results shows that mostly Mg doped ZnO thin films diffracted at ~36˚ and ~64˚ which corresponding to (1 0 1) and (2 2 0) crystal planes where (1 0 1) refer to ZnO phases and (2 2 0) refer to MgO phases.

The d-spacing and crystallite size of ZnO thin films that doped with Mg were calculated from the XRD result that obtained. From Bragg's Law which as shown in Eq (1), d-spacing of thin films can be obtained.

$$\lambda=2d\sin\Theta$$

$$d=\lambda/(2\sin\Theta) \quad \text{----------(1)}$$

where λ is the wavelength of x-ray (1.5406 Å), d is d-spacing in Å, Θ is the Bragg's angle, 2-theta (2Θ). On the other hand, by using Scherrer's formula as shown in Eq (4.2.1.2), the crystallite size can be obtained.

$$T=(0.9\lambda)/(\beta\cos\theta) \quad \text{----------(2)}$$

where T is crystallite size in nano meter, λ is wavelength of x-ray (0.15406 nm), β is full width at half maximum of the peak (FWHM) in radian and Θ is the Bragg's angle, 2-theta (2Θ).

Other than that, it could be found that the films were preferentially oriented in (2 2 0) plane at ~64˚ for phase of MgO. Mostly all samples show formation of ZnO wurtzite structure which corresponding to (1 0 1) plane except for the samples of 53000 and 102000. The highest peaks of intensity

of crystallinity of Mg doped ZnO thin film for (1 0 1) plane is 317 a.u. where the thin film is fabricated with 5 wt% Mg and spin speed of 2000 rpm.

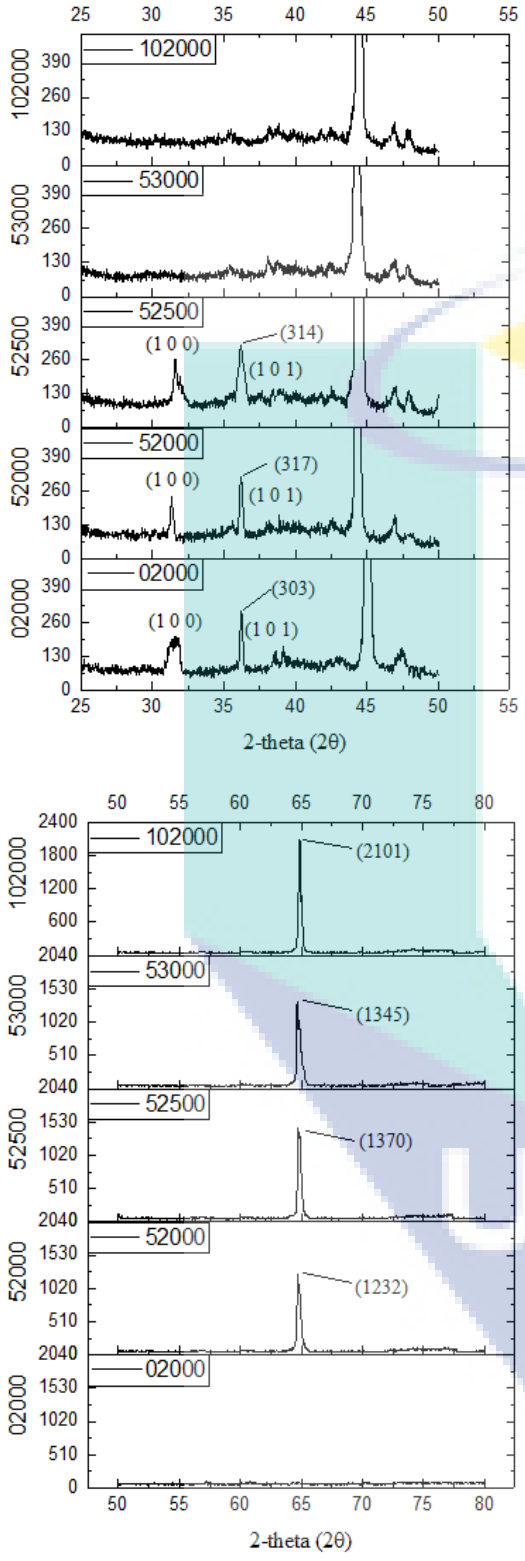

Figure 1: XRD Spectrum of All Samples

Moreover, all samples show formation of MgO phase which corresponding to (2 2 0) plane except for the sample of 02000 as there is no Mg doping provided for this sample. The highest intensity of crystallinity for (2 2 0) crystal planes of ZnO thin film is the thin film that doped with 10 wt% Mg and fabricated with spin speed of 2000 rpm which is 2101 a.u.. The results show that MgO phase which represent by (2 2 0) plane is formed as when Mg is used as the source of doping. However, the ZnO phase is disappeared in 53000 and 102000 samples which show that formation of ZnO is suppressed by the formation of MgO.

Table 1 shows the average crystallite size of different concentration of Mg of ZnO thin films and produced with different spin speed at constant annealing temperature. This results show that changes in concentration of doping and spin speed will affects the crystal sizes of thin films.

Table 1: Average Crystallite Size of Different Concentration of Mg of ZnO Thin Films

Concentration of Mg (wt%)	Spin Speed (rpm)	2-theta, 2Θ	(hkl)	d-spacing (Å)	Crystallite Size (nm)
0	2000	36.22	(101)	1.3036	21.4031
		-	-	-	-
5	2000	36.18	(101)	1.3049	12.3051
		64.72	(220)	0.8519	95.4954
5	2500	36.20	(101)	1.3043	13.1262
		64.78	(220)	0.8515	91.4062
5	3000	-	-	-	-
		64.66	(220)	0.8523	108.7135
10	2000	-	-	-	-
		64.86	(220)	0.8509	104.9434

The trend of graph of crystallite size for diffraction peaks (2 2 0) with different concentration is similar with Figure 2 which is the intensity of crystallinity peaks of ZnO thin film that doped with Mg with different concentration of Mg at constant spin speed of 2000 rpm and annealing temperature of 400˚C at diffraction phase for (b) Plane (2 2 0) (dot symbol). Therefore, it can be considered that the concentration of doping element is strongly affected the crystallite size of thin film in (2 2 0) plane. On the other hand, the crystallite size of thin films that fabricated using different spin speed for plane (1 0 1) as shown in Figure 5 shows a maximum point at 52500 samples for the trend of graph. However, the graph trend of thin film for plane (2 2 0) shows a minimum point at sample 52500 when the graph is plotted. Since both trend of graphs from Figure 5 is different from Figure 3, therefore, spin speed for fabricating the Mg doped ZnO thin film is not significantly affected the crystallite size of thin film formed. From Figure 4, the crystallite size of thin films for plane (1 0 1) is decreased as

concentration of Mg increases. However, the crystallite size of thin film for plane (2 2 0) increases as the concentration of Mg increases.

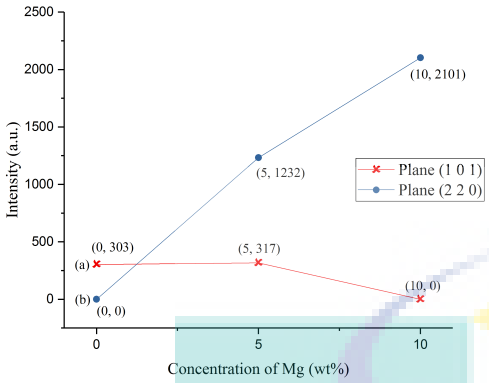

Figure 2: Intensity of Crystallinity of ZnO Thin Film that Doped with Mg with Different Concentration of Mg at Constant Spin Speed of 2000 rpm and Annealing Temperature of 400˚C at Diffraction Phase of (a) Plane (1 0 1) (cross symbol) and (b) Plane (2 2 0) (dot symbol)

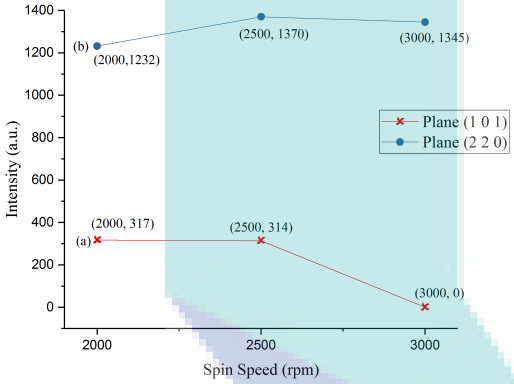

Figure 3: Intensity of Crystallinity of ZnO Thin Film that Doped with Mg with Different Spin Speed at Constant Concentration of Mg of 5 wt% and Annealing Temperature of 400˚C at Diffraction Phase of (a) Plane(1 0 1) (cross symbol) and (b) Plane (2 2 0) (dot symbol)

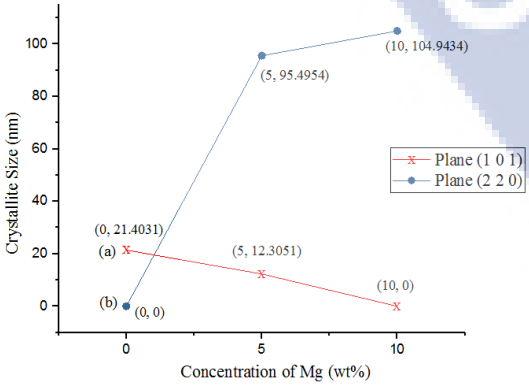

Figure 4: Crystallite Size of Mg ZnO Thin Film with Different Concentration of Mg at Constant Spin Speed of 2000 rpm and Annealing Temperature of 400˚C at Diffraction Phase of (a) Plane (1 0 1) (cross symbol) and (b) Plane (2 2 0) (dot symbol)

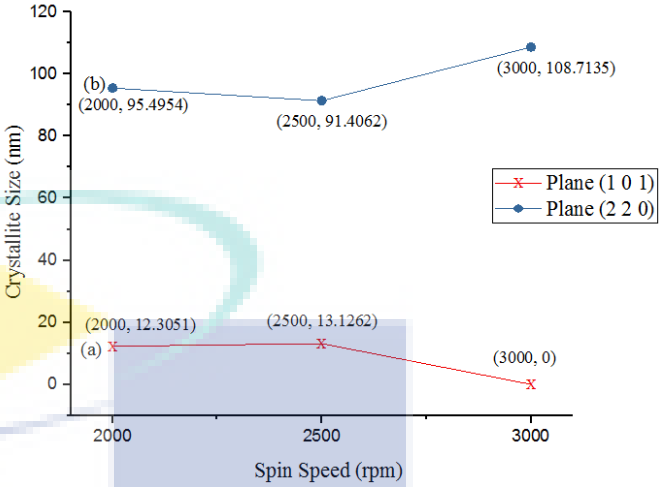

Figure 5: Crystallite Size of Mg ZnO Thin Film with Different Spin Speed at Constant Concentration of Mg of 5 wt% and Annealing Temperature of 400˚C at Diffraction Phase of (a) Plane(1 0 1) (cross symbol) and (b) Plane (2 2 0) (dot symbol)

B. Morphology Analysis

FESEM was used to study the surface morphology of ZnO thin films that doped with Mg. ZnO nanofilms were characterized under FESEM instead of SEM is due to limitation of magnification of SEM for surface morphology.

Surface morphology of undoped ZnO thin films with 0 wt% concentration of Mg and spin speed of 2000 rpm shows that the sample was in fiber-liked shaped. When the concentration of Mg is 5 wt%,this results shows that thin films consists of inhomogeneous particles with nano size was formed and it is different with undoped thin films. The grain size is increased as the thin film is doped with 5 wt% Mg and the structure changed from fiber-liked strips to uniform nanostructures. This indicates that incorporation of Mg cause the surface morphology of ZnO thin films to be improved. ZnO thin films that doped with 5 wt% concentration of Mg and spin speed of 2500 rpm shows that thin film was formed with worm-liked shapes and it is slightly different with circular shaped. The sample with 5 wt% concentration of Mg and spin speed of 3000 rpm shows that Mg doped ZnO thin film possessed uniform and dense distribution crystalline structure with nano size. ZnO thin films that doped with 10 wt% concentration of Mg and spin speed of 2000 rpm shows that the thin film was formed uniformly but with structure consists of porosity and cracking.

C. UV-Vis Analysis

Optical properties were obtained through UV-Vis analysis. UV-Vis was carried out in order to determine the transmittance spectrum and absorption spectrum for ZnO thin films that doped with different concentration and spin speed. Besides, transmittance measurement was determined from 300 nm to 900 nm. Transmittance value for thin films of ZnO that doped with different concentration of Mg and fabricated using

different spin speed was determined by Origin Pro software. Absorbance of samples was measured as a function of wavelength in the range of 200 nm to 900 nm. The first excitonic peak of samples was determined by Origin Pro software using absorption spectrum. The first excitonic peak was corresponding to electron changed from valence band to conductive band. Furthermore, the bandgap of doped and undoped ZnO thin films was calculated using the Eq. (3).

$$E_g = hv/\lambda \quad (3)$$

where E_g is bandgap energy, h is Plank's constant in eV (4.1357×10^{-15} eV), v is the velocity of light (3×108 ms^{-1}) and λ is the wavelength of first excitonic peak.

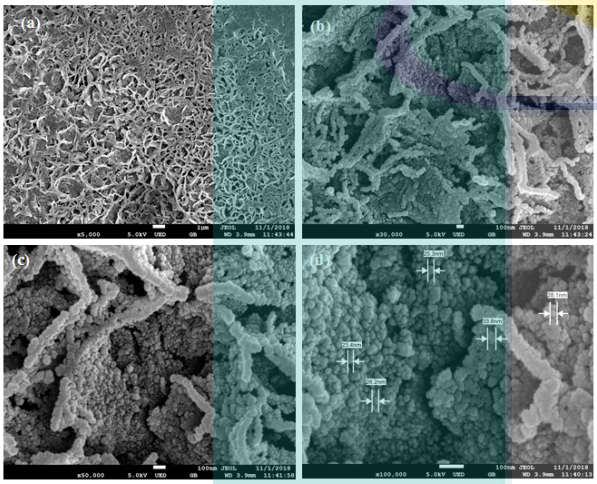

Figure 6: Surface morphology of ZnO thin films that doped with concentration of Mg of 0 wt% and spin speed of 2000 rpm in different magnification.

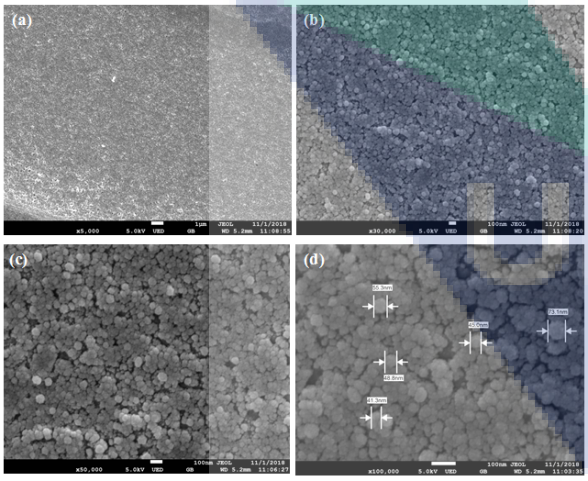

Figure 7: Surface morphology of ZnO thin films that doped with concentration of Mg of 5 wt% and spin speed of 2000 rpm in different magnification.

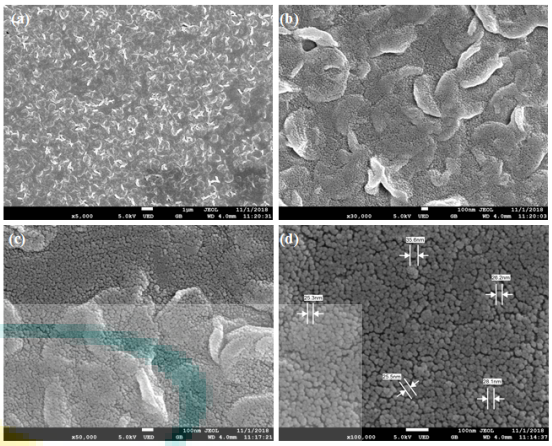

Figure 8: Surface morphology of ZnO thin films that doped with concentration of Mg of 5 wt% and spin speed of 2500 rpm in different magnification.

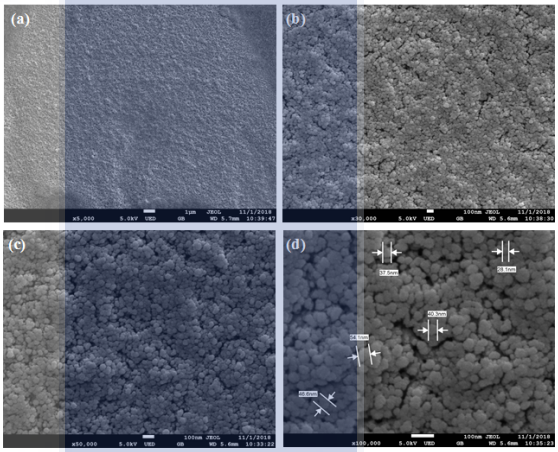

Figure 9: Surface morphology of ZnO thin films that doped with concentration of Mg of 5 wt% and spin speed of 3000 rpm in different magnification.

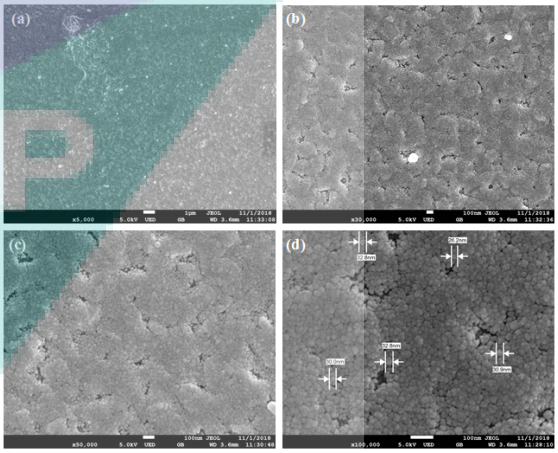

Figure 10: Surface morphology of ZnO thin films that doped with concentration of Mg of 10 wt% and spin speed of 2000 rpm in different magnification.

Figure 11 shows the transmission spectrum of different concentration and spin speed of ZnO thin films that doped with Mg. The results show that all thin films have average optical transparency over 80% in visible range. The 10 wt% Mg doped ZnO thin film fabricated with 2000 rpm has the lowest value of transmittance which is 83% while the highest transmittance value is 93% refer to 0 wt% Mg of doped ZnO thin film produced by spin speed of 2000 rpm. When higher concentration of Mg is doped into ZnO thin films, more nanoparticles of Mg will presents inside and cause the transmittance value to be decreased. According to some research, the decreasing trend of transmittance may be due to doping process which will increased the scattering of photons by crystal defects [25]. By varying spin speed, results show that when spin speed increases from 2000 rpm to 2500 rpm, the trasparency increases from 89% to 92.5%. However, when spin speed increases to 3000 rpm, the transparency of thin film decreases to 88%.

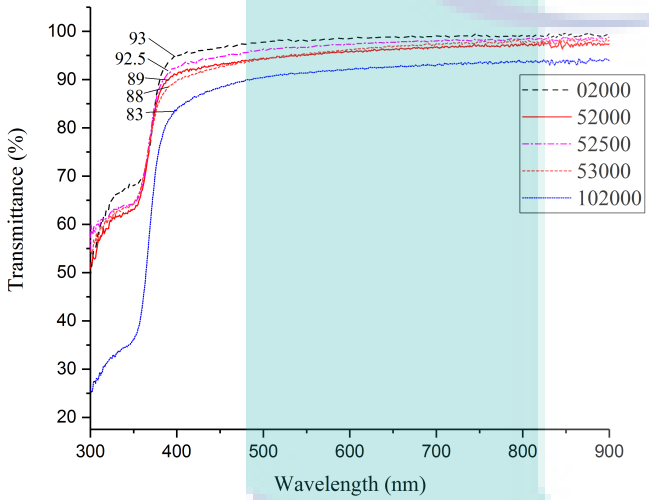

Figure 11: Transmittance Spectra of ZnO Thin Film that Doped with Mg by Varying Concentration of Mg and Spin Speed

Table 2: Energy Band gap of UV Emission Peak at Different Concentration of Mg and Spin Speed

Sample	Concentration of Mg (wt%)	Spin Speed (rpm)	First Excitonic Peak (nm)	Energy Band gap (eV)
02000	0	2000	360	3.4464
52000	5	2000	356	3.4851
52500	5	2500	352	3.5247
53000	5	3000	350	3.5449
102000	10	2000	348	3.5653

By varying concentration of Mg, the results show that the bandgap value increases with increases of Mg incorporation in ZnO thin films. Similar results were reported by various authors in their research [26-27]. This behaviour may attribute by the fact that MgO (7.8 eV) has a wider band gap compared to ZnO (3.37 eV) [28]. This has been shown in the Figure 2 of XRD analysis where intensity of crystallinity of crystal plane of (2 2 0) which refer to MgO increased as the concentration of doping increased. This showed that more crystal of MgO has been form and thus wider the band gap of thin films. Furthermore, bandgap of thin films formed with different concentration of Mg is significantly influenced by the concentration of Mg because the increasing trend of the bandgap and crystallinity of thin films is similar. Hence, it can be said that band gap energy of thin films that doped with different concentration at constant spin speed of 2000 rpm and annealing temperature of 400˚C is consistent with XRD result that represents the number of crystal growth of MgO thin film in plane (2 2 0). By varying spin speed, that bandgap energy of thin films increased as the spin speed increased. This increase in band gap energy may be due to increase of the formation of MgO crystal. As the spin speed is higher, the volume of thin films is lower and thus more MgO could be formed and lead to increase of band gap energy.

D. Photoluminescence Analysis

Photoluminescence spectrum normally provides information on the optically active defects and relaxation pathways of excited states. Figure 12 shows PL spectra of ZnO thin films doped with different concentration of Mg and fabricated using different spin speed. It shows that all the PL spectra located at two emission bands which are ultraviolet emission (~370 nm) and visible range (~ 580nm). The ultraviolet emission at around 370 nm related to energy band gap of ZnO is caused by the direct recombination of excitons of thin films. On the other hand, the visible range emission is normally due to the structural defects that caused by deep level emission such as vacancies of zinc or oxygen or interstitial of zinc or oxygen [29, 30].

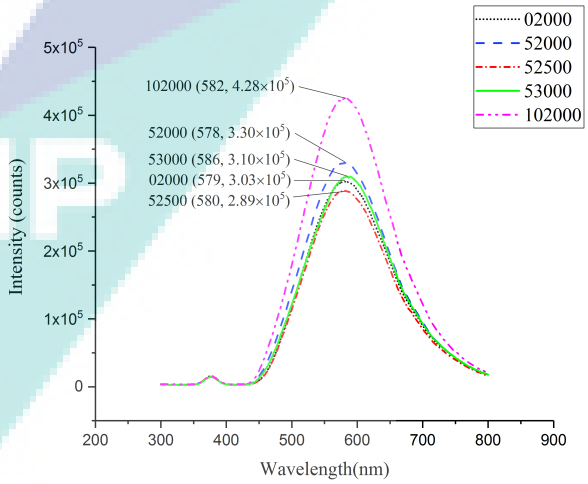

Figure 12: PL Spectrum of ZnO Thin Films that Doped with Mg with Different Spin Speed and Concentration of Mg

E. Electrical Analysis

The resistivity of thin films that doped with different concentration of Mg and spin speed was obtained by using four point probe method. The resistance of thin film was obtained and resistivity was calculated using formulae E1. (4):

$$\rho = RA/l \quad (4)$$

where R is resistance of thin films, A is area of thin films and l is length of thin films. Since the area and length of thin films could not be measured, therefore, the resistivity was presented in kilo ohm per □ where □ represents A/l .

Samples	Concentration of Mg (wt%)	Spin Speed (rpm)	Resistivity $(\frac{k\Omega}{\square})$
02000	0	2000	0.65
52000	5	2000	0.85
52500	5	2500	0.54
53000	5	3000	0.47
102000	10	2000	1.14

Table 3: Resistivity Value of Mg Doped ZnO Thin Films with Different Concentration of Mg and Spin Speed at Constant Annealing Temperature of 400˚C

Table 3 shows the resistivity value of ZnO thin films that doped with different concentration of Mg and spin speed. The results shows that ZnO thin films that doped with 10 wt% Mg and fabricated with spin speed of 2000 rpm has the highest value of resistivity which is 1.14 kΩ/□. On the other hand, ZnO thin films that doped with 5 wt% Mg and fabricated with 3000 rpm spin speed has the lowest resistivity value which is 0.47kΩ/□.

By varying concentration of Mg, the value of resistivity increased as the concentration of Mg increased. According to theory, Mg is a metal which conduct electricity. The valence band of Mg is overlaps with conduction band and there is no any band gap exists. Thus, this shows that Mg is a conductor. However, when Mg is doped into ZnO thin films, MgO is formed. MgO is an atoms that formed by ionic bond between Mg and O. The sharing of electron cause MgO becomes a stable atom and thus reduces the conductivity properties of Mg [28]. Therefore, as concentration of Mg is increased, the resistivity value of thin films is increased since more and more MgO is formed. This can be related to the intensity of crystallinity of crystal plane (2 2 0) which represents formation of MgO in thin films. The trend of graph for intensity of diffraction phase (b) plane (2 2 0) (dot symbol) as shown in Figure 2 is similar with resistivity of Mg doped ZnO thin films with different concentration. By varying spin speed, the resistivity value is decreased as the spin speed is increased. When the spin speed for fabricating the thin film is high, thinner layer of thin film is produced. When thinner the thin film, the area of thin films will reduces and hence the resistivity is decreased.

IV. CONCLUSION

The objectives of this research were to synthesis Mg doped ZnO thin film using sol gel method and spin coating technique and to characterize Mg doped ZnO thin film using XRD, FESEM, PL, UV-Vis and four point probe by varying spin speed and concentration of Mg dopants. Conclusively, ZnO thin films that undoped and doped with Mg have been successfully synthesized by using sol gel spin coating techniques. From XRD results, the films of Mg doped ZnO are synthesized with diffraction phases of crystal plane of (1 0 1) and (2 2 0) which represents ZnO and MgO respectively. FESEM shows that the thin films structure changed from fibre-liked shaped to circular inhomogeneous nanoparticles when Mg is used as doping source. This shows that doping is enhanced the surface morphology of thin films. Transmittance value for all ZnO thin films are over 80% in the visible range. On the other hand, the absorption spectra for all samples show sharp UV absorption edge in UV range. The optical bandgap increases as concentration of Mg and spin speed increases. However, PL spectra for all samples emitted electron at two emission band which are UV range (~370 nm) and visible range (~580 nm). The resistivity of Mg doped ZnO thin films are enhanced by introduction of Mg and increase with increase the concentration of Mg. However, the resistivity of Mg doped ZnO thin film that fabricated with different spin speed shows that the value decreases with increases of spin speed. If focus on the photonic application, the sample 102000 has the best result in term of characterization of PL since it has the highest intensity of peaks for PL.

ACKNOWLEDGMENT

This research was supported by internal grant of Universiti Malaysia Pahang under RDU1703194 and final year project fund.

REFERENCES

1. Seshan, K. (2002). Handbook of Thin-Film Deposition Processes and Techniques - Principles, Methods, Equipment and Applications (2nd Edition). Chapter 8 Sputtering and Sputter Deposition.
2. Kulkarni, S. S., Sawarkar Mahavidyalaya, S., & Shirsat, M. D. (2015). Optical and Structural Properties of Zinc Oxide Nanoparticles. International Journal of Advanced Research in Physical Science, 2(1), 14–18.
3. Fang, D., Li, C., Wang, N., Li, P., & Yao, P. (2013). Structural and optical properties of Mg-doped ZnO thin films prepared by a modified Pechini method. Crystal Research and Technology, 48(5), 265–272.
4. A.G.E. Sutjipto, M.H. Mazwir, L.Y. Har, M.A. Jusoh, R. Othman, "Effect of compaction pressure of green body and heating current on photoluminescence property of ZnO crystal grown by electric current heating method," IOP Conference Series: Materials Science and Engineering, 290(1), 012043, 2018.
5. Bautista Ruiz, J., Olaya Flórez, J., & Aperador, W. (2016). Effect of forming technique BixSiyOzcoatings obtained by sol- gel and supported on 316L stainless steel. Journal of Physics: Conference Series, 687(1).
6. A.G.E. Sutjipto, M. Takata, "The use of SEM to investigate the effect of an electron beam on the optically-visible flashover treeing of CaO added MgO ceramic," Journal of Materials Science 42(15), pp. 6036-6040, 2007.

7. A.G.E. Sutjipto, “The effect of CaO addition on the microstructural, mechanical and dielectric properties of pure MgO ceramic,” Key Engineering Materials, 345-346 II, pp. 1609-1612, 2007.
8. A.G.E. Sutjipto, T. Okamoto, M. Takata, “Appearance of flashover treeing on polycrystalline magnesia surface,” Key Engineering Materials, (181-182), pp. 231-234, 2000.
9. A.G.E. Sutjipto, Y.P. Asmara, M.A. Jusoh,” Behavior of MgO Based Ceramics under Electron Irradiation,” Procedia Engineering, 170, pp. 88-92, 2017.
10. Jufriadi, A.G.E. Sutjipto, R. Othman, R. Muhida, “Microstructure and electrical properties of AZO films prepared by RF magnetron sputtering,” Advanced Materials Research, 264-265, pp. 754-759, 2011.
11. Jufriadi, A.G.E. Sutjipto, R. Othman, R. Muhida, “Discharge, microstructural and mechanical properties of ZrO2 addition on MgO for plasma display panel materials,” Materials Research Innovations, 13(3), pp. 149-152, 2009.
12. A.G.E. Sutjipto, R. Muhida, M. Takata, “An SEM flashover: Technique to characterize wide band gap insulators,”Proceedings of the IEEE International Conference on Properties and Applications of Dielectric Materials 4062645, pp. 216-219, 2007.
13. S.H. Tan, N. A. Ismail, Materials Today: Proceedings, 5, 3193–3201, 2018.
14. Nanotechnology, T. F. (n.d.). “Thin Film Nanotechnology & Applications.”
15. Analysis of Global Research Activities With Future. (n.d.). Solar Cells, 1–17.
16. Thin Film Nanotechnology . (2016).
17. Chang, R. C., Chu, S. Y., Yeh, P. W., Hong, C. S., Kao, P. C., & Huang, Y. J. (2008). The influence of Mg doped ZnO thin films on the properties of Love wave sensors. Sensors and Actuators, B: Chemical, 132(1), 290–295.
18. Abed, C., Bouzidi, C., Elhouichet, H., Gelloz, B., & Ferid, M. (2015). Mg doping induced high structural quality of sol-gel ZnO nanocrystals: Application in photocatalysis. Applied Surface Science, 349, 855–863.
19. Shakti, N. (2010). Structural and Optical Properties of Sol-gel Prepared ZnO Thin Film. Applied Physics Research, 2(1), 19–28.
20. Shi, Q., Zhang, J., Zhang, D., Wang, C., Yang, B., Zhang, B., & Wang, W. (2012). Red luminescent and structural properties of Mg-doped ZnO phosphors prepared by sol-gel method. Materials Science and Engineering B: Solid-State Materials for Advanced Technology, 177(9), 689–693.
21. Chelouche, A., Touam, T., Tazerout, M., Djouadi, D., & Boudjouan, F. (2017). Effect of Li codoping on highly oriented sol-gel Ce-doped ZnO thin films properties. Journal of Luminescence, 188(April), 331–336.
22. Kim, Y. S., & Tai, W. P. (2007). Electrical and optical properties of Al-doped ZnO thin films by sol-gel process. Applied Surface Science, 253(11), 4911–4916.
23. Nithya, N., & Radhakrishnan, S. R. (2012). Effect of Thickness on the Properties ZnO Thin Films. Advances in Applied Science Research, 3(6), 4041–4047.
24. Garcés, F. A., Budini, N., Koropecki, R. R., & Arce, R. D. (2015). Structural Analysis of ZnO(:Al,Mg) Thin Films by X-ray Diffraction. Procedia Materials Science, 8, 551–560.
25. Jeetendra, S., Nagabhushana, H., Mrudula, K., Naveen, C. S., Raghu, P., & Mahesh, H. M. (2014). Concentration Dependent Optical and Structural Properties of Mo doped ZnTe Thin Films Prepared by e-beam Evaporation Method, 9, 2944–2954.
26. Verma, K., Chaudhary, B., Kumar, V., Sharma, V., & Kumar, M. (2017). Investigation of structural, morphological and optical properties of Mg: ZnO thin films prepared by sol-gel spin coating method. Vacuum, 146, 524–529.
27. Huang, K., Tang, Z., Zhang, L., Yu, J., Lv, J., Liu, X., & Liu, F. (2012). Preparation and characterization of Mg-doped ZnO thin films by sol-gel method. Applied Surface Science, 258(8), 3710–3713.
28. Tanaka, H., & Fujita, S. (n.d.). Fabrication of wide-band-gap Mg x Zn 1 − x O quasi-ternary alloys by molecular-beam epitaxy.
29. Band, V., & Band, C. (n.d.).) can conduct. To conduct electrons must acquire energy to jump from the valence to the conduction band. In electronic devices, this is usually supplied by a battery. # of conduction electrons , 1–3.
30. H. Saputra, R. Othman, A.G.E. Sutjipto, R. Muhida, R., M.H. Ani, “Gel-like properties of MCM-41 material and its transformation to MCM-50 in a caustic alkaline surround,” Materials Research Bulletin 47(3), pp. 732-736, 2012.

AGUS GETER EDY SUTJIPTO . <agusgeter@ump.edu.my>

Your paper has been accepted for publication in Postgraduate Symposium on Industrial Science and Technology 2019

Postgraduate Symposium on Industrial ... <9783035716641@scientific.net> Fri, Aug 30, 2019 at 10:31 AM
Reply-To: "Postgraduate Symposium on Industrial ..." <9783035716641@scientific.net>
To: Agus Geter Edy Sutjipto <agusgeter@ump.edu.my>

Dear Agus Geter Edy Sutjipto,

Your article «Sample Preparation of TiO_2 Added ZnO Using Powder Metallurgy Route and its Characteristics» has been accepted for publication in the «Postgraduate Symposium on Industrial Science and Technology 2019». Although no further action is required, you can verify the status of your article by logging in to the publisher's website :

Please to https://www.scientific.net and log in using the credentials below.
Username : agusgeter@ump.edu.my
Password : sfEGQ642

After you log in please select « Author » role near the top of the screen.

If any further changes in your article become necessary you must notify and obtain a permission from an Editor via E-mail PRIOR to uploading a new version.
Thank you very much.

Best regards,
Agus Geter Edy Sutjipto
agusgeter@ump.edu.my

Sample Preparation of TiO_2 Added ZnO using Powder Metallurgy Route and Its Characteristics

Agus Geter Edy Sutjipto[1, a *], Low Kai Ti[1,b], Yuli Panca Asmara[2], and Ari Legowo[3,c *]

[1]Faculty of Industrial Sciences & Technology, Universiti Malaysia Pahang, Malaysia

[2]Inti International University, Malaysia

[3]Aviation Engineering Technology and Science, Higher Colleges of Technology, Abu Dhabi Men's College, UAE

[a]agusgeter@ump.edu.my, [b]kaitilow@gmail.com, [c]alegowo@hct.ac.ae

*corresponding author

Keywords: TiO_2, ZnO, powder metallurgy, sensor, semiconductor

Abstract. Metal oxide semiconductor gas sensors have been widely utilized in a variety of different roles and industries. They are relatively inexpensive, robust, lightweight, long lasting and benefit from high material and quick response time compared to other sensing technologies. However, there are major challenges need to overcame by developers in order to construct a semiconductor metal oxide gas sensor that is efficient, and durable and most importantly can work at lower temperature. Therefore, in this research, TiO_2 dopants was introduced into conventional high purity ZnO gas sensor whereby the samples were prepared in pellet form using powder metallurgy route. The improvement in the mechanical properties as well as the electrical properties of the samples was wished to be observed through this research. The density measurement showed that the adding of TiO_2 was efficient to promote the densification of ZnO sample in which 9 wt% TiO_2 doped ZnO sample showed the highest density. The XRD results showed that the diffraction pattern was basically attributed to the wurtzite structure of ZnO. This was proven by the plane (1 0 1) had the highest intensity in all the samples except 6 wt% TiO_2 and 9 wt% TiO_2 doped ZnO sample. SEM showed that the grain size of ZnO decreased with the addition of TiO_2. This was caused by the formation of the new phase which was Zn_2TiO_4. The smaller the grain size, the higher the specific surface area and oxygen adsorption quantity, and therefore the higher the gas sensitivity is. UV-Vis showed that the wavelength of all samples was located around 380 nm. Therefore, the calculated exitonic energy was around 3.20 eV which was nearly matched with the theoretical band gap of ZnO (3.37 eV). The measurement of the resistivity using four point probe showed that the electrical resistivity of the samples decrease up to addition of 9 wt% TiO_2. This was attributed to increased carrier concentration. Vickers hardness test showed that the doping of TiO_2 had increased the hardness of the sample whereby the 9 wt% TiO_2 doped ZnO sample showed the highest value of hardness. The addition of TiO_2 into high purity ZnO has influenced the mechanical and electrical properties of ZnO. From observing the microstructural and density measurement to the measurement of the surface resistivity as well as the determination of the Vickers hardness value, it was found that 9 wt% TiO_2 doped ZnO was predicted as a candidate for substituting a conventional high purity ZnO as the gas sensor.

Introduction

Metal oxide semiconductor gas sensors have been widely utilized in a variety of different roles and industries. They are relatively inexpensive, robust, lightweight, long lasting and benefit from high material and quick response time if being compared with the other sensing technologies. By having all these features, they have been selected as a great candidate to measure and monitor trace

amounts of environmentally important gases such as carbon monoxide and nitrogen dioxide. Recent discoveries also prove that with the use of metal oxides as gas sensing materials at high working temperature can make the significant progress in moving away from bulky sensor architectures become reality [1].

Therefore, new approaches must be studied and explored so that the gas sensor can be operated at lower or room temperature. Recent studies has showed that UV light irradiation is one of the very useful way to improve the gas-sensing properties and reduces the working temperature [2] . To the best of our knowledge, few papers have been reported that there are two materials which have been proven to exhibit all of the properties required for a good gas sensing performance, namely zinc oxide (ZnO) [3], while the others, such as indium tin oxide (ITO), In_2O_3, CdO, $ZnSnO_4$, NiO, etc., have also been widely studied. However, several studies have reported that the properties of ZnO-based gas sensor still can be remarkably improved by introducing TiO_2 dopant into the sensing films [4], and the peculiar structure and morphology of the sensing materials can also be conducive to the low temperature gas-sensing performance.

Due to the simple manufacture technique, rapid response, low cost and recovery of semiconductor metal oxide (MOS) gas sensor, it has attracted a great attention in the past few years. Apart from that, due to emergence and rapid development of the science and new technology, the idea of integration of gas sensor components into smarts phone, tablets and wrist watches have become a popular issues among the developers, with the purpose of providing the individual with the ability to detect harmful chemicals and pollutants in the environment by using the always-on hand-held or wearable devices. However, there are major challenges need to overcame by developers in order to construct a semiconductor metal oxide gas sensor that is efficient, and durable and most importantly can work at lower temperature. In this case, the introduction of TiO_2 dopants into the conventional ZnO gas sensor play an important role in making the gas sensor become more user-friendly.

This paper presents the fabrication process of the TiO_2 doped ZnO sample using powder metallurgy route [5-21]. The progressions in microstructure of the samples were observed or examined by utilizing X-Ray diffraction (XRD) and scanning electron microscopy (SEM) and the samples were characterized also using the ultraviolet –visible (UV-Vis) Spectroscopy. Furthermore, the relationship between the electrical properties and mechanical properties of the sample with its varying weight fraction of TiO_2 was studied as well.

Experimental Setup

The ZnO and TiO_2 powders were applied for powder mixtures of various desired compositions. In this research, 5 sample, each with varying amount of TiO_2 powder with the fixed amount of ZnO powder. They are samples respectively which containing ZnO as their main constituent with 0 wt%, 3 wt%, 6 wt%, 9 wt%, and 12 wt% of TiO_2. For this purpose, 10 grams of ZnO powder with 99.95% purity was measured using digital weighing machine. After that, the amount of TiO_2 powder needed was weighted accordingly and mixed with the ZnO powder. by adopting powder metallurgy route. It contains three basic procedures which were powder grinding, die compaction and sintering. In this case, the powder was manually grinded instead of grinding using the ball mill. The mixed powder (ZnO and TiO_2) was grinded using agate mortar and pestle for about two hours to ensure the mixture is homogenous and yielding fine particle. After that, half of the amount of 30 ml ethanol was added into the TiO_2 doped ZnO powder gently. The mixture was grinded on hotplate manually and heated with temperature around 70.0°C. This was done to facilitate the evaporation of the ethanol. Following that, another half of the amount ethanol was added slowly into the mixture during grinding process. Grinding process was ended when the mixture became dry. After grinding process, the mixed powder was transferred to pelletizer mould as shown in **Error! Reference source not found.** to form the pellets. Prior to the transferring of the powder to pelletizer mould, the pelletizer mould was thoroughly cleaned with ethanol. This is because there should be no

presence of any lubricant which might contaminate the sample. Amount of mixed powder used to form each pellet was around 1.0 g and 3 pellets were prepared for each sample. The mass of each pellet was measured using the digital weighing machine. 1.0 g of the mixed powder was gently poured into the cavity of the pelletizer mould and hydraulic press was adopted for compaction of the pellets. The final step of powder metallurgy method was the sintering process. The pellets were sintered in a box metallurgical furnace as shown in **Error! Reference source not found.**. The box metallurgy furnace was used to sinter the pellet so that it was convenience for the pellets in handling into or out of the furnace. The pellets and powder were placed inside rectangular alumina crucible boats and circular alumina crucible boats respectively before handling into the box metallurgy furnace. Both the pellets and the powder were sintered at 1100°C to prevent formation of large grain size. The sintered rate was 16.5°C/minutes to prevent grain from growing rapidly. The sintering process took 5 hours to ensure a complete densification of pellets through high isolation of pores at grain edges and high neck growth. Characterization of sintered samples used XRD, SEM, UV-Vis, Surface electrical resistivity and Vickers hardness.

Results and Discussions

XRD. Figure 1 showed the comparison of XRD of all samples. The diffraction patterns was basically attributed to the wurtzite structure of ZnO. This was proven by the plane (1 0 1) had the highest intensity in all the samples except 6 wt% TiO_2 and 9 wt% TiO_2 doped ZnO sample. The highest intensity of 6 wt% TiO_2 doped ZnO sample was plane (1 1 0) while that of 9 wt% TiO_2 doped ZnO sample was plane (1 0 0). The sensing mechanism of ZnO based gas sensor is based on the surface of the semiconducting oxides. Therefore, the phase state is one of the important factors for gas sensitivity. It was found that Zn_2TiO_4 phase and ZnO phase exist in all the samples. Apart from ZnO and $Zn2TiO_4$ phase, TiO_2 phase also exist in the sensing material. The existence of the TiO_2 phase is due to the addition of excessive amount of TiO_2 powder. However, upon doping with 9 wt% TiO_2 and onward, TiO phase was exist instead of TiO.

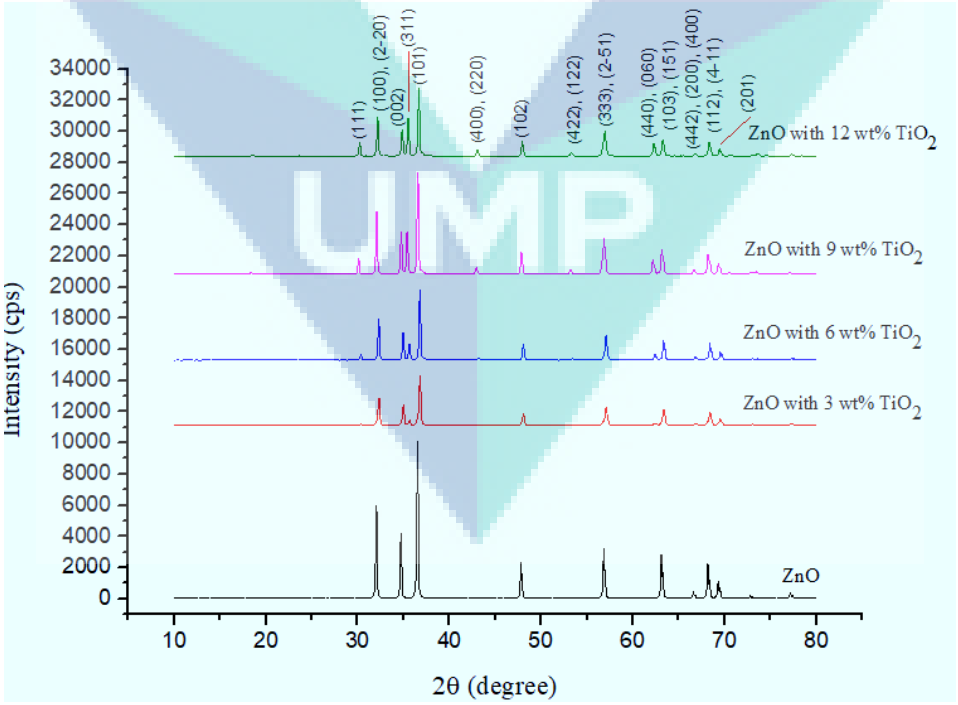

Fig. 1. XRD pattern for all samples of TiO_2 added ZnO.

SEM Images. Figure 2 shows the SEM images of all samples. It is clear that sample 4 with the composition of 9wt% TiO_2 visually less pores compared with others. The optimum densification

happened in this composition. Addition more TiO_2 will make reducing of densification. The grain growth will not further effective to increase the density.

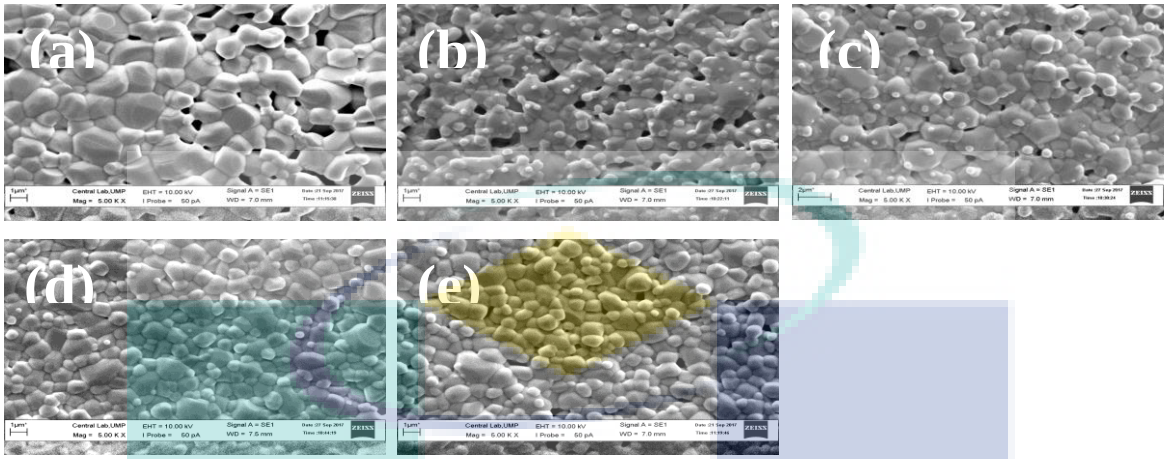

Fig. 2. SEM images for all samples of TiO_2 added ZnO respectively: (a) 0wt%, (b) 3wt%, (c) 6wt%, (d) 9wt% and 12wt% TiO_2 addition into high purity ZnO.

UV-vis. Figure 3 shows the UV-vis characterization for all samples (a) and table of threshold exitonic energy, absorbance and wavelength for all samples. The wavelength of first excitonic peak of each sample was found to be around 380 nm and the exitonic energy of most of the samples was around 3.20 eV which was nearly match with theoretical band gap 3.37 eV. The sample which doped with 3 wt% TiO_2 was found to absorb the longest wavelength which is equal to 380.5747 nm. The highest excitonic energy with the value of 3.3127 eV was exhibited by the sample when doped with 9 wt% TiO_2.

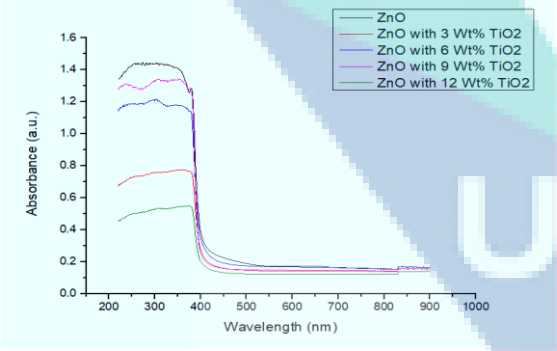

(a)

Sample	Absorbance (au)	Wavelength (nm)	Excitonic Energy (eV)
ZnO	1.2814	377.5549	3.2862
ZnO with 3 wt% TiO_2	0.7875	380.5747	3.2601
ZnO with 6 wt% TiO_2	1.1480	378.9760	3.2738
ZnO with 9 wt% TiO_2	1.2843	374.5350	3.3127
ZnO with 12 wt% TiO_2	0.5487	375.9561	3.3001

(b)

Fig. 3. UV-vis characterization for all samples (a) and table of threshold exitonic energy, absorbance and wavelength for all samples.

Electrical Resistivity. Error! Reference source not found. shows the electrical resistivity of each sample taken at three repetitions and average electrical resistivity of each sample respectively obtained using the four point probe technique respectively. It can be clearly seen that the electrical resistivity obtained for ZnO (0.6853 MΩ.m) is nearly match with the theoretical electrical resistivity of ZnO at room temperature which is equal to 0.75 MΩ.m. The electrical resistivity of the samples were observed to be decreasing when with increasing amount of TiO_2 being doped. However, upon the doping with 12 wt% TiO_2, the electrical resistivity increase again. For ZnO doped with TiO_2, the decrease in resistivity was due to the formation of the solid solution when Zn^{2+} was replaced with Ti^{4+}. Due to the almost similar ionic radii of both Zn^{2+} (0.074 nm) and Ti^{4+} (0.068 nm), the

reactions took place easily. This had lead to an increased carrier concentration and low resistivity for ZnO grains [22].

Table 1. Electrical resistivity for all samples

Sample	Average Electrical Resistivity (MΩ.m)
ZnO	0.6853
ZnO with 3 wt% TiO_2	0.4685
ZnO with 6 wt% TiO_2	0.2683
ZnO with 9 wt% TiO_2	0.1852
ZnO with 12 wt% TiO_2	0.1910

Vickers Hardness. For Vickers Hardness test (ASTM C1327-08), indentations were made on the surface of the pellets. The Vickers indenters had created a square impression and two surface-projected diagonal length were measured. The Vickers hardness was calculated form the ratio of applied load against area of contact of the indentation. Five indentations were made for each sample as shown in **Error! Reference source not found.** and average hardness was calculated and tabulated in 2. It can be clearly seen that the pellets exhibit the highest Vickers hardness with the value of 396 HVO.3 when being doped with 9 wt% TiO_2. In contrast, ZnO showed the lowest Vickers hardness with only 231.4 HVO.3.

Table 2. Vickers hardness for all samples

Sample	Averages Hardness (HVO.3)
ZnO	231.4
ZnO with 3 wt% TiO_2	297.1
ZnO with 6 wt% TiO_2	332.8
ZnO with 9 wt% TiO_2	396.8
ZnO with 12 wt% TiO_2	364.1

Summary

This research had proved that the 9 wt% TiO_2 doped ZnO was suitable to become a candidate for substituting a conventional high purity ZnO as the gas sensor. The addition of TiO_2 was able to promote densification of ZnO sample whereby 9 wt% TiO_2 doped ZnO showed the highest density. The analysis of the XRD results showed that the diffraction patterns of all the samples was basically attributed to the wurtzite structure of ZnO and there was the existence of a new phase Zn_2TiO_4 when doping with 3 wt% TiO_2 and onward. This can be proven by the plane (1 0 1) had the highest intensity in all the samples except 6 wt% TiO_2 and 9 wt% TiO_2 doped ZnO sample. Apart from that, from observing the microstructure of the samples, it was found that the doping of TiO_2 was able to decrease the grain size of the ZnO which believed to be effective in decreasing the working temperature of the gas sensor due to the increased surface activity of ZnO. Furthermore, the sample also exhibit the lowest electrical resistivity and highest Vickers hardness value when doped with 9 wt% TiO_2.

Acknowledgement

This study was supported by RDU grant of Universiti Malaysia Pahang RDU1703194 and Funding from Higher Colleges of Technology Abu Dhabi Men's College, UAE.

References

[1] C. Wang., L. Yin, L. Zhang, D. Xiang, & R. Gao, Metal oxide gas sensors: sensitivity and influencing factors. Sensors, 10(3), 2088-2106, 2010.

[2] P. Camagni, G. Faglia, P. Galinett, C. Perego, G. Samoggia, & G. Sberveglieri, Photosensitivity activation of SnO2 thin film gas sensors at room temperature. Sensors and Actuators B: Chemical, 31(1-2), 99-103, 1996.

[3] A. Bouaoud, A. Rmili, F. Ouachtari, A. Louardi, T. Chtouki, B. Elidrissi & H. Erguig, Transparent conducting properties of Ni doped ZnO thin films prepared by a facile spray pyrolysis technique using perfume atomizer. Materials Chemistry and Physics, 137(3), 843-847, 2013.

[4] C. Baratto, G. Sberveglieri, A. Onischuk, B. Caruso S. Di Stasio, S, Low temperature selective NO 2 sensors by nanostructured fibres of ZnO. Sensors and Actuators B: Chemical, 100(1), 261-265, 2004.

[5] A.G.E. Sutjipto, M.H. Mazwir, L.Y. Har, M.A. Jusoh, R. Othman: Effect of compaction pressure of green body and heating current on photoluminescence property of ZnO crystal grown by electric current heating method, IOP Conference Series: Materials Science and Engineering, 290(1), 012043, 2018.

[6] J. Bakri, Hens Saputra: A.G.E. Sutjipto, MFI Zeolite Membrane from Rice Husk for Biofuels Production, Applied Mechanics and Materials, Vol. 1787 (165), pp.104-108, 2012.

[7] A.G.E. Sutjipto, M. Takata: The use of SEM to investigate the effect of an electron beam on the optically-visible flashover treeing of CaO added MgO ceramic, Journal of Materials Science 42(15), pp. 6036-6040, 2007.

[8] A.G.E. Sutjipto: The effect of CaO addition on the microstructural, mechanical and dielectric properties of pure MgO ceramic, Key Engineering Materials, 345-346 II, pp. 1609-1612, 2007.

[9] A.G.E. Sutjipto, T. Okamoto, M. Takata: Appearance of flashover treeing on polycrystalline magnesia surface, Key Engineering Materials, (181-182), pp. 231-234, 2000.

[10] A.G.E. Sutjipto, Y.P. Asmara, M.A. Jusoh: Behavior of MgO Based Ceramics under Electron Irradiation, Procedia Engineering, 170, pp. 88-92, 2017.

[11] Jufriadi, A.G.E. Sutjipto, R. Othman, R. Muhida: Microstructure and electrical properties of AZO films prepared by RF magnetron sputtering, Advanced Materials Research, 264-265, pp. 754-759, 2011.

[12] A.R. Fatimah Azreen, A.G.E. Sutjipto, E.Y.T. Adesta: Fabrication of CuSiC composite by powder metallurgy route. Advanced Materials Research 264-265, pp. 748-753, 2011.

[13] Jufriadi, A.G.E. Sutjipto, R. Othman, R. Muhida: Discharge, microstructural and mechanical properties of ZrO2 addition on MgO for plasma display panel materials, Materials Research Innovations, 13(3), pp. 149-152, 2009.

[14] A.G.E. Sutjipto, R. Muhida, M. Takata: An SEM flashover: Technique to characterize wide band gap insulators, Proceedings of the IEEE International Conference on Properties and Applications of Dielectric Materials 4062645, pp. 216-219, 2007.

[15] H. Saputra, R. Othman, A.G.E. Sutjipto, R. Muhida, M.H. Ani: Gel-like properties of MCM-41 material and its transformation to MCM-50 in a caustic alkaline surround. Materials Research Bulletin. 47(3), pp. 732-736, 2012.

[16] H. Saputra, R. Othman, A.G.E. Sutjipto, R. Muhida, and M.H. Ani: Gel-like properties of MCM-41 material and its transformation to MCM-50 in a caustic alkaline surround, Material Research Bulletin, 47(3) pp. 732-736, 2012.

[17] A.R.F. Azreen, A.G.E. Sutjipto, E. Y. T. Adesta: Fabrication of CuSiC Composite by Powder Metallurgy Route, Advanced Materials Research, 264-265, pp 748-753, 2011.

[19] A.G.E. Sutjipto, Y.P. Asmara, M.A. Jusoh: Characteristic of MgO Based Ceramics under Electron Irradiation, Procedia Engineering (Elsevier), Vol. 170, pp. 88-92, 2017.

[20] R. Muhida, A.G.E. Sutjipto, Afzeri, T. Toyama, H. Okamoto: Relationship between average slope of textured substrate and poly-Si thin film solar cells performance. Materials Research Innovations 13 (3), pp. 246-248, 2009.

[21] A. R. F. Azreen, A.G.E. Sutjipto, A.S. Mohamad, Development of Cu-SiC composite for electrical discharge machining electrode using powder metallurgy technique, Advanced Materials Research, 576. pp. 203-207, 2012.

[22] J. Fan & R. Freer, The roles played by Ag and Al dopants in controlling the electrical properties of ZnO varistors. Journal of Applied Physics, 77(9), 4795-4800., 1995.

Universiti Malaysia PAHANG
Engineering • Technology • Creativity
UMP@ INSTITUTIONAL REPOSITORY (UMP IR)
Open Access Repository of UMP
Research & Publication
http://umpir.ump.edu.my

UMP INSTITUTIONAL REPOSITORY

Synthesis and characterizations of ZnO thin films deposited on aluminum metal substrate by sol-gel spin coating technique

Shaitir, Ali and Sutjipto, A. G. E. and Y., Shian (2018) *Synthesis and characterizations of ZnO thin films deposited on aluminum metal substrate by sol-gel spin coating technique.* In: Proceedings Book: National Conference for Postgraduate Research (NCON-PGR 2018), 28-29 August 2018 , Universiti Malaysia Pahang, Gambang, Pahang. pp. 133-138.. ISBN 978-967-22260-5-5

Pdf

Synthesis and Characterizations of ZnO thin17.pdf

Download (861kB) | Preview

DOI/Official URL: http://ncon-pgr.ump.edu.my/index.php/en/download/p...

Abstract

In this work, zinc oxide (ZnO) thin films were synthesized on aluminum substrate using sol-gel spin coating technique. The effect of changing in the annealing temperature (from 300 ◦C to 500 ◦C) and the rates of spin (from 1000rpm to 2000rpm) on the structural, optical and piezoelectric properties of the produced films are studied. Zinc acetate dehydrate, absolute ethanol and diethanolamine were used to act as sol gel precursor. Sol gel was coated on glass slide which wrapped by aluminum. The thin film was formed after preheating and annealing. The thin film was characterized by X-ray diffraction (XRD), Photoluminescence Spectroscopy (PL) and Ultraviolet-visible Spectroscopy (UV-Vis). X-ray analysis showed that thin films were preferentially diffracted around 65˚ which corresponding to (1 1 2) diffraction phase. From the PL results, there was only film with spin speed of 2000 rpm and annealing temperature of 300˚C had slightly left wavelength which was 380 nm. Annealing temperature would affect only the intensity of PL wavelength. From the results of UV-Vis, it was observed that when the spin speed was increased at same annealing temperature, the band gap was decreased. When the annealing temperature was increased at same spin speed, the band gap was decreased. This work provides a low cost and environment friendly material for Vibration sensing applications.

ITEM TYPE: Conference or Workshop Item (Lecture)

UNCONTROLLED KEYWORDS: Zinc oxide thin films; Sol-gel spin coating; Annealing temperature; Structural properties; Optical properties; Piezoelectric properties

SUBJECTS: Q Science > Q Science (General)

FACULTY/DIVISION: Faculty of Industrial Sciences And Technology

DEPOSITING USER: Pn. Hazlinda Abd Rahman

DATE DEPOSITED: 13 Dec 2018 04:50

LAST MODIFIED: 24 Jul 2019 03:05

URI: http://umpir.ump.edu.my/id/eprint/23059

DOWNLOAD STATISTIC: View Download Statistics

Actions (login required)

View Item

Synthesis and Characterizations of ZnO thin films deposited on aluminum metal substrate by sol-gel spin coating technique

Ali Shaitir [a], A.G.E. Sutjipto [b*], Y. Shian [c]
Faculty of Industrial Sciences & Technology
University Malaysia Pahang
Lebuhraya Tun Razak, 23600 Kuantan Pahang, Malaysia
[a] alishaiter@yahoo.com, [b] agusgeter@ump.edu.my

Abstract— In this work, zinc oxide (ZnO) thin films were synthesized on aluminum substrate using sol-gel spin coating technique. The effect of changing in the annealing temperature (from 300 ◦C to 500 ◦C) and the rates of spin (from 1000rpm to 2000rpm) on the structural, optical and piezoelectric properties of the produced films are studied. Zinc acetate dehydrate, absolute ethanol and diethanolamine were used to act as sol gel precursor. Sol gel was coated on glass slide which wrapped by aluminum. The thin film was formed after preheating and annealing. The thin film was characterized by X-ray diffraction (XRD), Photoluminescence Spectroscopy (PL) and Ultraviolet-visible Spectroscopy (UV-Vis). X-ray analysis showed that thin films were preferentially diffracted around 65° which corresponding to (1 1 2) diffraction phase. From the PL results, there was only film with spin speed of 2000 rpm and annealing temperature of 300°C had slightly left wavelength which was 380 nm. Annealing temperature would affect only the intensity of PL wavelength. From the results of UV-Vis, it was observed that when the spin speed was increased at same annealing temperature, the band gap was decreased. When the annealing temperature was increased at same spin speed, the band gap was decreased. This work provides a low cost and environment friendly material for Vibration sensing applications.

.

Keywords— Zinc oxide thin films; Sol-gel spin coating; Annealing temperature; Structural properties; Optical properties; Piezoelectric properties

1. INTRODUCTION

Zinc oxide is a non toxic, abundant, low cost and wide direct band-gap (3.2–3.4 eV) II–VI compound semiconductor [1–3]. This leaves it within the visible region having high optical transmission, suitable for solar spectrum [1]. Therefore, it has vast applications in optoelectronics device because of its structural, electrical and optical properties [4–9]. Due to these promising characteristics, thin films of ZnO have showed the considerable attention in the literature [1,10–12]. It is proposed that Multilayered ZnO thin films can increased the electrical properties of films [2]. Optimized multilayered ZnO films can be designed to have low resistivity and high solar transparencies in the visible region that are needed for the applications in solar cells and light emitting diodes [13].

The low cost and small time require for the synthesis of ZnO thin films for industrial requirements is always a need. Multilayered thin films of ZnO can be deposited by several methods such as magnetron sputtering [14], pulsed laser deposition [15] and spray pyrolysis [16]. Among them sol-gel technique is simple, low cost and large area deposition technique.

The review of literature showed that the properties of stacked ZnO thin films layers, deposited by sol-gel technique, which is cost effective and easy deposition technique, has not been studied yet. Current study will facilitate to fabricate optoelectronic devices with affordable cost. In present work, the structural, electrical and optical properties of multilayers of ZnO thin films deposited by sol-gel spin coating has been discussed [22-24].

.

2. METHODOLOGY

The stacked layers of ZnO thin films were prepared by using solgel method. The ZnO solution was prepared by dissolving 0.88 g of ‘‘Zinc acetate dehydrates” in the 20 ml of ‘‘2-methoxyethanol”. Then this solution was stirred with the help of magnetic stirrer at 60 ºC for 30 min. After that the ‘‘Mono ethanol amine” as a stabilizer was added in this solution and stirred the solution for 90 min at the temperature of 60 º C. The clear homogeneous solution of ZnO was obtained by aging this solution for 24 h.

The solution is now ready to prepared films. Now the aluminum substrate is fixed on spin coating system and its disc speed is changing (from 1000rpm to 2000rpm). The rotation time is 30s per sample. The drops of sol-gel solution are dropped on the aluminum substrate as per requirement of layers. After 30 s, the aluminum substrate is removed from spin coating disc and placed on the hot plate for almost 10 min to dry at 100 º C. The experiment is repeated to make thin films with multilayer.

The thin films are put in Furnace with changing in the annealing temperature (from 300 ˚C to 500 ˚C). Then the furnace is switched off and each sample is left to cool down until it reaches room temperature. Then samples are taken from the furnace and now they are ready to analyze.

3. RESULTS AND DISCUSSION

A. XRD results

From Figure 1, the angle of highest peak was ~45°. The lattice parameters of films were a = 3.4 Å and c = 5.1 Å. These values were similar to the values reported for good quality piezoelectric ZnO thin films [17]. For the plane of ZnO, it could be found that all the films were preferentially oriented in the (1 1 2) direction at ~65°. The presence of the (0 0 2) peak in some films, indicates that the as-deposited ZnO thin films have strong c-axis orientation perpendicular to the substrate. Higher degree of c-axis orientation and (0 0 2) preferred crystalline structure improve the piezoelectric properties of the ZnO thin film [18]. The presence of (0 0 2) diffraction phase was due to the precursor solution used was ZnAc which promotes the growth of crystal in (0 0 2) direction [19]. Some of the films could not find the peak of (0 0 2) may due to destructive interference happened.

Table 1 shows the average crystallite size of ZnO films with different spin speed and annealing temperature. When the annealing temperature was increased, the crystallite size was increased. The crystallite size was decreased from 0.5832 nm to 0.4955 nm and to 0.4512 nm. It had shown that temperature could affect material crystal sizes.

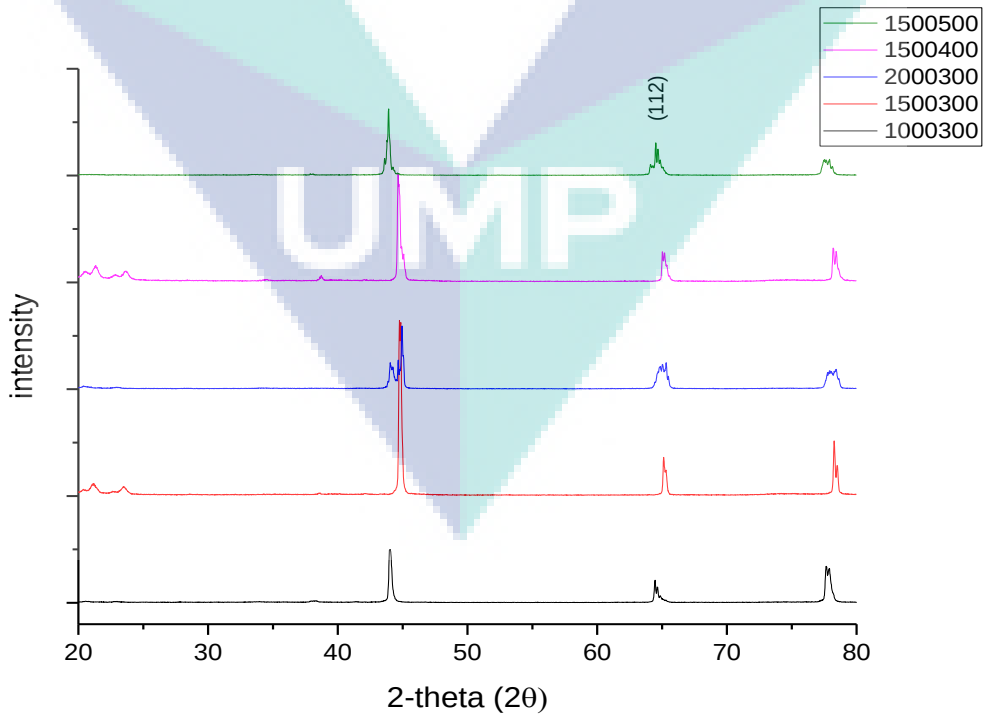

Figure 1: XRD pattern of ZnO thin films.

Table 1: (h k l) plane, d-spacing and crystalline size for the ZnO thin films with different spin speed and annealing temperature.

Sample	Spin Speed (rpm)	Anneal Temperature (°C)	2θ (°)	(h k l)	d-spacing	FWHM	Average Crystalline Size, nm
A	1000	300	43.9918 64.4470	(1 0 1) (1 1 2)	2.0566 1.44570	0.181 0.174	0.8405
B	1500	300	65.1421 74.0400	(1 1 2) (0 0 4)	1.43083 1.27900	0.151 2.260	0.5832
C	2000	300	34.3700 65.0830 78.3940	(0 0 2) (1 1 2) (1 0 4)	2.60700 1.43199 1.21882	1.100 0.260 0.256	0.4878
D	1500	400	34.4700 65.0300 74.1000	(0 0 2) (1 1 2) (0 0 4)	2.60000 1.43303 1.27800	0.560 0.142 2.500	0.4955
E	1500	500	33.6100 64.8820 75.5000	(0 0 2) (1 1 2) (2 0 2)	2.66400 1.43594 1.25900	0.900 0.143 4.000	0.4512

B. PL results

PL spectra of ZnO films were shown in Figure 2. The emission spectrum of ZnO thin film showed the peak was at narrow band ~380 nm. It was corresponding to band edge emission. It was due to free exciton emission. It has ultraviolet region. The PL spectrum also showed a wide broad peak of green emission at ~500 nm. The green emission was due to the existence of intrinsic defects, which are zinc vacancies and oxygen interstitial [20]. It could be observed that when the annealing temperature was increased, the wavelength intensity was increased. This was because of the oxygen and zinc atoms in interstitial site moved to lattice sites. It was also due to surface grain area increases [21]. From Figure 2, it can be seen that there was insignificant change in wavelength; this is because the wavelength shift only caused by composition of precursor but not annealing temperature and spin speed. Annealing temperature had only changed the intensity of wavelength [19].

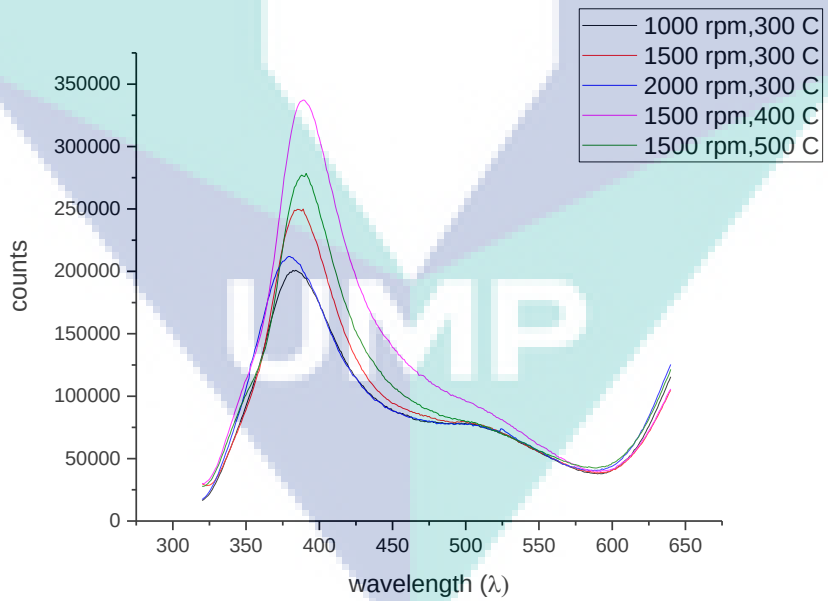

Figure 2: PL spectrum of ZnO thin film with different spin speed and annealing temperature.

C. UV-Vis Analysis

From Figure 3 to Figure 7 show the UV emission spectrum of ZnO with different spin speed and annealing temperature. Table 2 showed the energy band gap of each ZnO film with different spin speed and annealing temperature. It could be found that when increasing the annealing temperature, the energy band gap was decreased. The highest band gap (3.6109 eV) was belong to ZnO film with spin speed of 1000 rpm and annealing temperature of 300 °C.

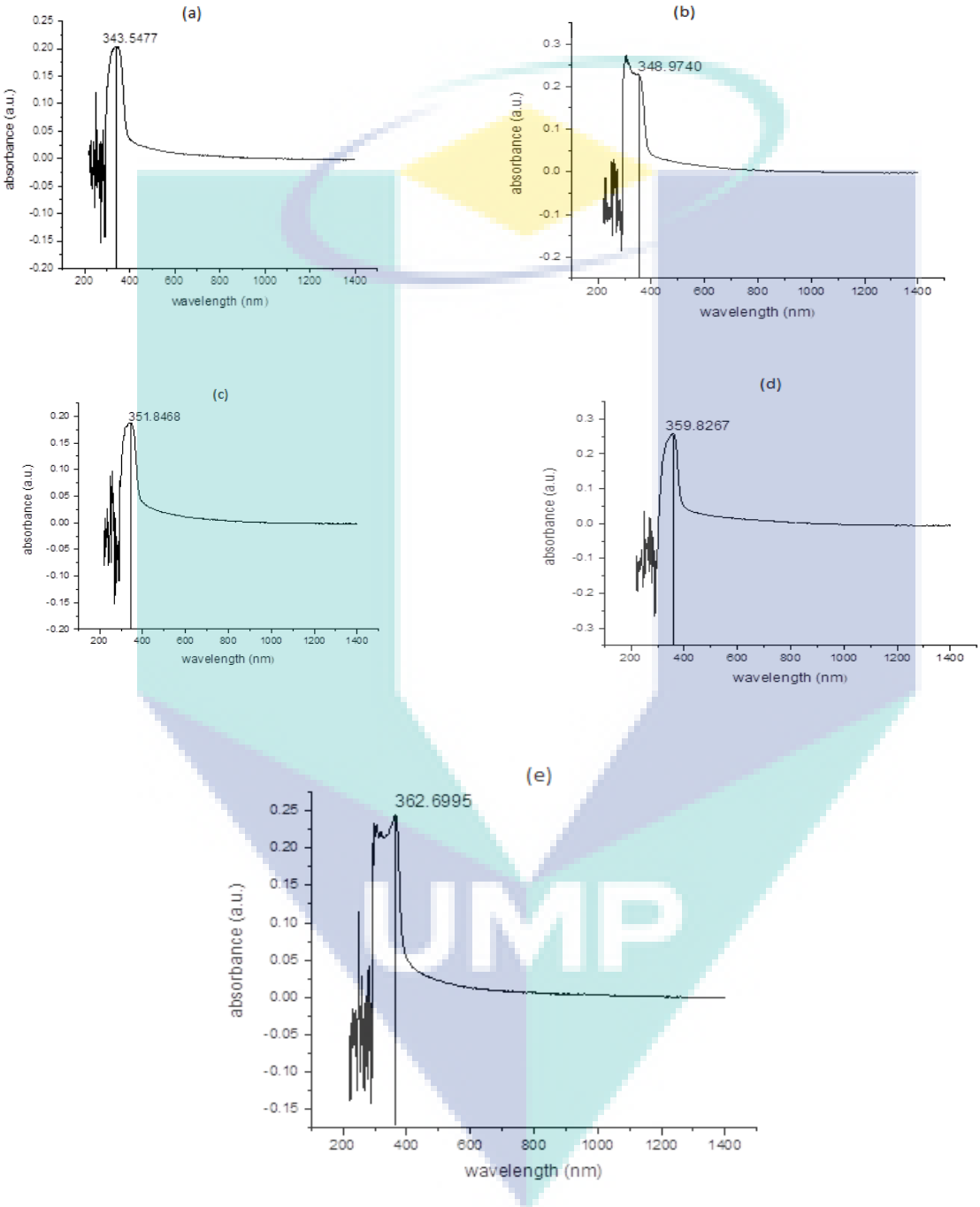

Figure 4: UV spectrum of ZnO film with (a-1000 rpm and 300 °C), (b-1500 rpm and 300 °C), (c- 2000 rpm and 300 °C), (d-1500 rpm and 400 °C), and (e- 1500 rpm and 500 °C) respectively.

Table 2: Energy band gap of UV emission peak at different spin speed and annealing temperature of ZnO thin film.

Sample	Spin Speed (rpm)	Anneal Temperature (°C)	First Excitonic Peak (nm)	Energy band gap (eV)
A	1000	300	343.5477	3.6109
B	1500	300	348.9740	3.5547
C	2000	300	351.8468	3.5257
D	1500	400	359.8267	3.4475
E	1500	500	362.6995	3.4202

4. CONCLUSIONS

In summary, ZnO multilayer thin films were prepared by sol-gel method. XRD confirms the hexagonal wurtzite structure. PL results shows that, there was only film with spin speed of 2000 rpm and annealing temperature of 300°C had slightly left wavelength which was 380 nm. Results of UV-Vis shows that, the band gap was decreased when (the spin speed or the annealing temperature) were increased.

ACKNOWLEDGMENT

This work was supported by Universiti Malaysia Pahang (UMP).

REFERENCES

[1] E.R. Rwenyagila, B.A-. Tuffour, M.G.Z-. Kana, O.A-. Ojo, and W.O. Soboyejo, "Optical properties of ZnO/Al/ZnO multilayer films for large area transparent electrodes," J. Mater. Res. 29, 2912, 2014.

[2] K. Sivaramakrishnan, and T. Alford, "Conduction and transmission analysis in gold nanolayers embedded in zinc oxide for flexible electronics," Appl. Phys. Lett., 96, 201109, 2010.

[3] M.A-. Kuhaili, M.A-. Maghrabi, S. Durrani, and I. Bakhtiari, "Investigation of ZnO/Al/ZnO multilayers as transparent conducting coatings," J. Phys. D. Appl. Phys., 41, 215302, 2008.

[4] M. Copuroglu, K. Koh, S.O. Brien, and G.M. Crean, "Comparative characterisation of zinc oxide thin films prepared from zinc acetate with or without water of hydration via the sol-gel method," J. Sol-Gel Sci. Technol., 52,432, 2009.

[5] D.C. Look, "Recent advances in ZnO materials and devices," Mater. Sci. Eng. B 80, 383, 2001.

[6] T. Minami, "Transparent conducting oxide semiconductors for transparent electrodes," Semicond Sci Technol., 20,S35. 2005.

[7] L. Spanhel, and M.A. Anderson, "Semiconductor clusters in the sol-gel process: quantized aggregation, gelation, and crystal growth in concentrated zinc oxide colloids," J. Am. Chem. Soc., 113, 2826, 1991.

[8] S.O. Brien, L. Koh, and G.M. Crean, "ZnO thin films prepared by a single step sol-gel process," Thin Solid Films, 516,1391, 2008.

[9] M. Ohyama, H. Kozuka, T. Yoko, and S. Sakka, "Preparation of ZnO films with preferential orientation by sol-gel method," Nippon Seramikkusu Kyokai Gakujutsu Ronbunshi, 104, 296, 1996.

[10] X. Wang, J. Song, J. Liu, and Z.L. Wang, "Direct-current nanogenerator driven by ultrasonic waves," Science, 316:102, 2007.

[11] Y. Yang, C. Song, X. Wang, F. Zeng, and F. Pan, "Giant piezoelectric d33 coefficient in ferroelectric vanadium doped ZnO films," Appl. Phys. Lett., 92, 12907, 2008.

[12] Y.C. Yang, C. Song, F. Zeng, F. Pan, Y.N. Xie, and T. Liu, "Induced ferroelectric behavior in V-doped ZnO films," Appl. Phys.Lett., 90, 242903, 2007.

[13] D. Sahu, and J.L. Huang, "Design of ZnO/Ag/ZnO multilayer transparent conductive films," Mater. Sci. Eng. B 130, pp.295, 2006.

[14] L.W. Lai, and C.T. Lee, "Investigation of optical and electrical properties of ZnO thin films," Mater. Chem. Phys., 110, pp. 393, 2008.

[15] V. Vaithianathan, Y.H. Lee, B.T. Lee, S. Hishita, and S.S. Kim, "Doping of As, P and N in laser deposited ZnO films," J. Cryst. Growth, 287, pp. 85, 2006.

[16] S. Studenikin, M. Cocivera , W. Kellner, and H. Pascher, "Band-edge photoluminescence in polycrystalline ZnO films at 1.7" J. Lumin, vol. 91, pp. 223, 2000.
[17] M. Kadota, and M. Minakata, "Piezoelectric Properties of Zinc Oxide Films on Glass Substrates Deposited by RF-Magnetron-Mode Electron Cyclotron Resonance Sputtering System," IEEE, Trans., Ultrason., Ferroelec., Frequency Control 1995, 42, pp. 345−350.
[18] R.O-. Ndong, G. Ferblantier, M. Kalfioui, A. Boyer, and A. Foucaran, "Properties of RF Magnetron Sputtered Zinc Oxide Thin Films," J. Cryst. Growth 2003, 255, pp. 130−135.
[19] P. Sagar, P. Shishodia, R. Mehra, H. Okada, A. Wakahara, and A. Yoshida, "Photoluminescence and absorption in sol-gel-deroved ZnO films," Journal of Luminescence, 2007, pp. 800-806.
[20] L. Xu, G. Zheng, M. Lai, and S. Pei, "Annealing impact on the structural and photoluminescence properties of ZnO thin films on Ag substrate," Journal of Alloys and Compounds, 2014, pp. 560-565.
[21] Y. Li, L. Xu, X. Li, X. Shen, and A. Wang, "Effect of aging time of ZnO sol on the structural and optical properties of ZnO thin films prepared by sol-gel method," Applied Surface Science, 2010, pp. 4543-4547.
[22] M.I. Khan, K.A. Bhatti, R. Qindeel, L.G. Bousiakou, N. Alonizan, and A. Fazal, "Investigations of the structural, morphological and electrical properties of multilayer ZnO/TiO2 thin films, deposited by sol–gel technique," Results Phys., 6, 2016, pp.156–60.
[23] J. Li, D. Yang, and X. Zhu, "Effects of aging time and annealing temperature on structural and optical properties of sol-gel ZnO thin films," AIP. Adv., vol. 7, 065213, 2017.
[24] L.H. San, N.S. Shiong, and Y.F. Kwong, "Sol–gel spin coating growth of magnesium-doped indium nitride thin films," Vacuum, vol. 155, pp.16-22, 2018.

PAPER • **OPEN ACCESS**

Effect of compaction pressure of green body and heating current on photoluminescence property of ZnO crystal grown by electric current heating method

To cite this article: A G E Sutjipto *et al* 2018 *IOP Conf. Ser.: Mater. Sci. Eng.* **290** 012043

View the article online for updates and enhancements.

IOP ebooks™

Bringing you innovative digital publishing with leading voices to create your essential collection of books in STEM research.

Start exploring the collection - download the first chapter of every title for free.

This content was downloaded from IP address 103.53.32.140 on 10/06/2019 at 21:04

IOP Conf. Series: Materials Science and Engineering **290** (2018) 012043 doi:10.1088/1757-899X/290/1/012043

Effect of compaction pressure of green body and heating current on photoluminescence property of ZnO crystal grown by electric current heating method

A G E Sutjipto[1], M H Mazwir[1], H L Yee[1], S R Misskon[2], A G M Shaitir[1], M A Jusoh[1] and R Othman[2]

[1]Material Technology Program, Faculty of Industrial Sciences & Technology, Universiti Malaysia Pahang (UMP), Gambang, 26300 Pahang, Malaysia
[2]Department of Science in Engineering, Faculty of Engineering, International Islamic University Malaysia (IIUM), Jalan Gombak, 53300 Kuala Lumpur, Malaysia

Corresponding author: agusgeter@ump.edu.my

Abstract. In this study, we reported the effect of applied compaction pressure on green body and electric current heating on ceramic bar on the ZnO crystal growth and its photoluminescence characteristic. Crystals grown on ZnO bar sintered by 1100 ^{o}C were mostly on (1 0 1) orientation. Sample with 3.0 ton and 3.0 A for applied pressure and current, respectively revealed the shortest photoluminescence (PL) wavelength of 409.5 nm with highest emission energy of 3.03 eV.

1. Introduction

ZnO has gained substantial interest in the research community because of its large exciton binding energy (60 meV) and wide direct band gap (Eg ~ 3.37 eV) at room temperature (R.T.). This large exciton binding energy paves the way for an intense near-band-edge excitonic emission such as lasing action at R.T. and higher temperatures, because this value is 2.4 times larger than that of the room temperature thermal energy (kBT = 25 meV). In addition, the interest in ZnO is fueled and fanned by its prospects in electronics and photonics applications, viz. transparent electrodes in solar cells, flat display devices and novel solid-state ultraviolet (UV) lasers owing to its direct wide band gap [1–7].

Many works have been done on the fabrication of ZnO micro/nanostructures with high aspect ratios using metalorganic chemical vapor deposition [8], thermal evaporation and thermal decomposition [9]. But these techniques appear to be involved process with many complex steps, require sophisticated equipment and rigorous experimental conditions. However, some of them have drawbacks like long reaction time, toxic templets and exotic metal catalysts, and low purity or poor crystallite quality of products, which may influence the quality and applications of ZnO. So there is still the need for developing a method that can produce the ZnO micro/nanostructures in laboratory environment with high quality, high repeatability and low cost process for a wide range of applications. Hence, a novel technique called ECH for the preparation of ZnO micro/nanocrystals [10-12].

When a certain direct current flowed through a sample of ZnO ceramic bar, the sample was Joule-heated, and the crystal growth occurred. ZnO is a key technological material. The lack of a centre of symmetry in wurtzite, combined with large electromechanical coupling, results in strong piezoelectric

Content from this work may be used under the terms of the Creative Commons Attribution 3.0 licence. Any further distribution of this work must maintain attribution to the author(s) and the title of the work, journal citation and DOI.
Published under licence by IOP Publishing Ltd

and pyroelectric properties and the consequent use of ZnO in mechanical actuators and piezoelectric sensors. In addition, ZnO is a wide band-gap (3.37 eV) compound semiconductor that is suitable for short wavelength optoelectronic applications. The high exciton binding energy (60 meV) in ZnO crystal can ensure efficient excitonic emission at room temperature and room temperature ultraviolet (UV) luminescence has been reported in disordered nanoparticles and thin films. The objective of this research was to investigate the effect of compaction pressure and current on the crystal growth and its PL characteristics.

2. Experimental procedures

The amount of 10 grams of ZnO powder with 99.00% purity was measured using digital weighing machine. The weighted ZnO powder was grinded manually with mortar and pestle for 6 hours at room temperature to achieve find particles. Ceramic bar of ZnO with average dimension of 13.00 mm x 2.50 mm x 1.00 mm each were formed by adopting powder metallurgy methods. It contained three basic steps which were powder grinding, die compaction and sintering. Firstly, half of the amount of 30ml ethanol was added into ZnO powder gently. The mixture was grinded on hotplate manually and heated with temperature around 70.0°C. Another half of the amount ethanol was added slowly into the mixture during grinding process. Grinding process was end once the mixture was dry. The amount of 1.5 gram ZnO powder was prepared to make green body using compaction die with dimension of 14.95 mm x 30 mm x 40 mm. Different green body was made by different in applying compaction pressure of 2 and 3 tons, respectively. The green body of different applied compaction pressure was then sintered under 1100 °C with rate of 16.5 °C/min for 3 hrs. The sintered ceramic was then cut into 13.00 mm x 2.50 mm x 1.00 mm each prior to ECH. The current applied into the ECH was vary from 2.5 to 3.5 A. Figure 1 shows the ECH process until the crystal grew on the surface of ceramic bar.

Figure 1. Electric current heating applied into ceramic bar for ZnO crystal growth. It is shown on the 3rd figure the crystal grew on the surface of ceramic bar.

Characterization and observation were carried out for XRD RIGAKU Miniflex II, UV-vis, scanning electron microscope Carl Zeiss EVO 50, and PL spectroscopy NIR 300/2.

3. Results and Discussion

Sample of SZ2, SZ3, SZ4, SZ12, SZ13, SZ14 and SZ15 were chosen to conduct ECH process. The treatment of each sample is listed in table 1.

Table 1. The percentage of relative density of ZnO bars after sintered used in this research.

Pressure Applied (Ton)	Current (A)	Sample	Volume (cm^3)	Density (g/cm^3)	Relative density (%)
2.0	2.50	SZ3	0.0249	5.1807	92.41
	3.00	SZ4	0.0248	5.2823	94.23
	3.50	SZ2	0.0263	5.3612	95.63
3.0	2.50	SZ15	0.0308	4.8377	86.29
	3.00	SZ12	0.0289	5.0519	90.12
	3.50	SZ13	0.0318	5.1887	92.56
	3.50	SZ14	0.0357	4.6779	83.44

Figure 2 shows the comparison of XRD of all samples where red colour of planes correspond to Cu powder and black colour of planes were contributed by ZnO crystal. The XRD results showed most of the crystals grew on the plane (1 0 1). The crystal was in rock like shape. This was proved by the plane (1 0 1) had the highest intensity in all the samples except SZ13 and SZ14. The highest intensity of crystal grew in SZ13 was plane (1 0 0). The highest intensity of crystal grew in SZ14 was contributed by Cu since large amount of Cu powder was placed on top of ZnO bar. This had affect the growth of ZnO crystal.

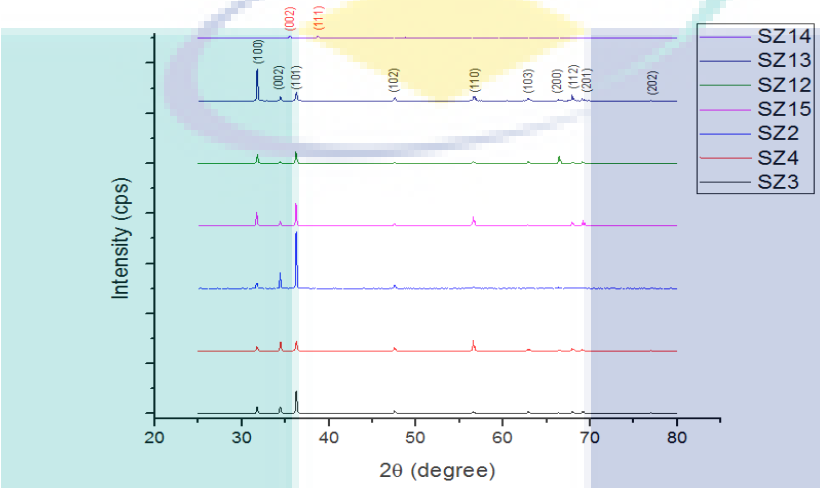

Figure 2. XRD of all samples where red colour of planes correspond to Cu powder and black colour of planes were contributed by ZnO crystal.

Figure 3 shows the comparison of the crystals grown and PL spectra between samples. Crystal like structures were grown on the surface of ceramic bars such as flower like (SZ12), grass like (SZ13),

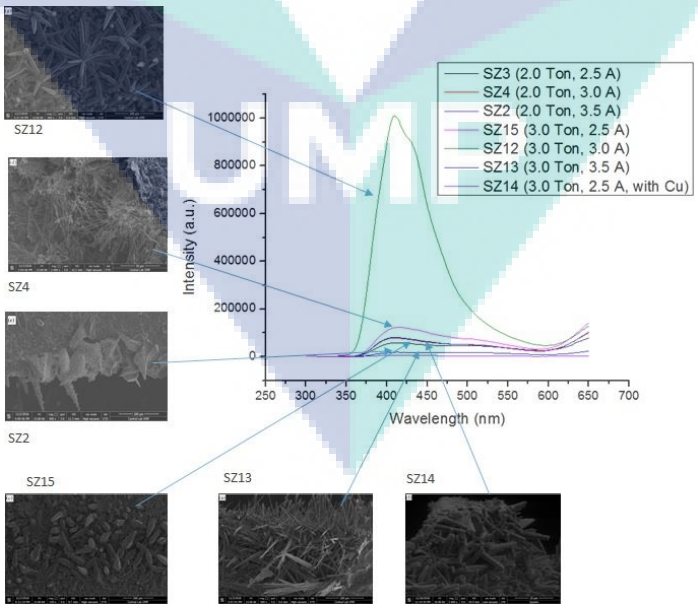

Figure 3. Comparison of SEM images and PL spectra between samples.

needle shape like (SZ4), KLCC tower like (SZ15), fish sting like (SZ2), and hexagonal shape like (SZ14). Under the PL spectrometer, the wavelength of samples SZ3, SZ4, SZ2, SZ15, SZ12, SZ13, and SZ14 were respectively 415, 411, 412, 413, 409, 412, and 415 nm. The shortest wavelength belonged to SZ12 has the highest intensity of about 1 million a.u. and 10 to 15 times higher than the other samples. The sample SZ12 which was under 3 tons and 3 A has the highest emission energy of 3.03 eV. This result was consistent with the result of UV-Vis spectrometer (see figure 4). The wavelength (in nm) and the excitonic energy (in eV) of SZ3, SZ4, SZ2, SZ15, SZ12, SZ13, and SZ14 are respectively 372 (3.34), 387 (3.21), 371 (3.34), 376 (3.30), 387 (3.20), 376 (3.30), and 376 (3.30). Sample 12 had emitted the longest wavelength and thus own the lowest excitonic energy. This showed that electron in SZ12 can be excited most easy among all samples.

4. Conclusion

In summary, it can be concluded that the sintered ZnO ceramic bar (SZ12) fabricated under 3 tons compaction pressure of green body with dimension of 13.0 mm x 2.5 mm x 1.0 mm and under ECH with input current of 3 A has the optimum value among the investigated samples. SZ12 sample revealed that it had the lowest exciton energy of 3.20 eV, the highest emission energy of 3.02 eV, the most significant crystal growth of flower like crystal.

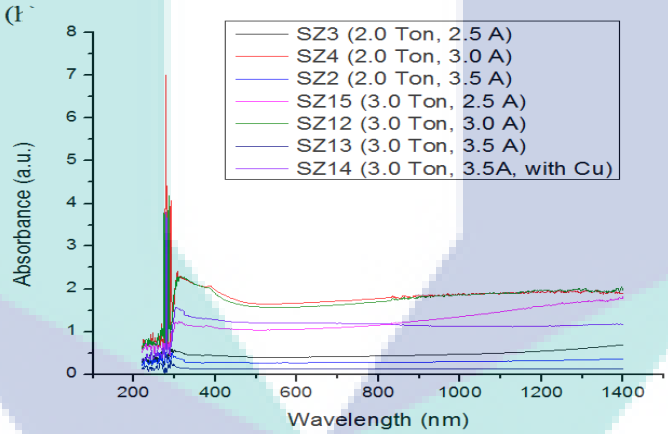

Figure 4. The result of UV-Vis spectrometer between samples.

Acknowledgement

This work was financially supported by Fundamental Research Grant Scheme 2016 (FRGS/1/2016/STG02/UMP/02/1), Ministry of Higher Education Malaysia and UMP Grant RDU1703194.

References

[1] R Sivakumar, T Tsunoda, Y Kuroki, T Okamot and M Takata 2012 *Mat. Chem and Phys* **134** 345– 349
[2] J Zhan, H Dong, S Sun, X Ren, J Liu, Z Chen, C Lienau and L Zhang 2016 *Adv. Optical Mater.* **4** 126–134
[3] D D Wang, G Z Xing, J H Yang, L L Yang, M Gao, J Cao, Y J Zhang and B Yao 2010 *J. Alloys Compd.* **504** 22
[4] R Sivakumar, K Punitha, C Sanjeeviraja, R Gopalakrishnan, 2014 *Materials Letters* **121** 141–144
[5] G H Nam, S H Baek, C H Cho and I K Park 2014 *Nanoscale*
[6] M Willander, L L Yang, A Wadesa, S U Ali, M H Asif, Q X Zhao and O Nur 2009 *J. Mater.*

Chem. **19** 1008
[7] A G E Sutjipto and L A Gafar 2012 *Contemporary Metallic Materials*, IIUM Press 141-146
[8] G Zhang, A Nakamura, T Aoki, J Temmyo and Y Matsui 2006 *Appl. Phys. Lett.* **89** 113112
[9] R Yousefi and B Kamaluddin 2009 *J. Alloys Compd*. **479** 11
[10] D Nezaki, S Takano, Y Kuroki, Y Kurihara, T Okamoto and M Takata 2000 *Trans. Mater. Res. Soc. Jpn.* **25** 205
[11] D Nezaki, T Okamoto and M Takata 2002 *Key Eng. Mater*. **228–229** 241
[12] H Yamasaki, K Minato, D Nezaki, T Okamoto, A Kawamoto and M Takata 2004 *Solid State Ionics* **172** 349

AGUS GETER EDY SUTJIPTO . <agusgeter@ump.edu.my>

Your paper has been accepted for publication in Postgraduate Symposium on Industrial Science and Technology 2019

Postgraduate Symposium on Industrial ... <9783035716641@scientific.net> Fri, Aug 30, 2019 at 10:31 AM
Reply-To: "Postgraduate Symposium on Industrial ..." <9783035716641@scientific.net>
To: Agus Geter Edy Sutjipto <agusgeter@ump.edu.my>

Dear Agus Geter Edy Sutjipto,

Your article «Sample Preparation of TiO_2 Added ZnO Using Powder Metallurgy Route and its Characteristics» has been accepted for publication in the «Postgraduate Symposium on Industrial Science and Technology 2019». Although no further action is required, you can verify the status of your article by logging in to the publisher's website :

Please to https://www.scientific.net and log in using the credentials below.
Username : agusgeter@ump.edu.my
Password : sfEGQ642

After you log in please select « Author » role near the top of the screen.

If any further changes in your article become necessary you must notify and obtain a permission from an Editor via E-mail PRIOR to uploading a new version.
Thank you very much.

Best regards,
Agus Geter Edy Sutjipto
agusgeter@ump.edu.my

Sample Preparation of TiO_2 Added ZnO using Powder Metallurgy Route and Its Characteristics

Agus Geter Edy Sutjipto[1, a *], Low Kai Ti[1,b], Yuli Panca Asmara[2], and Ari Legowo[3,c *]

[1]Faculty of Industrial Sciences & Technology, Universiti Malaysia Pahang, Malaysia

[2]Inti International University, Malaysia

[3]Aviation Engineering Technology and Science, Higher Colleges of Technology, Abu Dhabi Men's College, UAE

[a]agusgeter@ump.edu.my, [b]kaitilow@gmail.com, [c]alegowo@hct.ac.ae

*corresponding author

Keywords: TiO_2, ZnO, powder metallurgy, sensor, semiconductor

Abstract. Metal oxide semiconductor gas sensors have been widely utilized in a variety of different roles and industries. They are relatively inexpensive, robust, lightweight, long lasting and benefit from high material and quick response time compared to other sensing technologies. However, there are major challenges need to overcame by developers in order to construct a semiconductor metal oxide gas sensor that is efficient, and durable and most importantly can work at lower temperature. Therefore, in this research, TiO_2 dopants was introduced into conventional high purity ZnO gas sensor whereby the samples were prepared in pellet form using powder metallurgy route. The improvement in the mechanical properties as well as the electrical properties of the samples was wished to be observed through this research. The density measurement showed that the adding of TiO_2 was efficient to promote the densification of ZnO sample in which 9 wt% TiO_2 doped ZnO sample showed the highest density. The XRD results showed that the diffraction pattern was basically attributed to the wurtzite structure of ZnO. This was proven by the plane (1 0 1) had the highest intensity in all the samples except 6 wt% TiO_2 and 9 wt% TiO_2 doped ZnO sample. SEM showed that the grain size of ZnO decreased with the addition of TiO_2. This was caused by the formation of the new phase which was Zn_2TiO_4. The smaller the grain size, the higher the specific surface area and oxygen adsorption quantity, and therefore the higher the gas sensitivity is. UV-Vis showed that the wavelength of all samples was located around 380 nm. Therefore, the calculated exitonic energy was around 3.20 eV which was nearly matched with the theoretical band gap of ZnO (3.37 eV). The measurement of the resistivity using four point probe showed that the electrical resistivity of the samples decrease up to addition of 9 wt% TiO_2. This was attributed to increased carrier concentration. Vickers hardness test showed that the doping of TiO_2 had increased the hardness of the sample whereby the 9 wt% TiO_2 doped ZnO sample showed the highest value of hardness. The addition of TiO_2 into high purity ZnO has influenced the mechanical and electrical properties of ZnO. From observing the microstructural and density measurement to the measurement of the surface resistivity as well as the determination of the Vickers hardness value, it was found that 9 wt% TiO_2 doped ZnO was predicted as a candidate for substituting a conventional high purity ZnO as the gas sensor.

Introduction

Metal oxide semiconductor gas sensors have been widely utilized in a variety of different roles and industries. They are relatively inexpensive, robust, lightweight, long lasting and benefit from high material and quick response time if being compared with the other sensing technologies. By having all these features, they have been selected as a great candidate to measure and monitor trace

amounts of environmentally important gases such as carbon monoxide and nitrogen dioxide. Recent discoveries also prove that with the use of metal oxides as gas sensing materials at high working temperature can make the significant progress in moving away from bulky sensor architectures become reality [1].

Therefore, new approaches must be studied and explored so that the gas sensor can be operated at lower or room temperature. Recent studies has showed that UV light irradiation is one of the very useful way to improve the gas-sensing properties and reduces the working temperature [2] . To the best of our knowledge, few papers have been reported that there are two materials which have been proven to exhibit all of the properties required for a good gas sensing performance, namely zinc oxide (ZnO) [3], while the others, such as indium tin oxide (ITO), In_2O_3, CdO, $ZnSnO_4$, NiO, etc., have also been widely studied. However, several studies have reported that the properties of ZnO-based gas sensor still can be remarkably improved by introducing TiO_2 dopant into the sensing films [4], and the peculiar structure and morphology of the sensing materials can also be conducive to the low temperature gas-sensing performance.

Due to the simple manufacture technique, rapid response, low cost and recovery of semiconductor metal oxide (MOS) gas sensor, it has attracted a great attention in the past few years. Apart from that, due to emergence and rapid development of the science and new technology, the idea of integration of gas sensor components into smarts phone, tablets and wrist watches have become a popular issues among the developers, with the purpose of providing the individual with the ability to detect harmful chemicals and pollutants in the environment by using the always-on hand-held or wearable devices. However, there are major challenges need to overcame by developers in order to construct a semiconductor metal oxide gas sensor that is efficient, and durable and most importantly can work at lower temperature. In this case, the introduction of TiO_2 dopants into the conventional ZnO gas sensor play an important role in making the gas sensor become more user-friendly.

This paper presents the fabrication process of the TiO_2 doped ZnO sample using powder metallurgy route [5-21]. The progressions in microstructure of the samples were observed or examined by utilizing X-Ray diffraction (XRD) and scanning electron microscopy (SEM) and the samples were characterized also using the ultraviolet –visible (UV-Vis) Spectroscopy. Furthermore, the relationship between the electrical properties and mechanical properties of the sample with its varying weight fraction of TiO_2 was studied as well.

Experimental Setup

The ZnO and TiO_2 powders were applied for powder mixtures of various desired compositions. In this research, 5 sample, each with varying amount of TiO_2 powder with the fixed amount of ZnO powder. They are samples respectively which containing ZnO as their main constituent with 0 wt%, 3 wt%, 6 wt%, 9 wt%, and 12 wt% of TiO_2. For this purpose, 10 grams of ZnO powder with 99.95% purity was measured using digital weighing machine. After that, the amount of TiO_2 powder needed was weighted accordingly and mixed with the ZnO powder. by adopting powder metallurgy route. It contains three basic procedures which were powder grinding, die compaction and sintering. In this case, the powder was manually grinded instead of grinding using the ball mill. The mixed powder (ZnO and TiO_2) was grinded using agate mortar and pestle for about two hours to ensure the mixture is homogenous and yielding fine particle. After that, half of the amount of 30 ml ethanol was added into the TiO_2 doped ZnO powder gently. The mixture was grinded on hotplate manually and heated with temperature around 70.0°C. This was done to facilitate the evaporation of the ethanol. Following that, another half of the amount ethanol was added slowly into the mixture during grinding process. Grinding process was ended when the mixture became dry. After grinding process, the mixed powder was transferred to pelletizer mould as shown in **Error! Reference source not found.** to form the pellets. Prior to the transferring of the powder to pelletizer mould, the pelletizer mould was thoroughly cleaned with ethanol. This is because there should be no

presence of any lubricant which might contaminate the sample. Amount of mixed powder used to form each pellet was around 1.0 g and 3 pellets were prepared for each sample. The mass of each pellet was measured using the digital weighing machine. 1.0 g of the mixed powder was gently poured into the cavity of the pelletizer mould and hydraulic press was adopted for compaction of the pellets. The final step of powder metallurgy method was the sintering process. The pellets were sintered in a box metallurgical furnace as shown in **Error! Reference source not found.**. The box metallurgy furnace was used to sinter the pellet so that it was convenience for the pellets in handling into or out of the furnace. The pellets and powder were placed inside rectangular alumina crucible boats and circular alumina crucible boats respectively before handling into the box metallurgy furnace. Both the pellets and the powder were sintered at 1100°C to prevent formation of large grain size. The sintered rate was 16.5°C/minutes to prevent grain from growing rapidly. The sintering process took 5 hours to ensure a complete densification of pellets through high isolation of pores at grain edges and high neck growth. Characterization of sintered samples used XRD, SEM, UV-Vis, Surface electrical resistivity and Vickers hardness.

Results and Discussions

XRD. Figure 1 showed the comparison of XRD of all samples. The diffraction patterns was basically attributed to the wurtzite structure of ZnO. This was proven by the plane (1 0 1) had the highest intensity in all the samples except 6 wt% TiO_2 and 9 wt% TiO_2 doped ZnO sample. The highest intensity of 6 wt% TiO_2 doped ZnO sample was plane (1 1 0) while that of 9 wt% TiO_2 doped ZnO sample was plane (1 0 0). The sensing mechanism of ZnO based gas sensor is based on the surface of the semiconducting oxides. Therefore, the phase state is one of the important factors for gas sensitivity. It was found that Zn_2TiO_4 phase and ZnO phase exist in all the samples. Apart from ZnO and $Zn2TiO_4$ phase, TiO_2 phase also exist in the sensing material. The existence of the TiO_2 phase is due to the addition of excessive amount of TiO_2 powder. However, upon doping with 9 wt% TiO_2 and onward, TiO phase was exist instead of TiO.

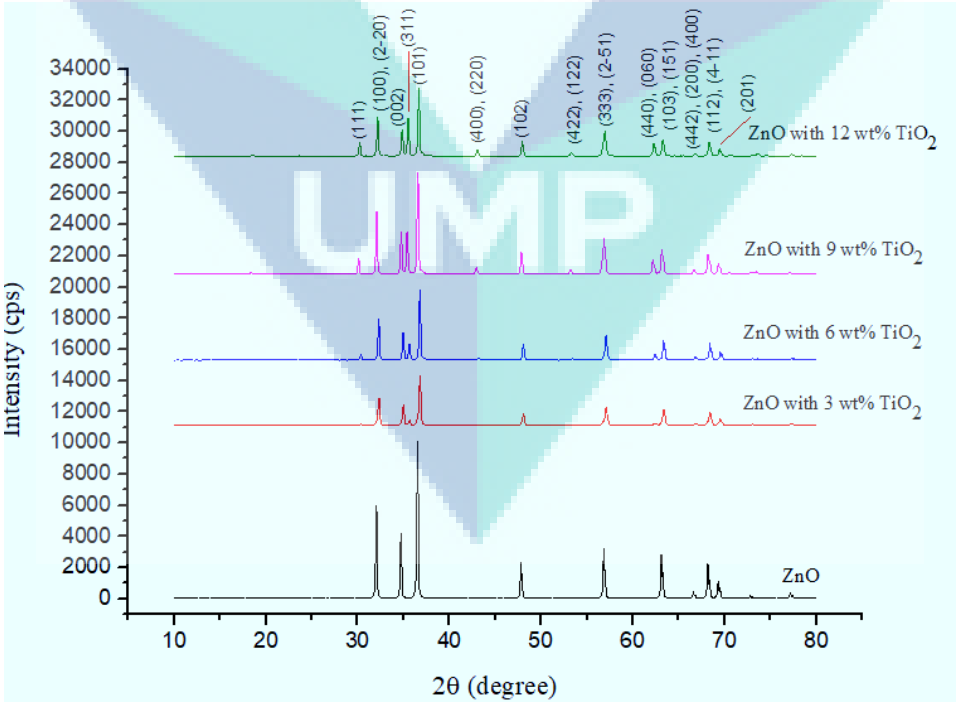

Fig. 1. XRD pattern for all samples of TiO_2 added ZnO.

SEM Images. Figure 2 shows the SEM images of all samples. It is clear that sample 4 with the composition of 9wt% TiO_2 visually less pores compared with others. The optimum densification

happened in this composition. Addition more TiO_2 will make reducing of densification. The grain growth will not further effective to increase the density.

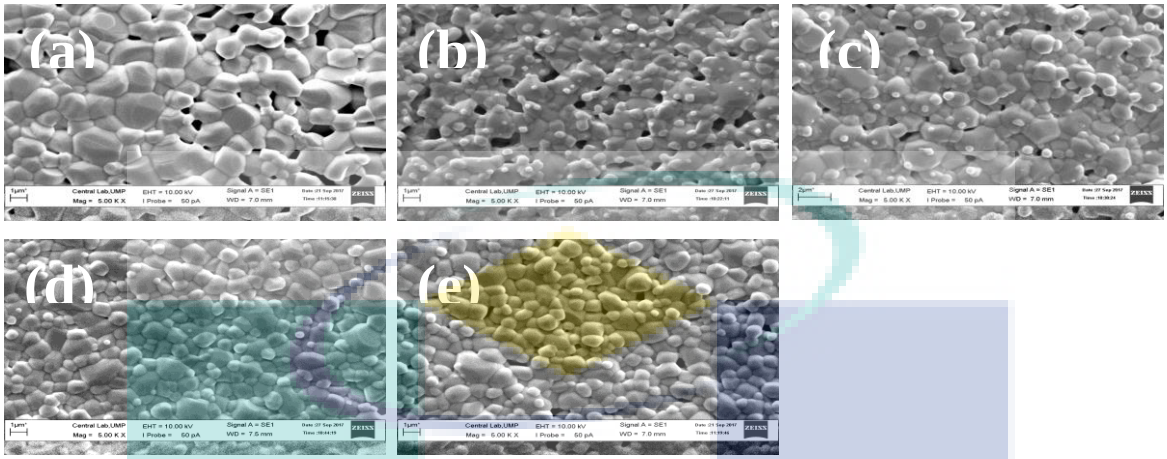

Fig. 2. SEM images for all samples of TiO_2 added ZnO respectively: (a) 0wt%, (b) 3wt%, (c) 6wt%, (d) 9wt% and 12wt% TiO_2 addition into high purity ZnO.

UV-vis. Figure 3 shows the UV-vis characterization for all samples (a) and table of threshold exitonic energy, absorbance and wavelength for all samples. The wavelength of first excitonic peak of each sample was found to be around 380 nm and the exitonic energy of most of the samples was around 3.20 eV which was nearly match with theoretical band gap 3.37 eV. The sample which doped with 3 wt% TiO_2 was found to absorb the longest wavelength which is equal to 380.5747 nm. The highest excitonic energy with the value of 3.3127 eV was exhibited by the sample when doped with 9 wt% TiO_2.

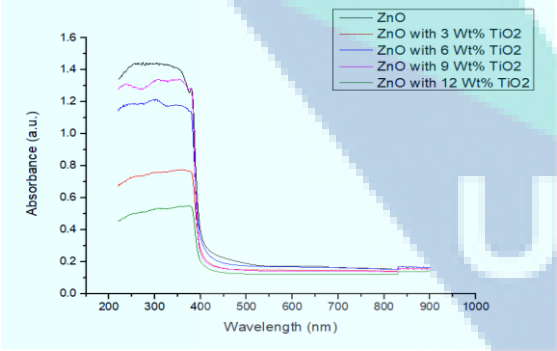

(a)

Sample	Absorbance (au)	Wavelength (nm)	Excitonic Energy (eV)
ZnO	1.2814	377.5549	3.2862
ZnO with 3 wt% TiO_2	0.7875	380.5747	3.2601
ZnO with 6 wt% TiO_2	1.1480	378.9760	3.2738
ZnO with 9 wt% TiO_2	1.2843	374.5350	3.3127
ZnO with 12 wt% TiO_2	0.5487	375.9561	3.3001

(b)

Fig. 3. UV-vis characterization for all samples (a) and table of threshold exitonic energy, absorbance and wavelength for all samples.

Electrical Resistivity. Error! Reference source not found. shows the electrical resistivity of each sample taken at three repetitions and average electrical resistivity of each sample respectively obtained using the four point probe technique respectively. It can be clearly seen that the electrical resistivity obtained for ZnO (0.6853 MΩ.m) is nearly match with the theoretical electrical resistivity of ZnO at room temperature which is equal to 0.75 MΩ.m. The electrical resistivity of the samples were observed to be decreasing when with increasing amount of TiO_2 being doped. However, upon the doping with 12 wt% TiO_2, the electrical resistivity increase again. For ZnO doped with TiO_2, the decrease in resistivity was due to the formation of the solid solution when Zn^{2+} was replaced with Ti^{4+}. Due to the almost similar ionic radii of both Zn^{2+} (0.074 nm) and Ti^{4+} (0.068 nm), the

reactions took place easily. This had lead to an increased carrier concentration and low resistivity for ZnO grains [22].

Table 1. Electrical resistivity for all samples

Sample	Average Electrical Resistivity (MΩ.m)
ZnO	0.6853
ZnO with 3 wt% TiO_2	0.4685
ZnO with 6 wt% TiO_2	0.2683
ZnO with 9 wt% TiO_2	0.1852
ZnO with 12 wt% TiO_2	0.1910

Vickers Hardness. For Vickers Hardness test (ASTM C1327-08), indentations were made on the surface of the pellets. The Vickers indenters had created a square impression and two surface-projected diagonal length were measured. The Vickers hardness was calculated form the ratio of applied load against area of contact of the indentation. Five indentations were made for each sample as shown in **Error! Reference source not found.** and average hardness was calculated and tabulated in 2. It can be clearly seen that the pellets exhibit the highest Vickers hardness with the value of 396 HVO.3 when being doped with 9 wt% TiO_2. In contrast, ZnO showed the lowest Vickers hardness with only 231.4 HVO.3.

Table 2. Vickers hardness for all samples

Sample	Averages Hardness (HVO.3)
ZnO	231.4
ZnO with 3 wt% TiO_2	297.1
ZnO with 6 wt% TiO_2	332.8
ZnO with 9 wt% TiO_2	396.8
ZnO with 12 wt% TiO_2	364.1

Summary

This research had proved that the 9 wt% TiO_2 doped ZnO was suitable to become a candidate for substituting a conventional high purity ZnO as the gas sensor. The addition of TiO_2 was able to promote densification of ZnO sample whereby 9 wt% TiO_2 doped ZnO showed the highest density. The analysis of the XRD results showed that the diffraction patterns of all the samples was basically attributed to the wurtzite structure of ZnO and there was the existence of a new phase Zn_2TiO_4 when doping with 3 wt% TiO_2 and onward. This can be proven by the plane (1 0 1) had the highest intensity in all the samples except 6 wt% TiO_2 and 9 wt% TiO_2 doped ZnO sample. Apart from that, from observing the microstructure of the samples, it was found that the doping of TiO_2 was able to decrease the grain size of the ZnO which believed to be effective in decreasing the working temperature of the gas sensor due to the increased surface activity of ZnO. Furthermore, the sample also exhibit the lowest electrical resistivity and highest Vickers hardness value when doped with 9 wt% TiO_2.

Acknowledgement

This study was supported by RDU grant of Universiti Malaysia Pahang RDU1703194 and Funding from Higher Colleges of Technology Abu Dhabi Men's College, UAE.

References

[1] C. Wang., L. Yin, L. Zhang, D. Xiang, & R. Gao, Metal oxide gas sensors: sensitivity and influencing factors. Sensors, 10(3), 2088-2106, 2010.

[2] P. Camagni, G. Faglia, P. Galinett, C. Perego, G. Samoggia, & G. Sberveglieri, Photosensitivity activation of SnO2 thin film gas sensors at room temperature. Sensors and Actuators B: Chemical, 31(1-2), 99-103, 1996.

[3] A. Bouaoud, A. Rmili, F. Ouachtari, A. Louardi, T. Chtouki, B. Elidrissi & H. Erguig, Transparent conducting properties of Ni doped ZnO thin films prepared by a facile spray pyrolysis technique using perfume atomizer. Materials Chemistry and Physics, 137(3), 843-847, 2013.

[4] C. Baratto, G. Sberveglieri, A. Onischuk, B. Caruso S. Di Stasio, S, Low temperature selective NO 2 sensors by nanostructured fibres of ZnO. Sensors and Actuators B: Chemical, 100(1), 261-265, 2004.

[5] A.G.E. Sutjipto, M.H. Mazwir, L.Y. Har, M.A. Jusoh, R. Othman: Effect of compaction pressure of green body and heating current on photoluminescence property of ZnO crystal grown by electric current heating method, IOP Conference Series: Materials Science and Engineering, 290(1), 012043, 2018.

[6] J. Bakri, Hens Saputra: A.G.E. Sutjipto, MFI Zeolite Membrane from Rice Husk for Biofuels Production, Applied Mechanics and Materials, Vol. 1787 (165), pp.104-108, 2012.

[7] A.G.E. Sutjipto, M. Takata: The use of SEM to investigate the effect of an electron beam on the optically-visible flashover treeing of CaO added MgO ceramic, Journal of Materials Science 42(15), pp. 6036-6040, 2007.

[8] A.G.E. Sutjipto: The effect of CaO addition on the microstructural, mechanical and dielectric properties of pure MgO ceramic, Key Engineering Materials, 345-346 II, pp. 1609-1612, 2007.

[9] A.G.E. Sutjipto, T. Okamoto, M. Takata: Appearance of flashover treeing on polycrystalline magnesia surface, Key Engineering Materials, (181-182), pp. 231-234, 2000.

[10] A.G.E. Sutjipto, Y.P. Asmara, M.A. Jusoh: Behavior of MgO Based Ceramics under Electron Irradiation, Procedia Engineering, 170, pp. 88-92, 2017.

[11] Jufriadi, A.G.E. Sutjipto, R. Othman, R. Muhida: Microstructure and electrical properties of AZO films prepared by RF magnetron sputtering, Advanced Materials Research, 264-265, pp. 754-759, 2011.

[12] A.R. Fatimah Azreen, A.G.E. Sutjipto, E.Y.T. Adesta: Fabrication of CuSiC composite by powder metallurgy route. Advanced Materials Research 264-265, pp. 748-753, 2011.

[13] Jufriadi, A.G.E. Sutjipto, R. Othman, R. Muhida: Discharge, microstructural and mechanical properties of ZrO2 addition on MgO for plasma display panel materials, Materials Research Innovations, 13(3), pp. 149-152, 2009.

[14] A.G.E. Sutjipto, R. Muhida, M. Takata: An SEM flashover: Technique to characterize wide band gap insulators, Proceedings of the IEEE International Conference on Properties and Applications of Dielectric Materials 4062645, pp. 216-219, 2007.

[15] H. Saputra, R. Othman, A.G.E. Sutjipto, R. Muhida, M.H. Ani: Gel-like properties of MCM-41 material and its transformation to MCM-50 in a caustic alkaline surround. Materials Research Bulletin. 47(3), pp. 732-736, 2012.

[16] H. Saputra, R. Othman, A.G.E. Sutjipto, R. Muhida, and M.H. Ani: Gel-like properties of MCM-41 material and its transformation to MCM-50 in a caustic alkaline surround, Material Research Bulletin, 47(3) pp. 732-736, 2012.

[17] A.R.F. Azreen, A.G.E. Sutjipto, E. Y. T. Adesta: Fabrication of CuSiC Composite by Powder Metallurgy Route, Advanced Materials Research, 264-265, pp 748-753, 2011.

[19] A.G.E. Sutjipto, Y.P. Asmara, M.A. Jusoh: Characteristic of MgO Based Ceramics under Electron Irradiation, Procedia Engineering (Elsevier), Vol. 170, pp. 88-92, 2017.

[20] R. Muhida, A.G.E. Sutjipto, Afzeri, T. Toyama, H. Okamoto: Relationship between average slope of textured substrate and poly-Si thin film solar cells performance. Materials Research Innovations 13 (3), pp. 246-248, 2009.

[21] A. R. F. Azreen, A.G.E. Sutjipto, A.S. Mohamad, Development of Cu-SiC composite for electrical discharge machining electrode using powder metallurgy technique, Advanced Materials Research, 576. pp. 203-207, 2012.

[22] J. Fan & R. Freer, The roles played by Ag and Al dopants in controlling the electrical properties of ZnO varistors. Journal of Applied Physics, 77(9), 4795-4800., 1995.